TEMPERATURE-RESPONSIVE SKIN-LIKE DIRECTIONAL LIQUID FLOW AND WATER REPELLENT FABRIC

PU YI

PhD

The Hong Kong Polytechnic University

2026

The Hong Kong Polytechnic University

School of Fashion and Textiles

Temperature-responsive Skin-like Directional Liquid Flow and Water Repellent Fabric

PU Yi

A thesis submitted in partial fulfilment of the requirements for the degree of Doctor of Philosophy

June 2025

Certificate of Originality

I hereby declare that this thesis is my own work and that, to the best of my knowledge and belief, it reproduces no material previously published or written, nor material that has been accepted for the award of any other degree or diploma, except where due acknowledgement has been made in the text.

_____(Signed)

PU Yi (Name of student)

Abstract

In the context of global climate change, high-temperature conditions are becoming increasingly prevalent. Outdoor workers during summer months frequently encounter extreme heat conditions that significantly affect comfort levels, with severe cases potentially leading to heat exhaustion or even life-threatening heat stroke. Acting as a second skin for the human body, clothing plays a critical role in maintaining thermoregulatory and moisture comfort. However, current garment technologies often fail to address thermal and moisture regulation requirements during heavy perspiration. Conventional moisture management textiles typically operate by rapidly transporting sweat away from the skin surface and facilitating quick liquid spreading for enhanced evaporative cooling. Nevertheless, these traditional fabrics exhibit significant limitations when excessive sweating takes place. When wet with excessive sweat, they become heavy, clingy, and uncomfortable after-chill against the skin. Prolonged wear of sweat-soaked garments may also cause potential health problems. Furthermore, unlike human skin, existing thermoregulatory textiles lack the ability to dynamically adjust their moisture management performance in response to temperature variations, which substantially restricts their practical utility in various applications. An ideal moisture management fabric should dynamically regulate the liquid water transport properties in response to temperature variations like human skin. If the moisture management fabric could enhance liquid water transport property at higher temperatures while suppressing liquid water transport to reduce evaporative cooling at lower temperatures, it will critically improve thermal and moisture comfort. This

research aims to develop temperature-responsive skin-like directional flow and water repellent fabrics as well as understanding the underlining mechanisms of its unique directional liquid water transport and water repellent properties. The research contains three parts: (1) development of fabrication method of skin-like fabrics for scalability, (2) development of poly([2-(Methacryloyloxy)ethyl] dimethyl-(3-sulfopropyl) ammonium hydroxide) (PDMAPS)-based temperature-responsive skin-like fabrics, and (3) development of poly(acrylamide-co-acrylonitrile) [poly(AAm-co-AN)]-based non-ionic temperature-responsive (NiTR) skin-like textiles.

To address the issues of conventional moisture management fabrics (e.g., heaviness and wet clinginess when saturated with sweat), skin-like fabrics have already been reported in previous work. However, the existing plasma-based fabrication method presents several drawbacks, including high energy consumption, low production efficiency, and poor durability. This study improved the fabrication process of existing skin-like fabric, proposing a new polyvinyl alcohol (PVA)-based fabrication approach of skin-like fabrics. First, PVA solution was printed onto the fabric surface by screen printing technique as a coverage pattern, followed by hydrophobic treatment via dip coating. After hot washing for the removal of PVA, the covered areas by PVA formed gradient wettability channels. These channels enabled directional liquid water transport from the inner side to the outer surface of the fabric, where droplets accumulated and rolled off, while most areas remain dry, which effectively prevented moisture-induced heaviness and coldness. Additionally, the predominantly hydrophobic outer surface provides water repellency against contamination. The

wettability, directional liquid transport property, water repellency, and air permeability of the prepared skin-like fabric were evaluated This method offered simplicity, cost-effectiveness, and compatibility with various substrates. The resulting samples demonstrated excellent durability and showed potential for industrial-scale production.

To achieve the temperature-responsive property on the skin-like fabric, zwitterionic upper critical solution temperature (UCST)-type temperature-responsive polymer PDMAPS was grafted onto the surface of the skin-like fabric using a “grafting-from” approach. Before the grafting process, 3-(trimethoxysilyl) propyl methacrylate (TMSPMA) was applied onto the fabric as a coupling agent to enhance grafting durability. The TMSPMA-treated fabric was then dip-coated with the [2-(Methacryloyloxy)ethyl] dimethyl-(3-sulfopropyl) ammonium hydroxide (DMAPS) monomer solution and subjected to ultraviolet (UV)-initiated graft polymerization, resulting in (PDMAPS)-based temperature-responsive fabric. The fabricated fabric not only remained the characteristics of skin-like fabric but also exhibited dynamically switchable moisture management properties in response to temperature changes. At higher temperatures, the fabric demonstrated enhanced liquid water transport efficiency, while at lower temperatures, it showed decreased liquid water transport capability and improved water repellency. The directional liquid water transport property, temperature responsiveness, water resistance, air permeability, and handle of the fabric were systematically evaluated. The mechanism of the temperature-responsive directional liquid transport property of the fabric was also discussed. This functional fabric holds potential as a multifunctional smart moisture management textile, particularly suitable

for next-generation intelligent sportswear applications. The combination of temperature-responsive behavior with inherent skin-like fabric properties offers promising opportunities for advanced textile development.

The (PDMAPS)-based temperature-responsive fabric, while offering advantages such as easy preparation and rapid temperature response, exhibits sensitivity to electrolyte concentration variations due to its zwitterionic nature. Since human sweat electrolyte levels fluctuate with health status and exercise intensity, the practical applications of (PDMAPS)-based temperature-responsive fabrics are limited. To solve this problem, we developed a non-ionic UCST-type temperature-responsive fabric. The non-ionic UCST-type temperature-responsive polymer, poly(AAm-co-AN) was grafted onto the cotton knitted fabric for the first time via a novel site-specific grafting method. The fabric underwent mixed silane pretreatment before grafting with the polymer, followed by photo-initiated grafting of poly(AAm-co-AN). The mixed silane contains a hydrophobic silane to adjust the fabric surface wettability, a grafting-functionalized silane to control the concentration of grafting sites on the fabric surface, and a silane crosslinker to increase the coating stability. By adjusting the ratio of the hydrophobic silane and the grafting-functionalized silane, the grafting ratio of poly(AAm-co-AN) could be controlled, enabling the surface to achieve stable temperature-responsive performance. By precisely controlling both the silane composition and acrylamide-to-acrylonitrile (AAm:AN) ratio, we fabricated NiTR fabrics with tunable transition temperatures, excellent reversibility, and remarkable electrolyte stability. The resulting smart textiles demonstrate superior performance in various applications including being

used for the substrate of skin-like fabric for personal moisture management, smart oil-water separation and advanced wound dressings, representing significant improvements over conventional temperature-responsive fabrics.

List of Publications

Research Papers

1. **Pu, Y.**, & Fan, J. (2024). Thermoresponsive skin-like fabric for personal comfort and protection. ACS Applied Materials & Interfaces, 16(8), 10960-10968.

2. Zhang, H. C., Kang, Z. X., Wu, Y. X., **Pu, Y.**, Jiang, S. K., Amir, S., ... & Fan, J. T. (2024). Double-side super-hydrophilic/superspreading fabric for ultrafast asymmetric sweat transport and in-situ power generation. Nano Energy, 128, 109919.

3. **Pu, Y.**, Liu, C.& Fan, J. Non-ionic UCST-type Temperature-responsive Textiles with Tunable Transitional Temperature and Stability against Electrolyte Variation. (Submitting)

Patents

1. Fan, J., & **Pu, Y.** (2024). 一种制备定向传输液体的材料的方法. (Patent No. ZL 202110879048.4).

2. Fan, J., & **Pu, Y.** A Temperature-responsive Switchable Wettability Fabric and Preparation Method Thereof. (Patent Submitting)

Acknowledgements

First and foremost, I would like to express my deepest gratitude to my chief supervisor, Prof. Jintu Fan. I am deeply grateful for his invaluable guidance, steadfast support, and constructive feedback throughout my research endeavor. His mentorship and suggestions have been profoundly beneficial to my academic development. I sincerely appreciate the exceptional research environment and resources he provided. Through his exemplary conduct, he has instilled in me rigorous research methodologies and life philosophies that will continue to guide me indefinitely.

I gratefully acknowledge Dr. Zhanxiao Kang, Dr Lun Lou, Dr. Hanchao Zhang, Dr. Shoukun Jiang, Dr. Jiale Chai, Dr. Can Wang, Dr. Amir Shahzard for the valuable suggestions contributed to this work.

I would also like to express my appreciation to the members of our research group: Miss Judy Soo, Miss Xuanxuan Du, Miss Yiying Zhou, Ms. Lijun Wang, Mr. Yang Hong, Mr. Jiahao Liang, Miss Jiayi Sui, Miss Luning Yuan, Miss Yuxi Wu, Mr. Youshen Chen, Dr. Mengjuan Zhou, Miss Yue Li, Miss Fengfei Deng, Miss Chang Liu, Miss Jie Meng, Mr. Yudong Wu, Mr. Yang Cao, Dr. Jialong Chai, and Dr. Xiang Ma. Their professional support and friendship significantly motivated my research efforts.

I wish to express my sincere appreciation for the support from the technicians and supporting colleagues in our department, including Dr. Chenghao Lee, Dr. Kevin Hui, Dr. Patrick Pang, Mr. Kwan-on Choi, Mr. Shui-wing Ng, Dr. Ling Lam, Ms. Sicily Ho, Ms. Susanna Ng, Mr. Oscar Chau, and Ms. Tracy Wu.

I extend my profound gratitude to my family for their unwavering support. My parents' silent dedication and steadfast encouragement formed the essential foundation for this research endeavor. Above all, I wish to express my special appreciation to my wife, Dr. Jing Yang for her unwavering companionship and constant encouragement throughout this journey.

Table of Contents

List of Figures

List of Tables

Chapter 1 Introduction

1.1 Research Background

As the second skin of people, clothing has the ability to regulate thermal and moisture balance of human body[1, 2]. With the development of living standards, wearing comfort of clothing has become increasingly important[3-5]. In Hong Kong's subtropical climate, outdoor workers frequently experience excessive sweating due to prolonged heat and humidity exposure. Construction workers, for instance, endure intense physical exertion while handling heavy materials under direct sunlight, often leading to severe perspiration. Similarly, patrolling police officers face constant sweat accumulation during their extended outdoor shifts, particularly when wearing protective gear. Other vulnerable occupations include road maintenance crews, delivery couriers, and city cleaners subjected to an environment that causes excessive sweating and associated thermal discomfort. Moisture management fabrics play an important role in thermal and moisture regulation. This kind of fabric has the capacity of absorbing moisture away from the skin, spreading moisture over a large surface area and then drying the sweating quickly. Most of these fabrics exhibit directional liquid transport property[6, 7].

Directional liquid transport is a considerably common phenomenon in nature[8, 9]. For example, body fluids can be directionally transported through biochemical membranes[10], water can be directionally transported from the root of the plant to the stem and leaves[11], spider silk can drive water droplets directionally[12]. In the area of

textile science, directional water transport properties of textiles are important factors for thermal and moisture comfort. For moisture management fabrics, sweat should be transported from the close-to-skin side to the outer side of the fabric but cannot be transported in the reverse direction. However, the traditional moisture management fabric with directional water transport properties has an all hydrophilic outer surface, so it is easily contaminated and could not resist external water. Furthermore, the fabric will be clammy, clingy and heavy after the outer surface is saturated. It may cause health problems. Therefore, it is critically important to establish a next generation moisture management fabric that can address current challenges.

As the second skin of the human body, ideal clothing should have the function of dissipating heat at a higher temperature and keeping warm in a cold environment[5, 13, 14]. If the moisture management fabrics can regulate their moisture management property with the change of temperature, their performance will be enhanced in many applications. To achieve this temperature-responsive property of the fabrics, one simpler way is to coat a layer of polymer with temperature-responsive properties on the surface of the fabric. These polymers are then able to change their wettability with the change of environment. Many researchers applied such polymers to different surfaces to achieve a reversibly switchable wettability surface for self-cleaning, microfluidic tools, tunable optical lens[15]. However, significant challenges arose when applying these polymers to textiles, particularly in achieving the desired hydrophilic-hydrophobic balance on the fabric surface and ensuring durability of the coating. These limitations currently hinder the advancement of temperature-responsive functional textiles.

1.2 Research Challenges

Generally, there are two key driving forces of the directional liquid transport, namely, the mechanical or capillary pressure and chemical potential, as well as the fluid surface tension and wetting behaviour[16]. Therefore, to achieve the directional liquid transport in fabric materials, it is essential to engineer the difference of these driving forces between two sides of fabrics through two primary approaches: One is constructing a surface energy difference (wettability difference) on both sides of the fabric, the other one is building a structural difference (pore size difference) through the cross-section direction of the fabric[17, 18]. These strategies are both able to be accomplished via surface modification (e.g., plasma treatment[16]) and multi-layer composition (e.g., layer by layer electrospinning[19]). These directional water transport fabrics have been widely used in areas including moisture management clothing[20], moisture sensor[21], oil-water separation[22], fog harvest[23]. However, conventional directional liquid transport fabrics with fully hydrophilic outer surfaces present several critical limitations, as described in Section 1.1. To solve these problems, our group developed a “skin-like” fabric[24] by mimicking the one-way liquid transport property of human skin. Using selective plasma treatment, gradient wettability channels were developed on a hydrophobic cotton fabric. Water can be easily transported from the close-to-skin side to the outer side through the wettability channels, but the fabric has an excellent water repellency due to the mostly hydrophobic outer surface. Nevertheless, it is difficult to achieve the large-scale production of the fabric, and the water transport property of this fabric is not stable due to the aging of plasma. Furthermore, the “skin-

like" fabric could not regulate the moisture management property according to the change of temperature like real human skin.

Numerous studies have successfully fabricated temperature-responsive fabrics by coating temperature-responsive polymers onto textile surfaces. The surface roughness or chemical groups of these temperature-responsive polymers can be altered with the change of temperature. Hence, the surface wettability of these polymers can be easily changed as temperature changes. Generally, the temperature-responsive polymer can be divided into two categories, i.e., lower critical solution temperature type (LCST-type) polymers and upper critical solution temperature type (UCST-type) polymers[25]. LCST-type polymers refer to polymers which are hydrophobic at a higher temperature and hydrophilic at a lower temperature, whereas UCST-type polymers have the opposite properties[26-28]. The surface coated by these polymers have the capacity of changing the surface wettability as the temperature changes. While there are numerous reports on LCST-type polymers, such as poly (N-isopropylacrylamide) (PNIPAAm)[29-32], UCST-type polymers are more suitable for smart moisture management textiles due to their property of being hydrophilic at higher temperatures and hydrophobic at lower temperatures. However, research on UCST-type polymers is relatively limited due to challenges in fabrication and performance instability.

1.3 Research Objectives

This research aims to develop skin-like UCST-type temperature-responsive directional flow and water repellent fabrics as well as understanding the underlining

mechanisms of its unique directional water transport and water repellent properties. The directional water transport rate of the fabric is expected to be greater than that of the existing skin-like fabric. Furthermore, the moisture management property of the fabrics can be tuned by changing the water transport rate of the fabric as temperature variation. The fabric is expected to have a higher water transport rate at higher temperatures to dissipate heat from human body and have a lower water transport rate at lower temperatures to keep warm. This fabric can be widely used in smart moisture management clothing such as smart sportswear.

The specific research objectives of this study are:

1. To explore novel processing techniques for fabricating the skin-like directional flow and water repellent fabrics.
2. To develop diverse skin-like UCST-type temperature-responsive moisture management fabrics by applying various temperature-responsive polymers with switchable wettability properties.
3. To compare the performance characteristics of different temperature-responsive textiles and expand their application scenarios.
4. To study the underlining mechanisms of directional fluid flow through the gradient wettability channels spatially distributed across the predominantly superhydrophobic fabric.
5. To investigate the effect of the properties of temperature-responsive polymers as well as the structural and processing parameters of the directional flow fabric on

the changes of pore size in the fabric, directional fluid flow rate, reverse liquid repellency and breakthrough pressure.

1.4 Research Significance

The development of smart moisture management fabrics holds significant potential for improving personal thermal and moisture comfort, particularly in extreme environments where conventional textiles fail to adapt dynamically. This study developed temperature-responsive skin-like fabrics, proposing a novel thermal and moisture management textile that addresses key limitations of traditional moisture management fabrics, with the following significance:

1. This study addressed the scalability challenge on the fabrication of skin-like fabric by establishing a PVA-based method via mature technologies for durable performance, providing critical technical guidelines for scale-up production.

2. This research successfully engineered temperature-responsive functionality into skin-like fabrics by grafting temperature-responsive polymers onto textile surfaces, enabling dynamic regulation of both water transport capacity and hydrostatic pressure resistance in response to temperature changes. Compared with skin-like fabrics, the temperature-responsive skin-like fabric demonstrated a 29.1% enhancement in water transport rate at higher temperatures, while achieving up to 28.9% improvement in hydrostatic pressure resistance at lower temperatures.

3. This study addressed a research gap in non-ionic UCST-type polymer-based fabrics by applying the “grafting-from” technique to immobilize poly(AAm-co-AN) polymers onto fabric surfaces. The developed temperature-responsive textile demonstrated tunable transition temperatures while exhibiting stability against electrolyte concentration variations.

4. This research addressed several limitations of traditional moisture management fabrics, with the materials developed in this study demonstrating enhanced personal comfort performance for outdoor activities.

5. The developed temperature-responsive fabric demonstrated promising potential across multiple applications, including thermal-moisture management, wound dressing, and oil-water separation, offering innovative solutions to various industrial challenges.

1.5 Outline of the Thesis

The structure of the thesis is as follows:

Chapter 1 introduces the research background, challenges, objectives and significance of the research.

Chapter 2 is the literature review for directional liquid flow textiles, temperature-responsive reversible wettability materials, introducing the categories, applications and mechanisms of these materials. Meanwhile, the polymer grafting methods are outlined.

Chapter 3 reports a developed preparation method of skin-like fabric for scalability. The existing plasma-based fabrication method is evaluated and proposed a novel PVA-based method for preparing the skin-like fabric. The newly developed method adopts well-established technologies, demonstration potential for industrial production of the skin-like fabric while offering energy-efficient and cost-effective advantages. The fabricated skin-like fabric using PVA-based method exhibits excellent directional liquid transport capability and remarkable durability.

Chapter 4 reports on the development of a (PDMAPS)-based temperature-responsive skin-like fabric by applying zwitterionic temperature-responsive polymer, PDMAPS, onto the surface of the skin-like fabric prepared by PVA-based method. The prepared fabric exhibits temperature-responsive moisture management capacity, demonstrating enhanced water transport efficiency at elevated temperatures and reduced water transport rate under cooler conditions.

Chapter 5 reports on the development of a [poly(AAm-co-AN)]-based non-ionic UCST-type temperature-responsive (NiTR) skin-like fabric. Firstly, a NiTR cotton knitted fabric is prepared as the substrate of skin-like fabric by grafting poly(AAm-co-AN) onto mixed silane treated fabrics. A novel treatment strategy is developed to precisely modulate the hydrophilic-hydrophobic balance on the surface of the fabric while optimizing the grafting density of the temperature-responsive polymer. The prepared fabric exhibits tunable transition temperature and stability against electrolyte concentration variations. Then, the NiTR skin-like fabric is prepared using the NiTR fabric as substrate by PVA-based method.

Chapter 6 demonstrates the potential applications of NiTR fabric, including skin-like fabric for personal thermal and moisture management, oil-water separation, and wound dressing.

Chapter 7 summarizes the conclusions and proposes the limitations of the research work as well as the suggestions for future research.

Chapter 2 Literature Review

2.1 Directional Liquid Flow Textiles

Directional liquid flow textiles exhibit anisotropic liquid transport properties, enabling directional liquid movement. Unlike conventional wicking fabrics that allow bidirectional diffusion, these engineered one-way liquid transportation significantly enhance the thermal and moisture management efficiency of the fabric[33]. Specifically, sweat can be directionally transported either through-plane (from the skin-facing surface of the fabric to the outer layer) or in-plane (on the fabric surface), optimizing wearing comfort and functional performance. The directional liquid flow phenomenon is quite common in nature[8, 9, 11, 34]. Certain shorebirds transport water toward their mouths by a bidirectional beak motion (rapid opening and closing)[35] (Figure 2.1a); Desert beetles collect water using hydrophilic bumps on their hydrophobic back[36] (Figure 2.1b); spider silk with spindle knots can drive water droplets towards spindle knots from other areas[12] (Figure 2.1c). There are two general strategies for achieving directional liquid flow on textiles: (1) constructing a surface energy difference on textiles[17] or (2) building a structural difference on different areas of textiles[37]. Both strategies are able to be achieved via surface treatment or multi-layer composition, including dip coating, spray coating, electrospinning, and laminating. Beyond personal thermal and moisture management, these directional liquid flow textiles exhibit broad applications across interdisciplinary fields due to their asymmetric wettability and capillary gradient effects, such as wound dressing, oil-water separation, moisture sensor,

and fog harvest. Here, Mechanism, recent developments, and applications of directional flow textiles will be introduced in this section.

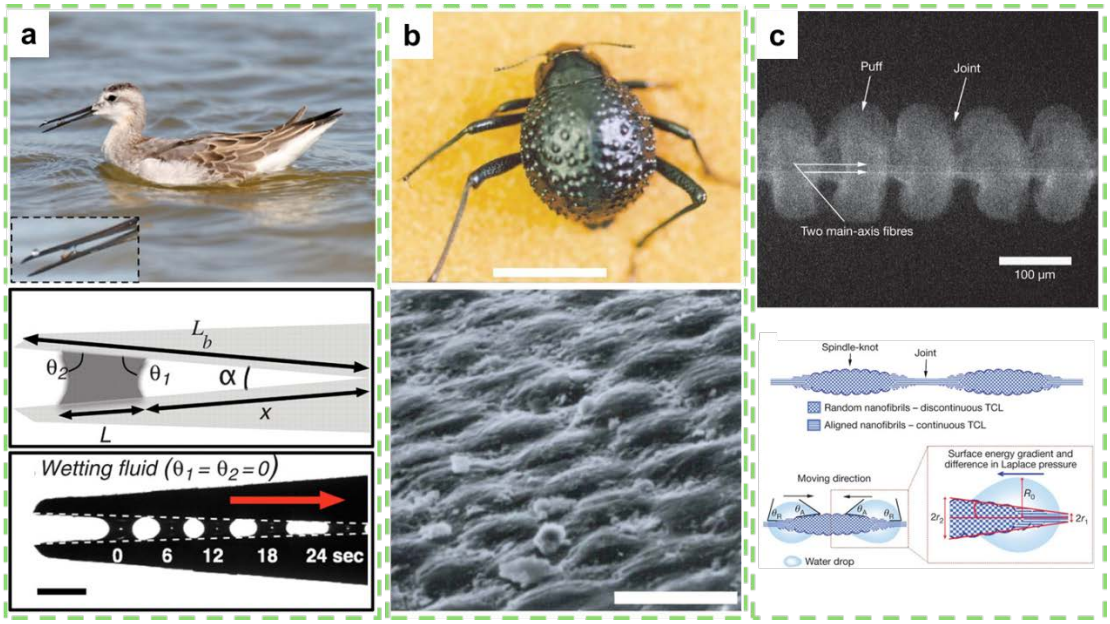

Figure 2.1 Directional liquid transport phenomenon in nature. (a) shorebird beak [35]. (b)Desert beetles[36]. (c) Spider silk[12].

2.1.1 Mechanism of Directional Liquid Flow Textiles

To elucidate the mechanism of directional liquid flow in textiles, a fundamental understanding of wetting behavior is essential. Wetting refers to the interfacial phenomenon where a liquid adheres to and spreads across a solid surface, governed by the thermodynamic equilibrium between adhesive (liquid-solid) and cohesive (liquid-liquid) interactions[38]. The degree of wetting is quantitatively characterized by the contact angle (θ). This behavior is primarily determined by two key factors: the chemical composition (and thus surface energy) of the solid surface and its micro/nanoscale topography[39], which can be described by Young's model, the Wenzel model and the Cassie-Baxter model.

Young's model[40] explains the wetting behavior on an ideally smooth and chemically homogenous solid surface (Figure 2.2a). The Young's equation is expressed as:

$$\gamma_{SG} - \gamma_{SL} - \gamma_{LG} \cos\theta_0 = 0 \tag{2.1}$$

Where γ_{SG}, γ_{SL}, γ_{LG} denote the interfacial energies of solid-gas, solid-liquid, and liquid-gas, respectively. θ_0 corresponds to the Young's contact angle. However, such perfectly smooth and homogenous surfaces are practically unachievable. Consequently, the Wenzel model and the Cassie-Baxter model were proposed to explain the wetting behavior on rough surfaces. The Wenzel model[41] describes complete liquid penetration into surface roughness without air entrapment (Figure 2.2b), which could be expressed as follows:

$$\cos\theta = r\cos\theta_0 = r\frac{\gamma_{SG} - \gamma_{SL}}{\gamma_{LG}} \tag{2.2}$$

Where θ represents the apparent liquid contact angle on the rough solid surface. Compared with the Young's model, the roughness factor *r* was introduced to describe the roughness of the solid surface. Here, *r* is always greater than 1, so the roughness on the surface amplifies the intrinsic wettability of the surface, i.e., a hydrophobic surface will be more hydrophobic, and a hydrophilic surface will be more hydrophilic. The Cassie-Baxter model[42, 43] applies when surface topography prevents complete wetting, resulting in composite liquid-solid-gas interfaces (Figure 2.2c). The apparent contact angle can be calculated by the equation:

$$\cos\theta = f_1(\cos\theta_0 + 1) - 1 \tag{2.3}$$

Where f_1 denotes the area fraction of liquid-solid surface contact.

In textile science, wetting behavior exhibits fundamentally different characteristics depending on surface morphologies. When textiles undergo chemical surface treatments that enable complete liquid penetration, the Wenzel model appropriately describes the resulting wetting phenomena[44]. This model accounts for enhanced wettability through surface roughness amplification, where liquid intimately contacts all surface asperities. Conversely, textiles engineered with nanostructures that trap air pockets demonstrate Cassie-Baxter wetting behavior, characterized by composite solid-liquid-air interfaces[44]. In such cases, the inability to achieve complete wetting surface from the persistence of nanoscale air gaps beneath the liquid phase.

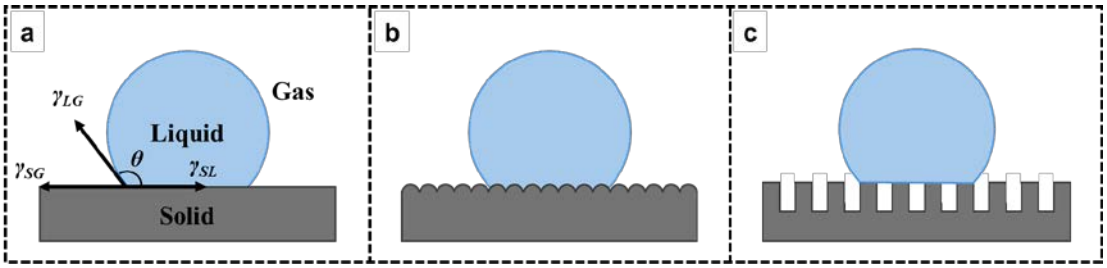

Figure 2.2 Wetting states of liquid on different solid surfaces. (a) Young's model. (b) Wenzel model. (c) Cassie-Baxter model.

Directional liquid transport in textiles is fundamentally governed by capillary effects after wetting behavior, particularly through the diameter gradient mechanism. The underlying principle originates from capillary action in microscale conduits. Capillary tubes refer to tubes with very small diameter. When these narrow tubes are

immersed in a liquid, it can be observed that the liquid in the capillary tubes are lower or higher than the surrounding liquid level[45]. This is driven by the intermolecular adhesion (F_1, solid-liquid interaction) between the solid and liquid, as well as the cohesion (F_2, liquid-liquid interaction) within the liquids[46]. When the surface energy of capillary tube exceeds the surface tension of the liquid ($F_1 > F_2$), the resulting contact angle (θ) becomes less than 90°, forming a concave meniscus that elevates the liquid column (Figure 2.3a). Conversely, when the surface energy of capillary tube is lower than the surface tension of the liquid ($F_1 < F_2$), θ exceeds 90°, creating a convex meniscus that depresses the liquid level (Figure 2.3c). The transitional state ($F_1 = F_2$, θ = 90°) yields a planar interface with no net liquid displacement (Figure 2.3b). It has been confirmed that the height to which the liquid level rises in the capillary tube is related to the difference between F_1 and F_2, as well as the diameter of the capillary tube. The height of capillary rise (h) exhibits a positive correlation with both the force differential ($\Delta F = F_1 - F_2$) and the inverse of radius of the capillary tube (r). As described by the Jurin's law[47, 48]:

$$h = \frac{2\gamma \cos\theta}{\rho g r} \tag{2.4}$$

Where h is the liquid height, γ represents surface tension of the liquid, θ is the contact angle, ρ is the mass density of the liquid, g is the gravitational acceleration, r is the tube radius. This relationship demonstrates that narrower capillaries (smaller r) and stronger adhesive-cohesive force imbalances (lager ΔF) synergistically enhance liquid elevation.

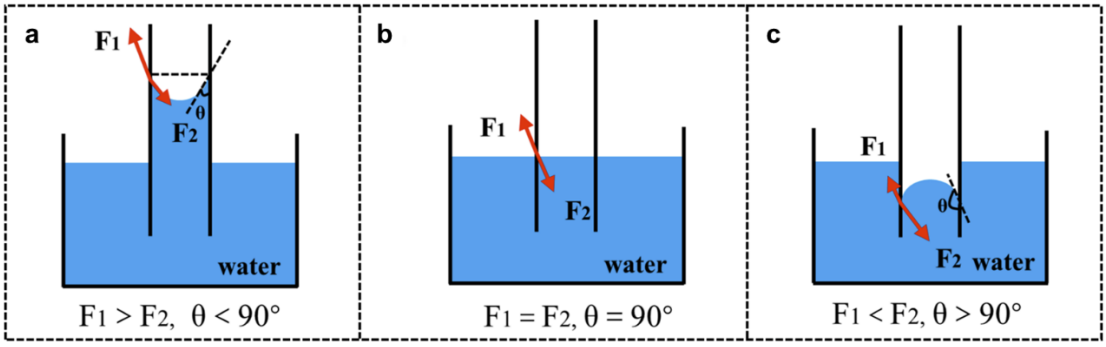

Figure 2.3 The capillary effect. (a) The water level rises when $F_1 > F_2$. (b) The plane meniscus when $F_1 = F_2$. (c) The water level descends when $F_1 < F_2$.[46]

Mass transport analysis demonstrates that capillary action and atmospheric pressure differentials serve as the primary diving forces for liquid transport in porous media[49]. In textile systems, structural porosity plays a vital role in directional liquid transport[50, 51]. The capillary diameter gradients effect can be enhanced through two primary approaches: (1) establishing a controlled wettability gradient via surface modification or multi-layer composition, which increasing ΔF in the textiles; (2) engineering a progressive reduction in pore size across the fabric (building narrower r). These two strategies build asymmetric capillary forces in different areas of the textiles, enabling a continuous directional liquid transport along fabrics.

2.1.2 Constructing Wettability Difference on Textiles

Building wettability difference (or surface energy gradients) across distinct regions of a textile has emerged as a primary strategy for engineering directional liquid transport fabrics. Directional liquid flow textiles prepared by this method allow liquid directionally to be transported from the more lyophobic side to the more lyophilic side while effectively suppressing reverse flow[52, 53]. This directional transport property is

mainly driven by two key forces: (1) Laplace pressure, arising from curvature asymmetry, and (2) capillary forces, governed by wettability contrast[54, 55]. Based on their wettability profiles, such fabrics are classified into two principal categories[8]. One is Janus wettability textiles, featuring abrupt, binary wettability boundaries[19, 56]. The other one is wettability gradient textiles, exhibiting continuous surface energy variation[57, 58]. Both designs control fluid flow via interfacial energy gradients despite different spatial wettability distributions.

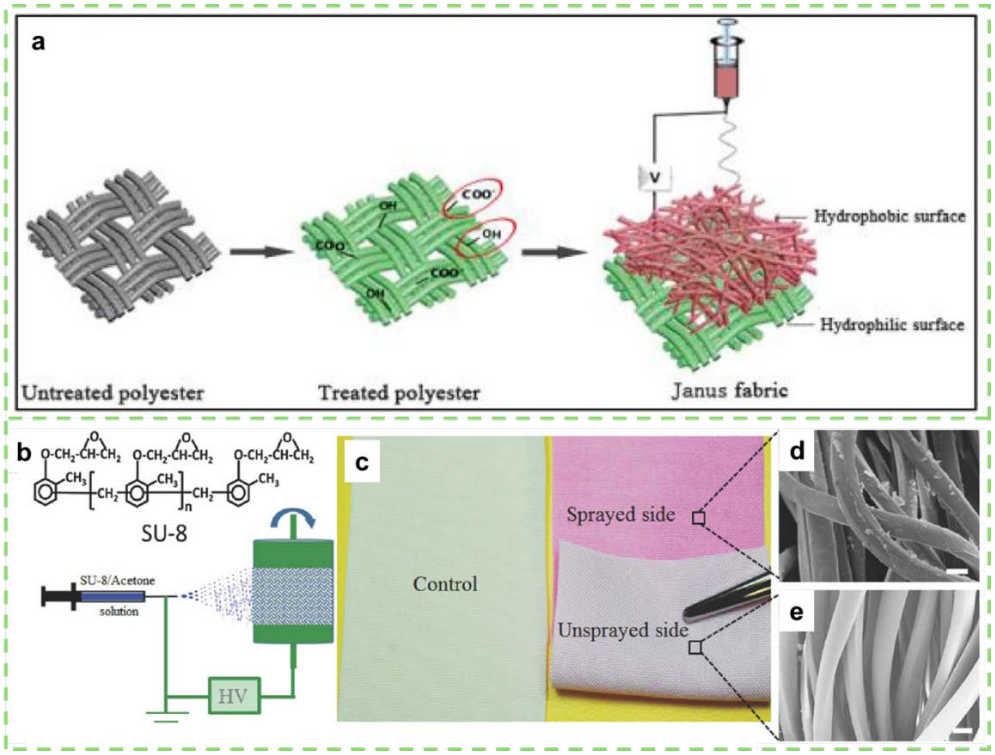

Figure 2.4 Methods for preparing Janus wettability textiles. (a) Schematic diagram illustrating the fabrication procedure of the Janus fabrics by electrospinning.[59] (b) Schematic diagram illustrating the fabrication procedure of the Janus fabrics by spray coating; (c) photos of untreated side of polyester fabric (control) and treated side of fabric (a red dye was added to finishing agent to indicate the coating layer); (d,e) SEM images of the electrosprayed and un-electrosprayed fabric sides (scale bar, 20 μm).[6]

Janus wettability textiles are typically constructed through the integration of two layers of textiles with different wettability properties. Electrospinning has emerged as a particularly convenient fabrication method for realizing such Janus wettability textiles. In 2019, Huang et al[59] prepared a Janus fabric via electrospinning technique (as shown in Figure 2.4a). Polyester fabric was first treated with sodium hydroxide (NaOH) to increase the content of active groups, thereby enhancing its hydrophilicity. Then, a layer of hydrophobic polystyrene (PS) was deposited on the hydrophilic polyester via electrospinning. By tuning the thickness of hydrophobic layer, the fabric showed a directional water transport feature. Similarly, Chen et al.[60] developed a directional liquid transport nonwoven by electrospinning for self-driven lithium extraction. A layer of hydrophobic polyvinylidene fluoride (PVDF) containing Li-ion sieve particles was deposited on a cotton layer. After laminating, a composite asymmetric nonwoven (CAN) was prepared. Water containing Li ions can be directionally transported from the hydrophobic PVDF layer to the hydrophilic cotton layer, absorbing Li ions in the hydrophobic layer.

An alternative approach for preparing Janus wettability textiles involves finishing techniques, particularly single-side spray coating. This method typically deposits a hydrophobic layer via spray coating onto a hydrophilic textile substrate. By controlling the thickness of coating precisely, the optimized directional liquid flow performance could be achieved. Compared to electrospinning techniques, this spray coating approach offers significantly greater scalability for industrial production. A directional water transport fabric prepared by electrospraying a thin layer of hydrophobic SU-8 on

to a hydrophilic polyester was developed by Zeng et al. (as shown in Figure 2.4b-e)[6]. The directional liquid transport property was tested using moisture management tester (MMT) and was durable against repeated washing. Peng et al.[61] presented a directional sweat transport window based on Janus fabric for sweat sensors. A directional sweat transport fabric prepared by single side spray coating was integrated between two hydrophilic cotton layers. In this all-fabric-based sweat sensor, the spontaneous unidirectional liquid transport capability of the Janus textile, combined with the high hydrophobicity of the sensing zone, ensured continuous delivery of fresh sweat to the electrochemical interface for real-time monitoring. In addition to unidirectional water transport fabrics, Janus wettability textiles can also function as directional oil-transport materials. Zhou et al.[62] demonstrated a directional oil transport Janus fabric prepared by electrospraying. The prepared material demonstrated different wettability on two sides. One side of this fabric was hydrophilic and oleophilic, and the other side was hydrophilic and oleophobic. This property enabled directional oil transport both in the air and under water, which could be extended to develop an oleophilic/oleophobic diode.

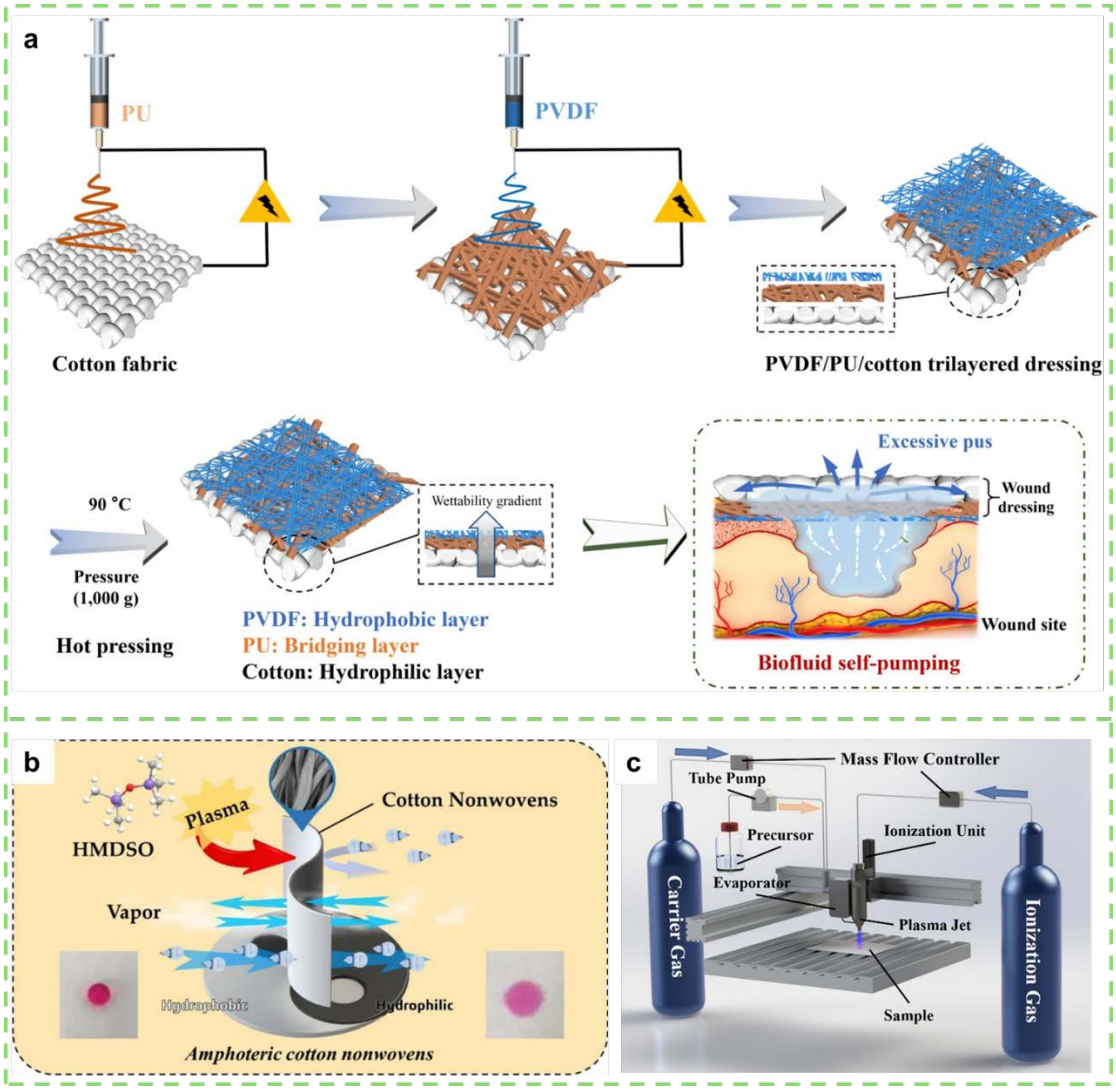

Figure 2.5 Methods for preparing textiles with gradient wettability gradient. (a) Schematic diagram of fabricating the PVDF/PU/cotton trilayered dressing via electrospinning.[63] (b) Amphoteric cotton nonwovens prepared by one side surface modification; (c) Schematic diagram of the atmospheric pressure plasma system operating with computer-controlled motion and velocity of the plasma jet.[16]

The Janus wettability textiles present challenges in balancing the liquid transport capacity in the positive direction and prevention of water penetration in the reverse direction[20]. Textiles with gradient wettability offer an effective solution to these challenges. These fabrics are typically engineered either by incorporating an interlayer between two layers of distinct wettability properties[20, 64] or applying single side surface

treatments to create continuous wettability variation along the thickness direction of fabrics[65]. Liu et al.[63] developed a trilayered fabric with gradient wettability prepared by electrospinning for wound dressing (Figure 2.5a). A bridge polyurethane (PU) layer was introduced between hydrophobic PVDF layer and hydrophilic cotton layer. The bridge layer endows the dressing with a wettability gradient which effectively prevents liquid backflow. A similar three-layer wettability gradient electrospinning structure was also implemented in medical protective clothing to prevent blood penetration[66]. Pu et al.[16] presented a directional water transport cotton nonwovens with gradient wettability prepared by single side atmospheric plasma deposition (Figure 2.5b-c). The treated cotton nonwoven exhibited excellent directional liquid transport properties while maintaining other essential performance characteristics.

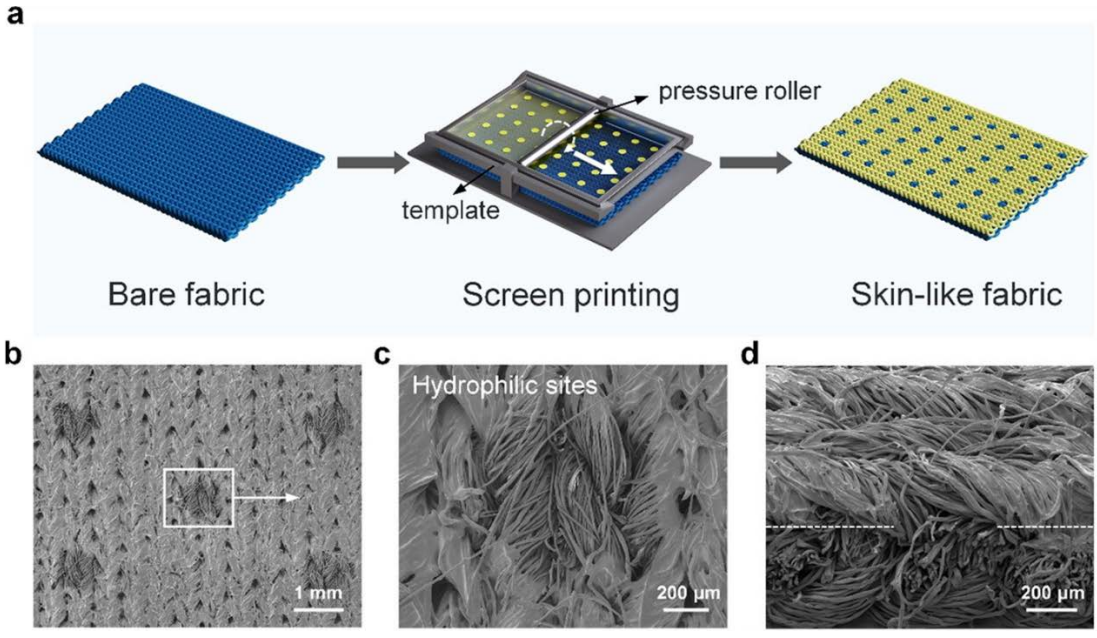

Figure 2.6 Distinctive pattered surface technique for preparing the directional liquid flow textiles. (a) Preparation of skin-like fabric via patterned screen printing. (b) SEM image of the fabric from the coated side and its (c) enlarged image. (d) Cross-section image of the skin-like fabric.[67]

Apart from these two approaches for creating wettability difference in textiles, a distinctive pattered surface technique has emerged as an alternative strategy[7, 68]. This method typically employs spray coating or screen printing methods to achieve selective surface modification (see Figure 2.6). The prepared fabrics feature a fully hydrophilic top side, while the back side exhibits a partially hydrophobic pattern rather than complete hydrophobicity. Such patterned textiles enable accelerated liquid transport from the patterned (partially hydrophobic) side to the hydrophilic side through the hydrophilic wettability channels within the hydrophobic patterned regions[67, 69]. Yang et al.[70] printed commercial hydrophobic agents onto the surface of hydrophilic polyester fabrics via different patterned printing screen. The researchers systematically investigated the effects of knitting structure and hydrophilic ratio of the finishing pattern on directional water transport efficiency. The research revealed that the fabric with a rib air structure and 69% hydrophilic area ratio has the best moisture management property. Zhao et al.[71] also printed a commercial hydrophobic agent onto a nano-ZnO coated cotton fabric via a honeycomb patterned printing screen. The treated fabric exhibited a high directional liquid transport property as well as high thermal conductivity, enabling the fabric to meet the demand for a comfortable microclimate to the human body.

2.1.3 Building Structural Difference on Textiles

The other method to develop the directional liquid transport textiles is building a structural difference on both sides of the fabrics. According to Jurin's law[47, 48], a smaller diameter of capillary tube increased the capillary force. Thus, fabrics with different pore

sizes between two sides of the fabric exhibit directional liquid transport property. Liquid tends to transport from the larger pore size side to the smaller pore size side but not vice versa[72, 73]. The directional liquid transport is driven by the Laplace pressure due to the curvature and size difference[33].

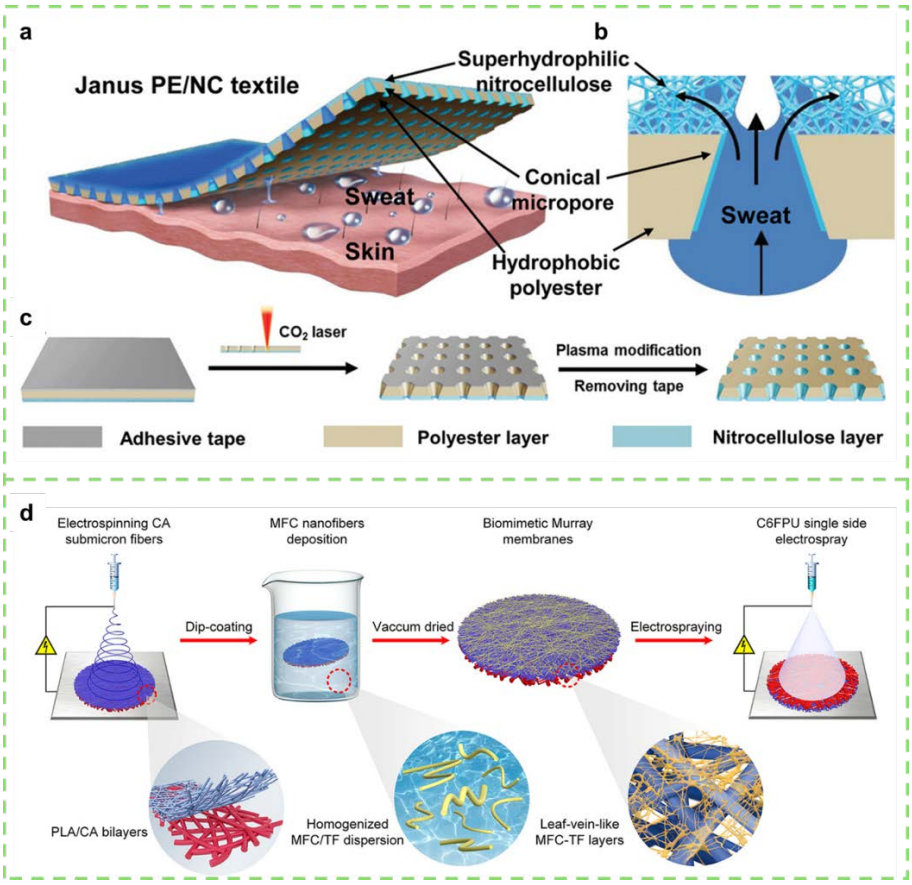

Figure 2.7 Directional liquid flow textiles prepared by building structural difference. (a) Schematic illustrating the sweat output pathways of the human body covered with the directional liquid flow fabric with structural difference; (b) Conical micropores across the directional liquid flow fabric; (c) Fabrication of the directional liquid flow fabric with structural difference. The regular micropore array is drilled in the textile via laser drilling, then the drilled textile is modified with plasma.[74] (d) Schematic illustration of the fabrication of biomimetic porous Murray membranes by elecrospinning.[37]

Based on this principle, a bioinspired directional liquid flow membrane was demonstrated by Dai et al.[74] Conical micropores were developed on the hydrophobic polyester membrane via laser ablation (Figure 2.7a-c). Liquid could be directionally transported from the larger pore side to the smaller pore side and spread on the hydrophilic nitrocellulose layer. Wang et al.[37] presented a biomimetic fibrous Murray membranes by compositing three layers of membrane with varies pore size (Figure 2.7d). This membrane showed ultrahigh directional liquid transport properties and outstanding quick-dry properties. In addition to the above-mentioned textiles, fully hydrophilic directional water transport fabrics without chemical finishing have been successfully developed. As demonstrated by Chen et al. in 2010[75], an innovative all-knitted “Plant Cool” fabric was engineered. By mimicking the branching structure of a plant, the fabric had less branches on one side and more branches on the other side making a difference in pore size on two sides of the fabric. The directional water transport fabric possessed a significantly greater initial water absorption rate, one-way transport capacity and air permeability. This purely structural approach achieved directional liquid transport without chemical treatments, establishing a new paradigm for next-generation sportswear textiles.

2.1.4 Other Directional Liquid Flow Textiles

Despite extensive research on textiles with directional liquid transport capabilities, conventional directional flow textiles still exhibit significant limitations in practical applications. Most traditional directional liquid transport fabrics feature fully hydrophilic outer surfaces, which tend to become heavy, sticky, and clammy upon

saturation, potentially compromising wearer comfort and hygiene. Meanwhile, all hydrophilic outer surfaces lead to the fabrics easily being contaminated. A novel class of directional liquid flow textiles with hydrophobic outer layer has emerged to address these limitations effectively.

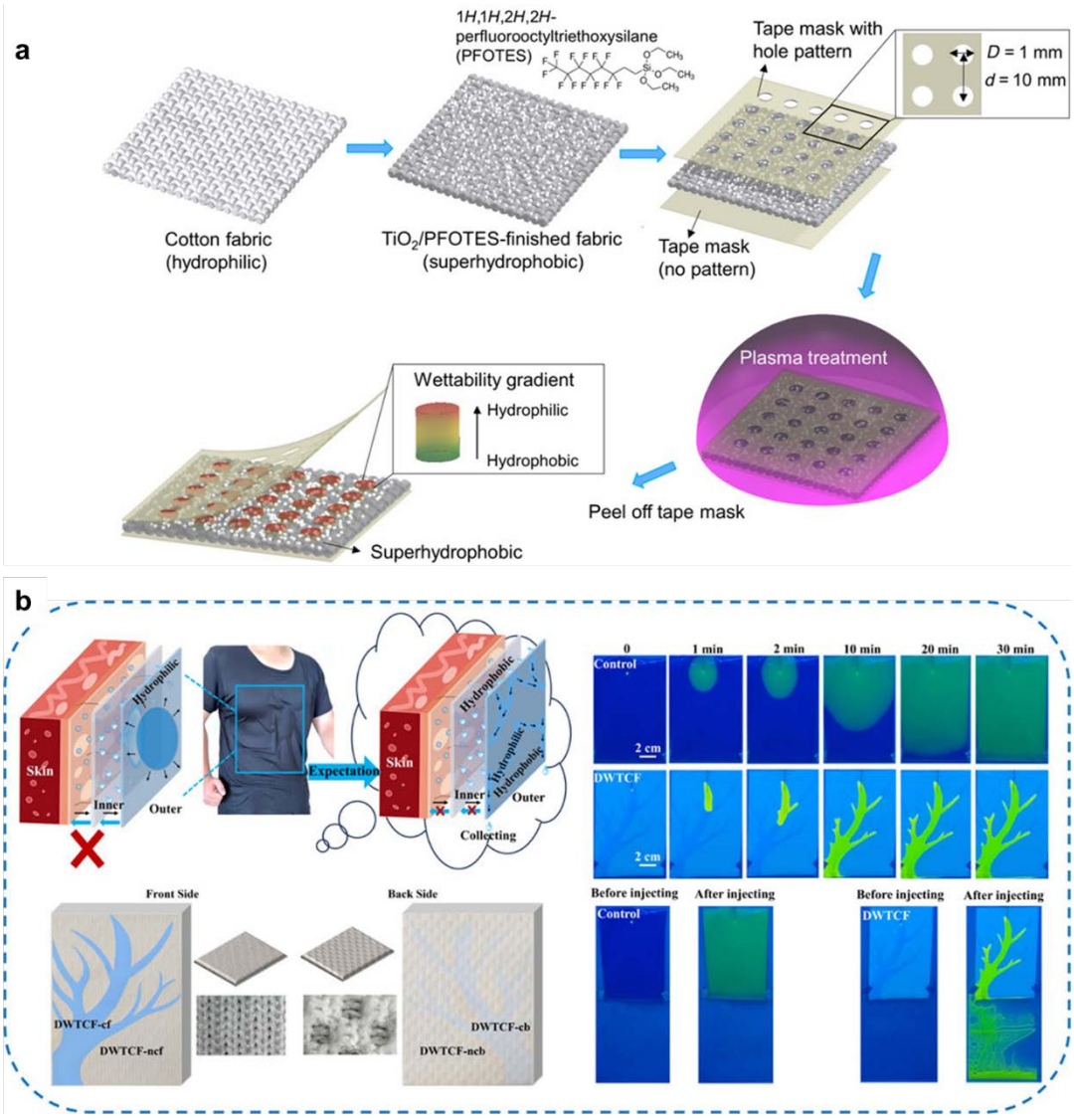

Figure 2.8 Other directional liquid flow textiles. (a) Schematic illustration and fabrication process of a skin-like fabric with both directional water transport and water repellency.[24] (b) In-plain directional liquid transport textiles prepared by screen printing.[76]

Lao et al.[24] developed a novel “skin-like” fabric with a hydrophobic outer layer in 2020 (Figure 2.8a). Human skin is an ideal directional material as it secrets liquid sweat and protects the body from external liquid contaminants. By mimicking the human skin, wettability channels with gradient wettability were constructed on a hydrophobic cotton fabric by selective plasma treatment. The gradient wettability channels act as sweat glands on human skin, directionally transporting liquid water from the skin side of the fabric to the outer side. Then the transported water accumulated on the outer surface and dripped down instead of spreading. Such “skin-like” fabric also can resist external bulk water due to the most hydrophobic outer surface. Subsequently, Zou et al.[77] improved the fabric by designing wettability gradient channels with different geometric shapes, significantly enhancing its directional water transport efficiency. Later, Ma et al.[78] applied Cu^{2+} onto the “skin-like” fabric to integrating antibacterial properties, providing a versatile and practical approach for developing fabrics that actively manage sweat diffusion from human skin while simultaneously inhibiting microbial growth, thereby preventing bacterial infections. Similarly, Peng et al.[79] demonstrated an artificial sweating skin (i-TRANS) with the directional water transport and water repellent properties by selective spray coating poly(dimethylsiloxane) (PDMS) on a normal fibrous wicking material. The gradient wettability channels on the substrate enable transporting liquid directionally without trapping undesired excess water. This fabric was used as an artificial skin for different types of devices, including hot plate and manikin.

The directional liquid flow textiles primarily facilitate liquid transport through the thickness direction of the fabrics (through-plain direction). However, achieving in-plain directional water transport with rapid lateral diffusion on surface of the fabric is also critical. To realize this in-plain directional liquid flow capability, wettability gradients or structural variations should be engineered across distinct regions of the surface of the textiles. Such in-plain directional liquid flow fabrics are particularly valuable for sportswear applications, where they actively regulate thermal and moisture comfort of the human body during high-intensity sweating conditions.

To investigate the methods for preparing in-plain directional flow textiles, Chen et al.[80] coated hydrophobic agents with different concentrations along a knitted stripes by screen printing. Experimental results confirmed that water droplet could be rapidly transferred from hydrophobic section to hydrophilic section of stripe. This research provided foundational guidelines for preparing textiles with controlled in-plain directional liquid transport capabilities. Liu et al.[81] referenced the directional liquid transport mechanism of desert beetles, cacti, nepenthes and rivers, constructing different hydrophilic wettability shapes on the surface of knitted fabrics with various structures. The coated fabrics showed excellent in-plain directional liquid transport properties as well as ideal moisture and air permeability for wearing. In 2024, Wang et al.[76] printed a hydrophobic agent on plant cool fabric to build branched hydrophilic flow paths (Figure 2.8b). Compared to traditional fabrics, the liquid is discrete and flows just in the treelike channel of the directional water transport and collection fabric, being transported continuously, collected and removed from the end of the fabric. The

fabric was dry and light due to this effect, providing a novel strategy for the design and development of sweat management sports garments.

2.1.5 Applications for Directional Liquid Flow Textiles

Directional liquid flow textiles have emerged as promising materials for personal thermoregulation and moisture management, owing to their ability to rapidly wick sweat from the skin-contact layer to the outer surface, thereby maintaining a dry and cool microclimate adjacent to the skin[82]. Beyond these inherent comfort-enhancing properties, the intrinsic wettability asymmetry of these fabrics enables diverse fluid manipulation applications, including wound dressing (directional exudate removal), oil-water separation (selective permeability), atmospheric moisture harvesting (fog collection), and humidity sensing (moisture-responsive electrical signals).

Pi et al.[83] developed a Janus fibrous wound dressing functionalized with TiO_2 nanoparticles to achieve directional exudate transport. The asymmetric wettability of the membrane enabled continuous pumping of wound fluids from the injury site to external environment, maintaining an optimal low-moisture environment for tissue regeneration. Furthermore, the immobilized TiO_2 nanoparticles provided effective antibacterial activity, synergistically enhancing wound healing efficiency. Chi et al.[22] presented an amphibious Janus fabric for oil-water separation. By coating superhydrophobic-oleophobic and superamphiphobic materials on two sides of the fabric respectively, the asymmetric oil wettability enables unidirectional oil penetration through the textile while blocking water permeation, thereby achieving highly efficient

oil-water separation. Huang et al.[23] prepared a Janus fabric with asymmetric water wettability by electrospinning, achieving a high water harvesting capacity. Wang et al.[21] integrated electrically conductive metal wires on Janus fabric and developed a high response moisture sensor for making “smart” clothing.

The reviewed studies have made substantial progress in developing directional liquid transport textiles through two primary strategies, engineering wettability gradients (e.g., hydrophobic/hydrophilic patterning) and designing structural asymmetries (e.g., pore gradient architectures), often synergistically combining both approaches. These fabrications have achieved remarkable unidirectional transport efficiencies while maintaining breathability. Despite these advances, current directional liquid transport textiles predominantly remain conventional all hydrophilic outer layers, which suffer from the limitations of moisture saturation and skin adhesion (as discussed in section 2.1.4). Although “skin-like” fabric designs have been proposed to make up for the shortcomings, most of these materials rely on fabrication techniques such as selective plasma treatment, resulting in prepared fabrics with insufficient stability and limited scalability. A critical research gap remains in developing cost-effective manufacturing approaches capable of producing fabrics that exhibit directional liquid transport properties and hydrophobicity which repels external water.

2.2 Temperature-responsive Reversible Wettability Materials

Temperature-responsive textiles represent a class of advanced smart materials capable of dynamically and reversibly modulating their wettability, morphological

structure, and thermal insulation properties in response to thermal stimuli[15, 30]. This adaptive behavior enables precise control over heat dissipation and moisture permeability, allowing these textiles to actively regulate personal thermal and moisture comfort during exposure to extreme or rapidly fluctuating temperatures[84]. Beyond comfort enhancement, such smart textiles demonstrate multifunctional utility across diverse domains, including atmospheric moisture harvesting[85, 86], selective oil-water separation[87], soft robotic actuation systems[88], and drug delivery[89]. The unique combination of physiological protection and energy conservation has generated significant interdisciplinary research interest in recent years. Temperature-responsive textiles are typically fabricated through two primary approaches: surface functionalization of conventional textiles via coating or grafting temperature-responsive polymers[90, 91] (e.g., PNIPAAm, PDMAPS), or electrospinning blended solutions containing both temperature-responsive and structural polymer components[92]. The coating/grafting method enables precise localization of responsive properties at fiber surfaces, while electrospinning allows for tunable bulk responsiveness through controlled phase distribution in composite nanofibers. The temperature-responsive polymers discussed herein can be classified into two fundamental categories based on their phase transition behavior[93-95]: lower critical solution temperature (LCST-type) materials (Figure 2.9a) and upper critical solution temperature (UCST-type) materials (Figure 2.9b). This section systematically reviews both polymer classes, including their distinctive thermal responsiveness mechanisms and recent advancements in textile applications.

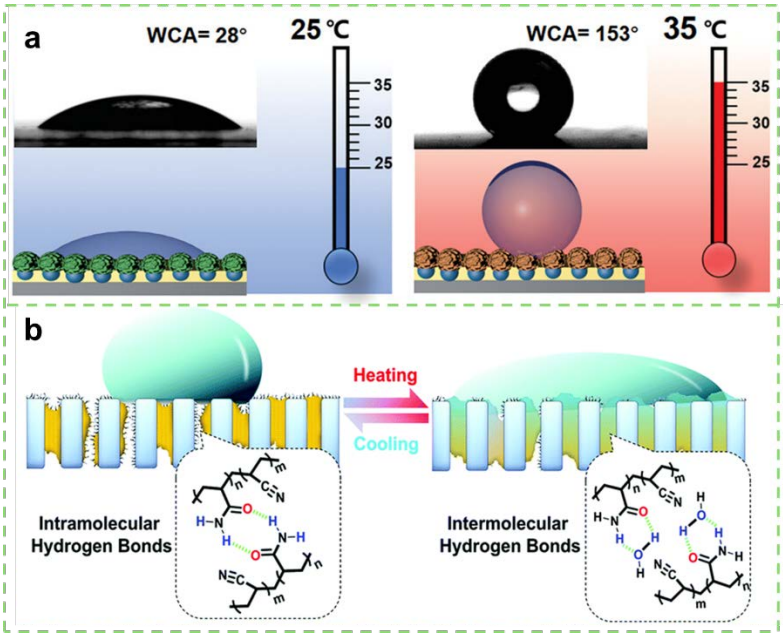

Figure 2.9 The illustration of (a) LCST-type materials[84] and (b) UCST-type materials[28].

2.2.1 LCST-type Polymers

LCST-type polymers represent a class of intelligent temperature-responsive materials that demonstrate remarkable phase transition behavior in aqueous environments[32, 96]. These polymers maintain a distinctly hydrophilic character when the ambient temperature remains below their critical transition point (T < LCST), exhibiting strong hydrogen bonding with water molecules that results in extended polymer chain conformations and excellent solubility[29, 97]. However, when the temperature exceeds this critical threshold (T > LCST), the polymers undergo a dramatic and reversible transformation to a hydrophobic state, driven primarily by entropy-dominated dehydration of the polymer chains[98]. This unique thermal responsiveness stems from the delicate balance between polymer-water hydrogen bonding and hydrophobic interactions of the polymer backbone[29]. The sharp transition

between these two distinct states typically occurs within a narrow temperature window making LCST-type polymers particularly valuable for applications requiring precise thermal control of surface properties. In textile applications, this behavior enables the creation of smart fabrics that can autonomously regulate moisture permeability and heat transfer in response to environmental or body temperature fluctuations, offering significant potential for advanced personal thermal management systems[84].

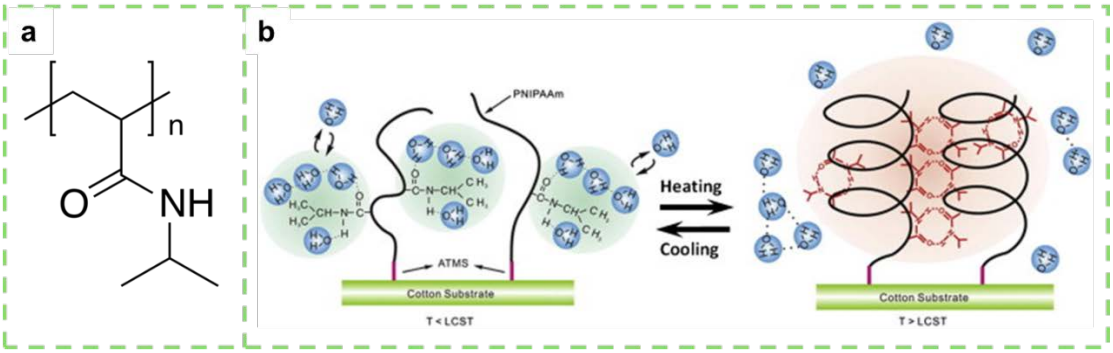

Figure 2.10 LCST-type PNIPAAm temperature-responsive materials. (a) Chemical structure of PNIPAAm. (b) Illustration of hydrophobic-hydrophilic transition of PNIPAAm grafted cotton substrate with the temperature variation[91].

The most extensively studied LCST-type polymer is PNIPAAm (as shown in Figure 2.10a), owing to its sharp transition temperature near physiological temperature of human (approximately 32°C)[31, 99]. The temperature-responsive property of this polymer is caused by the competition of the entropic and enthalpic contributions to the free energy of PNIPAAm chains. When temperature is lower than 32°C, the enthalpic contributions overtake the entropic contributions, the hydrophilic C=O and N-H groups in the molecular chain interacting easily with water molecules, resulting in the surface of the polymer hydrophilic. But when the temperature becomes higher (above the

LCST), the entropic contributions are much more. The molecular chain of PNIPAAm tends to form intramolecular hydrogen bonding between C=O and N-H groups, thus the polymer becomes hydrophobic (shown in Figure 2.10b)[99, 100].

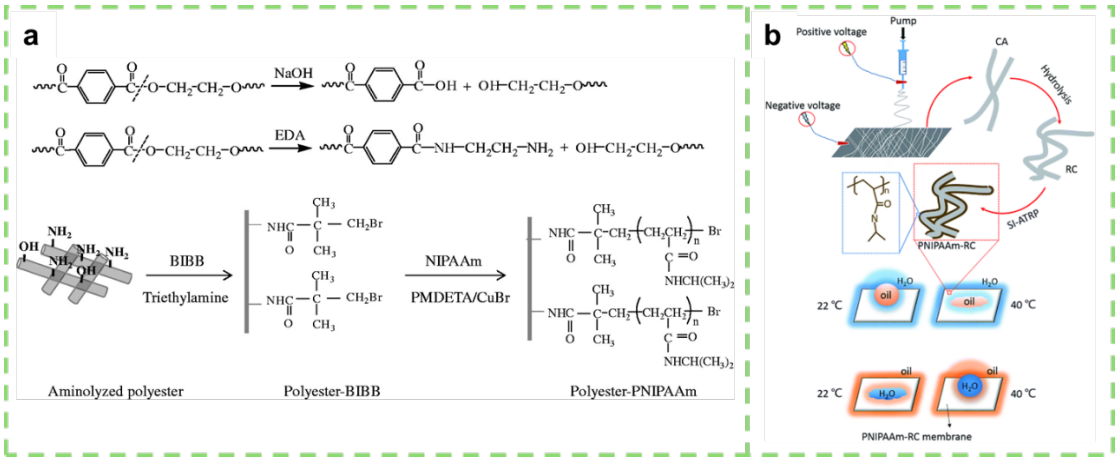

Figure 2.11 Preparation methods for LCST-type temperature-responsive fabrics. (a) The scheme of aminolysis and PNIPAAm grafting on polyester surfaces[101]. (b) The fabrication process of PNIPAAm-RC nanofibers undergoing electrospinning[87].

PNIPAAm have been coated or grafted onto the surface of various fabrics for preparing temperature driven smart textiles. Yang et al.[91] in-situ grafted PNIPAAm on a cotton fabric via atom transfer radical polymerization (ATRP). They studied the interaction between water and grafted PNIPAAm using the solid-state nuclear magnetic resonance (NMR) technique. Then, Wu et al.[101] developed a temperature-responsive polyester textile with switchable surface wettability. The pristine polyester fabric was first subjected to surface amination through alkali deweighting to introduce additional reactive groups. Subsequently, PNIPAAm was grafted onto the modified polyester surface via ATRP (shown as Figure 2.11a). This smart fabric exhibited reversible water contact angle changes, transitioning from 0° to 120° when the temperature exceeded

the LCST of PNIPAAm. PNIPAAm has also been copolymerized with other functional materials and grafted onto textile substrates to achieve additional properties beyond temperature-responsiveness. Chen et al.[90] reported a thermo-responsive wound dressing prepared by grafting chitosan and PNIPAAm onto polypropylene (PP) nonwoven fabrics via plasma polymerization. In daily use, the PNIPAAm grafted wound dressing is hydrophobic at the skin temperature above the LCST, keeping the tissue connected well to wound dressing layer due to the moist condition. When changing wound dressings requiring material-tissue separation, applying low-temperature treatment (below the LCST of PNIPAAm) renders the polymer hydrophilic, causing water absorption of the wound dressing layer. This enables gentle removal of the dressing from the wound without damaging newly regenerated skin tissue[90].

Other studies have prepared temperature-responsive nanofiber membranes via solution electrospinning by blending PNIPAAm with additional structural polymers. Gu et al.[92] reported a thermo-responsive biocompatible nanofiber membrane with switchable wettability property created by electrospinning in 2010. PNIPAAm and poly(L-lactide) (PLLA) was used for preparing the nanofiber membrane, and the films possessed a “bead on string” structure. The membrane could switch from superhydrophilic (contact angle was about 20°) to superhydrophobic (contact angle was higher than 120°) when the temperature increased from 20°C to 50°C. Furthermore, the electrospinning process and addition of PLLA did not change the thermo-sensitivity of PNIPAAm. The nanofiber membrane had properties of tunable surface morphologies and better biocompatibility. Wang et al.[87] demonstrated an electrospun temperature-

responsive nanofiber using PNIPAAm-modified regenerated cellulose (RC) (see Figure 2.11b). This membrane exhibited a smart controllable oil-water separation function. The oil-water separation mode could be switched between oil-removal and water-removal by simply changing the temperature.

In addition to PNIPAAm, other polymers such as poly(diethylene glycol monomethyl ether methacrylate) $PMEO_2MA$[102] and poly(oligo(ethylene glycol) methacrylate) POEGMA[103] also exhibit LCST behavior. These materials have similarly been utilized to create temperature-responsive smart surfaces. However, LCST-type polymers exhibit wettability that correlates positively with temperature, making it challenging to achieve increased contact angles upon heating. This inherent limitation constrains their application in systems requiring an inverse wettability response (i.e., enhanced hydrophobicity at lower temperatures). For textile applications, ideal thermoregulatory behavior would involve enhanced hydrophilicity at elevated temperatures (e.g., during exercise) to promote evaporative cooling, coupled with increased hydrophobicity at reduced temperatures to improve thermal insulation.

2.2.2 UCST-type Polymers

UCST-type polymers exhibit opposite properties from LCST-type polymers. They show hydrophobicity at lower temperatures (T < UCST) and exhibit hydrophilicity when temperature exceeds their UCST. The unique inverse thermal response enables UCST-type polymers to be widely applied to textile-based thermal management where conventional LCST systems prove inadequate. Despite this potential, UCST-type

polymers remain underexplored due to synthesis challenges and instability in transition behavior under varying environmental conditions[26]. Currently, UCST-type polymers are classified into two categories based on their molecular chain composition[104]: zwitterionic polymers and non-ionic polymers, distinguished by the presence or absence of ionic functional groups.

Zwitterionic polymers

Zwitterionic UCST-type polymers currently represent the most widely studied and applied category of temperature-responsive polymers exhibiting upper critical solution temperature behavior. These materials have been successfully grafted onto textile surfaces to develop smart fabrics with switchable wettability properties, demonstrating significant potential for oil-water separation[105] and advanced personal moisture management applications[106-108]. Among these, Poly(sulfobetaine), including poly(pentafluorophenyl acrylate) (pPFPA) and PDMAPS[25, 27] constitute a prominent subclass of zwitterionic polymers characterized by their molecular chains containing both cationic and anionic groups. The temperature-dependent wettability switching of these polymers originates from reversible association and dissociation between these oppositely charged groups in response to thermal stimuli[105, 109]. Wang et al.[106] engineered a reversible water transport diode by coating UCST-type PDMAPS and LCST-type $PMEO_2MA$ onto opposite sides of a cotton fabric. Since these temperature-responsive polymers share similar transition temperatures (26–27°C), the wettability of the two fabric sides remained consistently opposed. At temperatures below the transition threshold, liquid underwent directional transport from the UCST-

functionalized side to the LCST-functionalized side. Conversely, when the temperature exceeded the critical point, the transport direction reversed, with liquid moving from the LCST side to the UCST side. This bidirectional pumping capability endowed the fabric with advanced thermoregulatory properties: in hot environments, it promoted skin cooling through directional liquid transport and subsequent evaporation, while in cold conditions, it minimized heat loss to prevent sudden temperature drops (Figure 2.12a). Qi et al.[105] developed a temperature-responsive cotton textile functionalized with PDMAPS for switchable oil-water separation. Below the UCST, the coated fabric exhibited chain collapse and hydrophobic characteristics, enabling selective oil transport while blocking water permeation. When heated above the transition temperature, the polymer chains swelled into a hydrophilic state, reversing the selectivity to permit water transport while rejecting oil. This bidirectional switching behavior allowed the fabric to adaptively separate oil or water based on environmental temperature changes (Figure 2.12b).

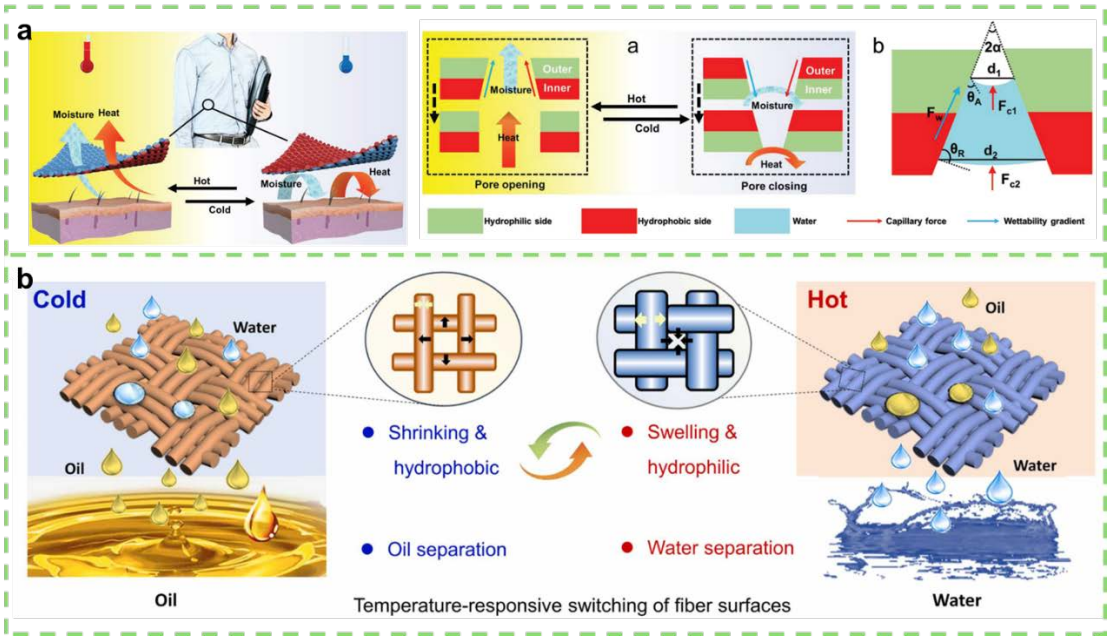

Figure 2.12 Application of UCST-type polymers on textiles. (a) UCST-type polymers modified textiles for thermal and moisture management[106]. (b) UCST-type temperature-responsive textiles for oil-water separation[105].

Despite their promise, zwitterionic polymer-based materials face significant practical limitations. A key challenge is the strong dependence of their phase transition temperature on both the polymer concentration and the surrounding electrolyte concentration[93, 109]. This sensitivity creates reliability issues in real-world applications. For medical uses like wound dressings or wearables, variations in human body fluid composition and health status[110-112] can unpredictably alter the transition behavior, resulting in inconsistent performance. Similarly, in environmental applications such as oil-water separation, the complex and variable ionic composition of seawater or industrial wastewater often leads to unstable operation. Furthermore, most current zwitterionic polymers offer limited tunability of their transition temperatures and

inability to adapt to specific application needs, significantly constraining their practical utility.

Non-ionic polymers

In contrast to zwitterionic UCST type polymers, non-ionic UCST type polymers do not include ions in their molecular chains[113]. Instead, their temperature-responsive wettability switching arises from the dynamic association and dissociation of intermolecular and intramolecular hydrogen bonds between hydrogen donors and acceptors within their structure[114, 115]. While several non-ionic UCST polymers, such as poly(N-acryloylglycinamide) (PNAGA)[116], poly(N-acryloylglycinamide-co-N-acetylacrylamide) (PNAcAAm)[117], and poly(acrylamide-co-acrylonitrile) [poly(AAm-co-AN)][118], have been explored, their complex synthesis has limited widespread research. A significant advancement occurred in 2012 when Seuring and Agarwal[109] developed a universal synthetic strategy for these materials, revitalizing interest in their design and applications. In their study, they proposed three key requirements for synthesizing non-ionic UCST type polymers with tunable transition temperature: (1) There must be groups which can form reversible hydrogen bonds in molecular chains; (2) The ionic groups introduced during the preparation process should be minimized; (3) The hydrophilic-hydrophobic balance of the polymer must be controlled to allow tuning of the phase transition temperature. Among these non-ionic UCST type polymers, poly(AAm-co-AN) has emerged as particularly promising due to precise UCST tunability via comonomer ratio adjustment (Figure 2.13a) and minimal thermal hysteresis during heating/cooling cycles[114].

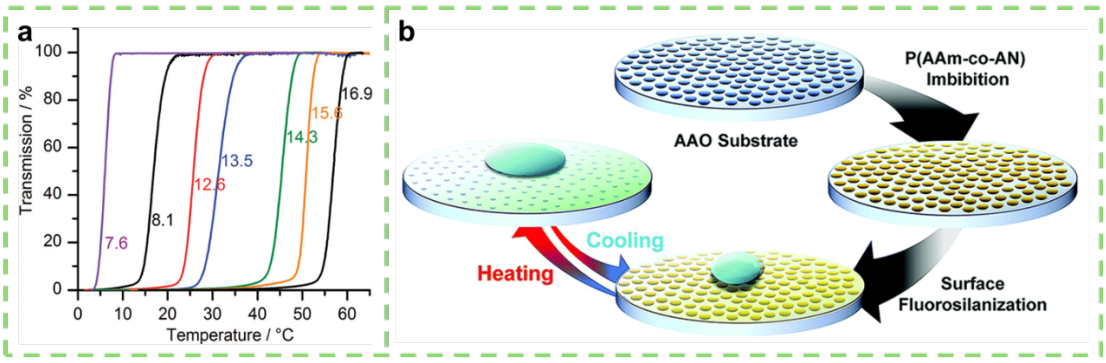

Figure 2.13 Tunability transition temperature of poly(AAm-co-AN) and the application. (a) Turbidity cooling curves of poly(AAm-co-AN)s with different copolymer compositions; The numbers state the acrylonitrile content in mol% (error 1.0-1.4 mol%)[109]. (b) The fabrication process of the smart surface with switchable wettability using poly(AAm-co-AN)[28].

Otsuka et al.[113] incorporated poly(AAm-co-AN) into cosmetic formulations as a temperature-responsive functional component. This polymer enables easy removal of cosmetic products through hot water washing, leveraging its hydrophilic transition at elevated temperatures. Due to the non-ionic nature of poly(AAm-co-AN), the UCST behavior of the polymer remains unaffected by sweat exposure, ensuring stable performance under physiological conditions. Chen et al.[52] built a smart surface with UCST behavior thermo-responsive property. The poly(AAm-co-AN) was coated on a porous anodic aluminum oxide plate (AAO) (Figure 2.13b). The water contact angle of the surface decreased from 103° to 60° as the temperature increased from 30°C to 80°C. The authors also found that the hydrophobic treated thermo-responsive surface had a wider response rate due to the synergistic effect from the hydrophobic coating and the poly(AAm-co-AN). However, the methodology employed in this study was limited to physically coating the polymers onto the substrate surface, resulting in mere physical

adhesion between the materials. This approach yields poor surface durability due to the absence of stronger chemical bonding. Furthermore, these approaches prove inadequate for textile applications due to the difficulty in precisely controlling the surface hydrophilic-hydrophobic balance on fibrous substrates. The complex three-dimensional structure and chemical heterogeneity of textile surfaces further exacerbate these limitations, making conventional coating techniques ineffective for achieving reliable temperature-responsive performance.

In summary, temperature-responsive materials can be classified into LCST-type and UCST-type categories based on their distinct phase transition behaviors. While UCST-type materials demonstrate greater suitability for textile applications compared to their LCST-type counterparts, their widespread adoption has been constrained by the challenge in synthesis and property instability. Non-ionic UCST-type polymers, despite offering advantages such as electrolyte-independent stability and tunable transition temperatures for broader potential applications, face significant implementation barriers in smart surface technologies, particularly in intelligent textiles, due to the difficulty in controlling the surface hydrophilic-hydrophobic balance on substrates.

2.3 Polymer Grafting Methods for Surface Modification

Surface functionalization of textiles through polymer grafting has emerged as the predominant modification technique in advanced materials engineering. Fundamentally, grafting reactions enable the synthesis of architecturally complex branched copolymers by chemically anchoring functional polymers onto substrate surfaces via covalent

bonding[119, 120]. This process typically involves the covalent bonding of side chains containing specific functional groups (e.g., hydroxyl, amine, or carboxyl moieties) to the substrates, thereby introducing new surface characteristics including enhanced hydrophilicity, electrical conductivity, or improved biocompatibility[121-123]. Unlike conventional physical coating methods that rely on weak intermolecular interactions, the covalent attachment in grafting provides interfacial stability and durability, being a critical advantage that has driven its widespread adoption in textile engineering for durable surface modifications. Based on the mechanism of molecular growth, there are three distinct grafting approaches, including “grafting-to”, “grafting-from”, and “grafting-through” methods (Figure 2.14)[124]. This section systematically presents three fundamental approaches for grafting polymers onto substrate surfaces, along with their respective procedural methodologies.

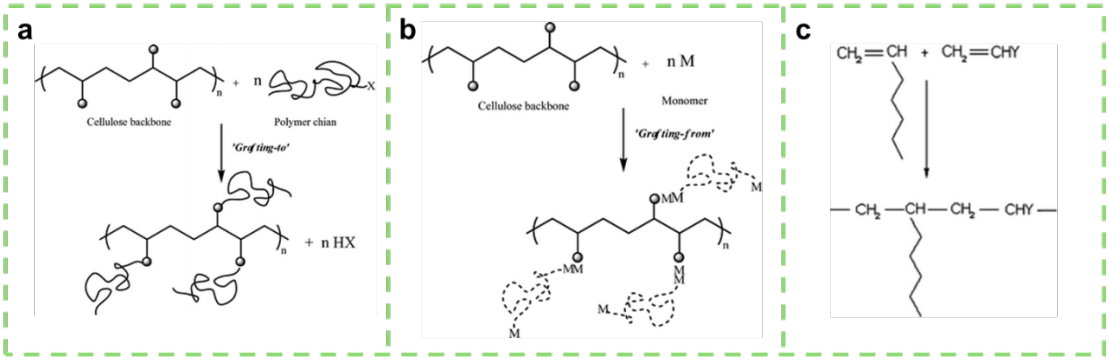

Figure 2.14 Approaches for grafting polymers onto substrates. (a) “grafting-to” approach, (b) “grafting-from” approach, and (c) “grafting-through” approach[121].

2.3.1 “Grafting-to” Approach

The "grafting-to" approach involves the covalent bonding of pre-synthesized polymer chains to substrate surfaces through targeted chemical reactions[125, 126]. This

methodology requires: (1) synthesis of end-functionalized polymers with reactive groups (e.g., -COOH, -NH_2, or -OH); (2) activation of substrate surfaces via chemical treatment or coupling agents to generate complementary reactive groups; and (3) formation of stable covalent linkages between the active groups of polymers and activated substrate surface. The process specifically proceeds through the reaction between the terminal functional groups of pre-formed polymers and the active groups present on the substrate backbone.

A superhydrophobic cotton fabric was prepared by the "grafting-to" approach[126]. Poly[(methyl methacrylate)-*b*-(trifluoroethyl methacrylate)] (PMMA-*b*-PTFMA) was first prepared via reversible addition-fragmentation chain transfer (RAFT) polymerization. Then, the prepared copolymer was grafted to the surface of a cotton fabric. The grafted fabric showed a durable superhydrophobicity and excellent stability against laundering and abrasion. Wang et al.[125] grafted quaternary ammonium compounds (QACs) onto cotton fabrics to prepare antibacterial fabrics by a "grafting-to" method. QAC polymers with functional end groups were prepared via free radical polymerization. Then, the polymers reacted with the functionalized cotton fabric, forming covalent bonding. This strategy enabled a durable antibacterial effect without significant affecting other wearable properties of the cotton fabric.

2.3.2 "Grafting-from" Approach

The "grafting-from" approach involves the direct growth of polymer chains from substrate surfaces through surface-initiated polymerization[127, 128]. This method

comprises three fundamental steps: (1) Initiation, where immobilized initiators generate active species (e.g., free radicals) that form reactive sites on the substrate; (2) Propagation, during which monomers polymerize from these surface-bound active sites, extending the grafted polymer chains; and (3) Termination, occurring either through radical recombination or chain transfer mechanisms[129]. “Grafting-from” has become the predominant technique for textile surface modification due to its ability to achieve high grafting densities, as the fully accessible of the reactive groups to the chain ends of the growing polymers[121].

Polyurethane (PU) was grafted onto cotton fabric surfaces using a “grafting-from” approach. In this process, the monomer and initiator were first dissolved in an organic solvent, followed by application onto the cotton substrate through dip-coating. Polymerization was then thermally initiated at elevated temperatures, resulting in covalently bonded PU chains growing directly from the fabric surface. The graft-modified cotton fabric demonstrated exceptional durability, maintaining both high wash resistance and anti-crease properties[130]. Yang et al.[131] prepared a temperature-responsive fabric by applying LCST-type polymer poly(diethylene glycol monomethyl ether methacrylate)-co-poly (ethylene glycol) methyl ether methacrylate [P(MEO2MA-co-OEGMA500)] onto the surface of cotton fabric by “grafting-from” method. The surface of the cotton fabric was first treated with silane coupling agent 3-(trimethoxysilyl) propyl methacrylate (TMSPMA) to introduce the grafting site. Then, the polymer grown from the grafting site of the fabric in the monomer solution. The

grafted fabric exhibited excellent LCST temperature-responsive properties, enabling effective thermal and moisture management capabilities.

2.3.3 “Grafting-through” Approach

The grafting-through approach involves copolymerizing macromolecular polymerizable substrates with low molecular weight comonomers to generate architecturally defined branched copolymers. This technique requires two key components: (1) substrate polymer chains with polymerizable end groups and (2) reactive low molecular weight monomers. Compared to alternative grafting strategies, this approach enables the synthesis of more structurally uniform copolymers with precisely controlled topological complexity[121].

In 2016, Sejoubsari et al.[132] successfully fabricated polymer brushes on activated cellulose surfaces using a “grafting-through” approach, achieving thicker and smoother brush layers compared to those produced via “grafting-from” methods. Building on this technique, Xu et al.[132] developed Janus cotton fabrics through a “grafting-through” process. Their methodology involved: (1) atomized spraying of acrylic acid (AA) aqueous solution onto both fabric sides, followed by thermal initiation of esterification between AA and cellulose hydroxyl groups for surface grafting; (2) copolymerization with monomer methacryloxyethyltrimethyl ammonium chloride (DMC) on one side to impart antibacterial properties; and (3) polyethylene glycol-400 (PEG-400) grafting via esterification on the opposite side for antifouling functionality. This approach

demonstrated minimal substrate damage while producing uniform, finely structured grafted layers with low monomer consumption.

2.4 Summary of Past Work and Research Gap

In this chapter, studies about directional liquid flow textiles, temperature-responsive reversible wettability textiles and grafting methods for surface modification have been reviewed.

This chapter first reviews the mechanism of directional liquid flow phenomenon through textiles, which are mainly driven by capillary force and Laplace pressure. The strategies for preparing the directional liquid flow textiles including constructing wettability difference and building structural difference on textiles are introduced. Both strategies are aimed at constructing an asymmetric capillary force on both sides of fabric. The discussion subsequently explores applications enabled by these directional transport properties, including personal moisture management, selective oil-water separation, and atmospheric water harvesting, all facilitated by the unique wetting behavior of these materials. While current directional transport textiles predominantly feature fully hydrophilic exterior surfaces, leading to undesirable saturation-induced heavy, clammy, and clingy. Although recent "skin-like" fabric designs have attempted to address these limitations, a significant challenge remains in developing cost-effective manufacturing processes for industrially scalable production of directional liquid transport textiles with water-repellent properties.

Then, the categories and mechanism of temperature-responsive reversible wettability textiles are reviewed. Based on the wettability and phase transition behavior, the temperature-responsive materials can be classified into two categories, lower critical solution temperature type (LCST-type) and upper critical solution temperature type (UCST-type). These two materials exhibit opposite wettability transitions in response to temperature variations. Specifically, while LCST-type materials demonstrate increasing hydrophobicity with rising temperature, the UCST-type materials exhibit enhanced hydrophilicity with increasing temperature. Both classes of materials contain molecular chains incorporating both hydrophilic and hydrophobic functional groups, exhibiting distinct temperature-dependent wettability behaviors. Compared with LCST-type materials, UCST-type materials offer unique advantages for inverse thermal response applications (hydrophilic at higher temperature), particularly in textile-based thermal management where conventional LCST systems prove inadequate. However, existing zwitterionic UCST textiles face critical limitations, including non-tunable transition temperatures and electrolyte-dependent performance, which severely restrict their practical utility given the individual variability in bodily fluid composition. Non-ionic UCST-type polymers have not been widely adopted in textile applications due to the significant challenge of achieving optimal hydrophilic-hydrophobic balance on fabric substrates.

Finally, this chapter reviews the polymer grafting methods for surface modification. Compared to simply physically coating polymers onto the fabric, grafting polymers onto the surface of the textiles exhibits excellent durability due to the covalent

bonding between polymers and substrates. The three approaches for grafting are introduced including “grafting-to”, “grafting-from”, and “grafting-through” approaches. The “grafting-from” approach has emerged as the dominant strategy for textile surface functionalization, owing to its capacity to produce exceptionally high grafting densities. This established methodology provides critical guidance for the grafting technique employed in this study.

Chapter 3 Development of Fabrication Method of Skin-like Fabrics for Scalability

3.1 Introduction

As modern living standards continue to rise, increasing attention has been directed toward improving the thermal and moisture comfort of clothing[3-5]. This concern is particularly relevant in Hong Kong, where extreme summer heat exposes outdoor workers to excessive sweating that significantly compromises personal comfort and, in severe cases, may lead to health issues. Moisture management fabrics offer an effective solution by actively regulating physical comfort. They allow sweat to be rapidly transported away from the skin and subsequent evaporation. Moisture management fabrics that directionally transport sweat away from the skin have been extensively reported these years[6, 7]. However, a critical limitation persists in current designs, that their predominantly hydrophilic outer surfaces lack protection against external water penetration.

Directional liquid transport, as a fundamental mechanism for efficient moisture management, represents one of the most essential functional properties in advanced textile engineering. This remarkable phenomenon is commonly observed throughout biological systems in nature, where various organisms have evolved directional water transport capabilities to maintain physiological homeostasis. Inspired by these natural prototypes, researchers have developed biomimetic textiles with directional liquid transport functions through engineered surface architectures. Conventional approaches

to creating directional liquid flow textiles primarily rely on establishing asymmetric properties across fabric surfaces, typically achieved through constructing asymmetric wettability or creating hierarchical pore size distributions. Traditional directional liquid transport textiles possess fully hydrophilic outer layers to generate directional capillary forces. However, when the outer layers become saturated with moisture, it tends to be heavy, clammy, and clingy, which compromise wearing comfort. Furthermore, the hydrophilic outer surfaces make these fabrics easy to be contaminated from external sources.

A skin-like fabric was proposed to solve this problem[24]. By mimicking the structure of human skin, numerous wicking channels with gradient wettability were constructed on a hydrophobic treated cotton fabric via selective plasma treatment. The gradient wettability channels acted as sweat glands on human skin, which could directionally transport sweat away from the body. Owing to the hydrophobic character of the outer layer, transported water accumulated along the wettability gradient channels and subsequently formed droplets that detached from the surface rather than laterally spreading. Subsequently, numerous skin-like fabric designs have emerged, such as “i-TRANS”[79]. These textiles exhibit both directional liquid transport properties and water repellency. However, the fabrication processes for these textiles face challenges in scalability and cost efficiency, significantly limiting their practical application in daily life.

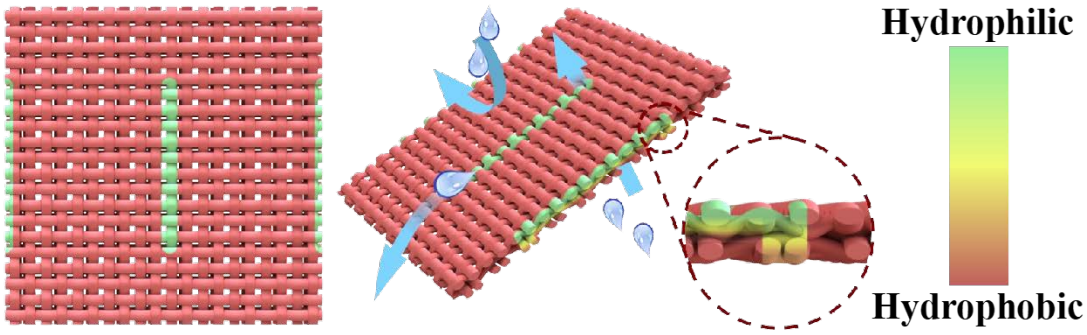

Figure 3.1 illustration of skin-like directional liquid flow fabric and gradient wettability channels developed on the cotton fabric.

In this chapter, the innovative scalable fabrication processes for creating skin-like fabric are investigated. The existing plasma-based fabrication method for skin-like fabric is evaluated, with its key limitation identified. A new PVA-based preparation approach for is proposed as an alternative. This approach involves printing a PVA solution onto the surface of hydrophilic cotton fabrics, thereby forming a covered area. Due to the viscosity of the PVA solution, a polymer concentration gradient covering is established in the thickness direction of the wetted fabric. Subsequently, the printed fabric is dried and treated with a commercial fluorine-free hydrophobic agent. Finally, the printed PVA is removed by washing with hot water. The presence of the printed PVA prevents the covered area from contacting with the hydrophobic agent, resulting in the formation of wettability gradient channels on the hydrophobic fabric. The prepared textile demonstrates directional liquid transport properties, driven by capillary force through these engineered gradient wettability channels, while maintaining overall water repellency due to the predominantly hydrophobic outer surface (as shown in Figure 3.1).

3.2 Evaluation of Existing Plasma-based Fabrication Method

The development of skin-like fabrics relies critically on selective treatment to engineer partially controlled wettability gradients. By differentially modifying distinct regions of the textile substrate, wettability gradient channels can be precisely constructed. Common methods for achieving selective treatment include plasma treatment, spray coating, and screen printing. The spray coating method was finally considered unsuitable for fabricating skin-like fabrics due to two inherent technical limitations. First, this approach provides inadequate control over liquor pick-up during application, resulting in inconsistent treatment deposition. More critically, the inherent wicking properties of hydrophilic surfaces cause uncontrolled spreading of the coating agent, preventing the formation of stable through-thickness wettability gradients essential for directional liquid transport. These fundamental constraints led to the exclusion of spray coating from our fabrication strategy. In this section, existing plasma-based fabrication processes for creating skin-like fabrics are explored[24]. Building upon the previous work reported by our group which demonstrated mask-assisted selective plasma treatment for skin-like fabric production, we initially adopted this method to optimize processing parameters. The plasma treatment approach, utilizing a perforated physical mask to create patterned wettability contrasts, served as the foundational technique for establishing gradient channels.

3.2.1 Materials

A plant-structured woven cotton fabric, developed by the School of Fashion and Textiles at The Hong Kong Polytechnic University based on previous research from our group[133], was employed as the substrate. The fabric exhibited a thickness of approximately 0.42 mm and the fabric weight was measured as 135 $g \cdot m^{-2}$. By mimicking the branching morphology of plant stems, the cross section of the fabric features a bifurcated structure, comprising two distinct sides with different pore sizes (see Figure 3.2). The side with the smaller pore size was designated as the top side or the outer surface and the other side was noted as the back side or the inner surface. This structural asymmetry facilitates directional liquid transport from the larger pore size side to the smaller pore size side through capillary action. Additional commercial fabrics used in this chapter were purchased from local suppliers. Prior to further treatment, all fabrics were thoroughly washed with an 80°C aqueous solution of 5% sodium hydroxide (NaOH) for 2 h to remove residual surface finishing. Acetic acid (AR) was purchased from Dieckmann (Hong Kong) Chemical Industry Co., Ltd. The fluorine-free hydrophobic agent, RUCO®-DRY ECO PLUS, and its crosslinking component, RUCO®-LINK XCR, as well as the hydrophilic agent FERAN® ICS was purchased from Rudolf Chemie (HK) Limited.

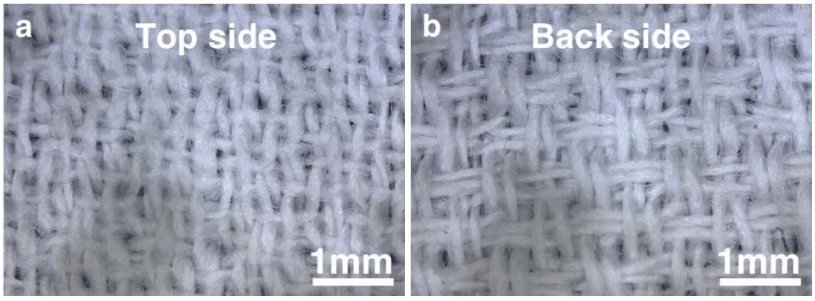

Figure 3.2 The microscopic image of the top side (a) and the back side (b) of the plant-structured fabric.

3.2.2 Fabrication Processes

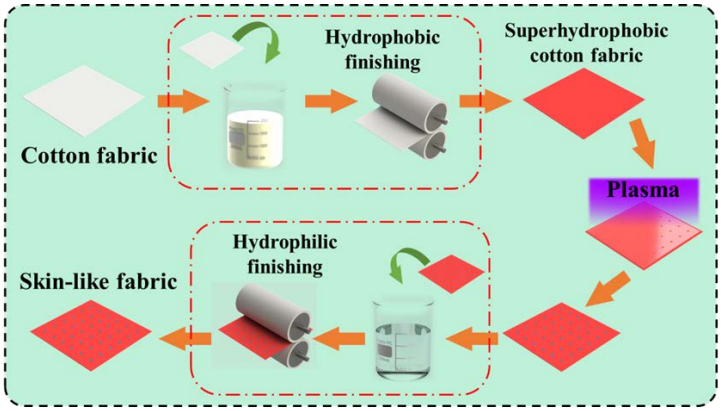

Figure 3.3 Illumination of preparation method for skin-like fabric via selective plasma treatment process.

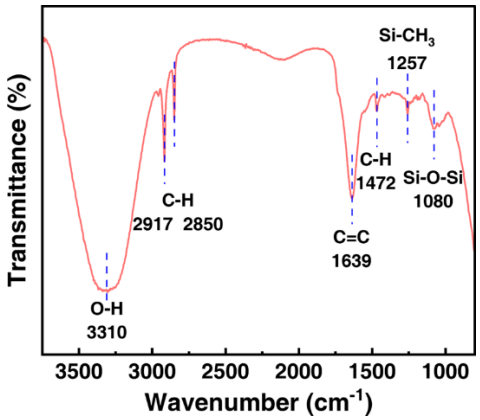

Figure 3.4 The FTIR spectra of the hydrophobic agent ®RUCO-DRY ECO PLUS.

The initial fabrication strategy employed selective plasma treatment to develop skin-like fabrics with directional water transport properties and water repellency (see Figure 3.3)[24]. The process began with pristine cotton fabrics undergoing hydrophobic finishing treatment to establish a superhydrophobic surface. The hydrophobic treatment solution was formulated by dissolving 80 g of RUCO®-DRY ECO PLUS in 1 L of deionized water, followed by the addition of 40 g of RUCO®-LINK XCR as a crosslinking agent. The solution pH was subsequently adjusted to 5 using acetic acid. This hydrophobic agent is a kind of silicone-based hydrophobic agent and free of organic halogen compounds inclusive of fluorocarbon compounds. The FTIR spectra of the hydrophobic agent is shown in Figure 3.4. The fabric was immersed in the hydrophobic agent solution and processed through a padding mangle (VFM type, Mathis AG, Switzerland) to achieve 70% liquor pick-up while removing excess finishing solution. Following padding, the fabric was air-dried at ambient temperature and then thermally cured at 160°C for 1 minute using a convection oven (Model DHG-9036A, Jinghong Experimental Equipment Co., Ltd., Shanghai, China), which imparted durable hydrophobicity to the treated substrate.

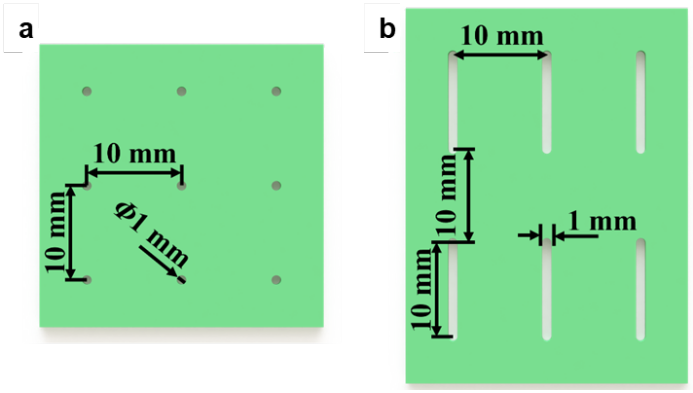

Figure 3.5 Desing of the laser cut screens. (a) Diagram of the round hole screen and (b) the elongated hole screen.

These pretreated substrates were then subjected to plasma treatment with a laser cut round hole screen covered. The screen was prepared by laser cutting using polyethylene terephthalate (PET) plates with thickness of 1 mm. As shown in Figure 3.5a, on the round hole screen, there were evenly distributed small holes with a diameter of 1 mm with the holes spacing 10 mm and the thickness of the screen being 1 mm. This selective treatment created distinct wettability zones: the plasma treated area transitioned to hydrophilic while covered areas remains their original hydrophobicity. However, the plasma induced hydrophilicity degraded rapidly due to surface reorganization and radical recombination.

To keep the hydrophilicity, an additional hydrophilic finishing was applied. To prepare the hydrophilic treatment solution, 60 g of hydrophilic agent FERAN® ICS was dissolved into 1 L of DI water. The plasma treated fabric was then immersed into the hydrophilic agent solution and then processed through a padder to remove excess

finishing solution. Afterwards, the fabric was dried at room temperature and then thermally cured at 160°C for 1 minute in an oven.

3.2.3 Characterization

The wettability and directional liquid flow property of the fabric were evaluated through water contact angle (CA) measured by a contact angle tester (Model SDC-350, Dynetech Intelligent Technology Co., Ltd., Guangdong, China). Testing was performed with water droplet volume of 5 μL, with five measurements taken per sample and the results reported as mean values.

3.2.4 Results and Discussion

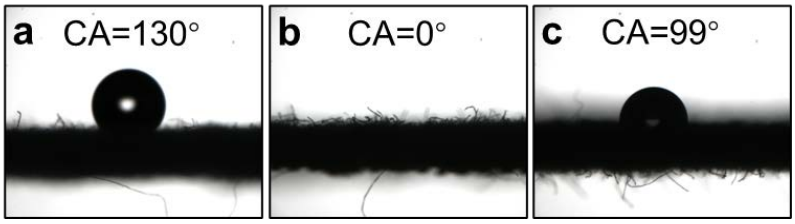

Figure 3.6 Wettability of the skin-like fabric prepared by plasma-based method. Water contact angle of (a) the hydrophobic treated area, (b) the top side and (c) the back side of the wettability channels area.

The directional liquid transport property and water repellency of the fabric largely depend on the surface wettability. Therefore, the wettability of the prepared skin-like fabric was first measured by the water contact angle tester. As shown in Figure 3.6, the hydrophobic treated area exhibited a high contact angle of 130°. In contrast, the plasma treated area showed wettability differences, with 0° on the top side and 99° on the back side. This difference resulted from the free radical induced by plasma, which enabled

effective hydrophilic coating. The attenuated plasma penetration depth created a wettability gradient across the cross-section of the fabric, with reduced hydrophilicity on the back side compared to the fully hydrophilic top surface. This wettability difference enabled the directional liquid flow property through this fabric. The water dripped onto the back side of the fabric can be directionally transported to the top side of the fabric (see Figure 3.7).

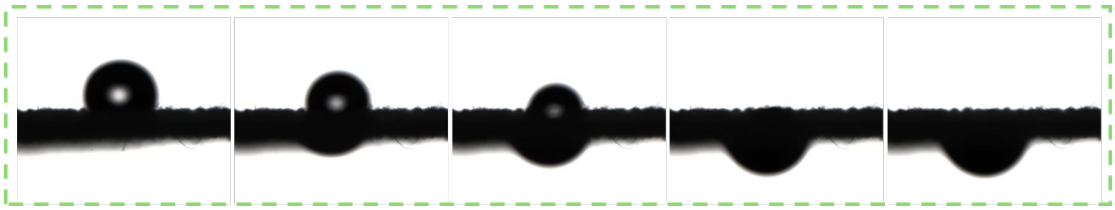

Figure 3.7 Directional liquid flow property of the skin-like fabric prepared by plasma-based process.

However, the as-prepared fabrics initially exhibited hydrophilicity to the wettability gradient channels, but complete hydrophobic recovery occurred after washing (see Figure 3.8). This may be caused by the aging of free radical induced by plasma treatment, which compromises the stable grafting of hydrophilic agents onto hydrophobic surfaces. Consequently, the hydrophilic coatings detached during washing, resulting in the restoration of the hydrophobicity on the fabric surface. Furthermore, the plasma treatment process proved impractical for large-scale production due to its slow processing speed, low throughput, and high energy consumption.

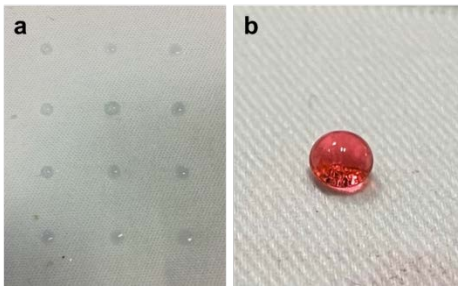

Figure 3.8 The skin-like fabric treated by selective plasma treatment process. (a) The hydrophilic wettability gradient channels. (b) Complete hydrophobic recovery of the fabric after washing.

3.3 Proposed PVA-based New Fabrication Method

3.3.1 Materials

The plant-structured cotton woven fabric was used as substrate as stated in Section 3.2.1. Polyvinyl alcohol (PVA, 1799L, 99% purity) was purchased from Shandong Usolf Chemical Technology Co., Ltd. (China). The hydrophobic agent and crosslinking component used in this section were the same as that in Section 3.2.1.

3.3.2 Fabrication Processes

In this technique, the wettability channels area to be developed on the surface of the fabric should be covered before the hydrophobic treatment to create precisely controlled wettability gradients. To realize the directional liquid transport and water repellent properties of the skin-like fabric, water soluble polymer PVA was selected as the covering agent due to easy removal by hot water. The PVA solution was prepared by dissolving a predetermined ratio of PVA solids in deionized (DI) water. Prior to dissolution, the PVA powder was immersed in DI water and continuously stirred for 12 hours to ensure complete swelling. The swollen PVA mixture was subsequently heated

to 80°C under continuous stirring for 4 h to achieve complete dissolution. In this study, five PVA aqueous solutions with varying concentrations in weight (5, 8, 11, 14, and 17 wt%) were systematically prepared for comparative analysis. Screen printing techniques were selected to apply the PVA onto the fabric. To assess the practical applicability of this method, the pristine fabric was first coated by PVA via screen printing using a dot patterned screen which was stated in Section 3.2.2. Afterwards, the printed fabric was treated by a commercial hydrophobic agent. The PVA then removed from the surface of the fabric by hot washing (see Figure 3.9). This approach was ultimately validated as feasible, with detailed results presented in Section 3.3.4.

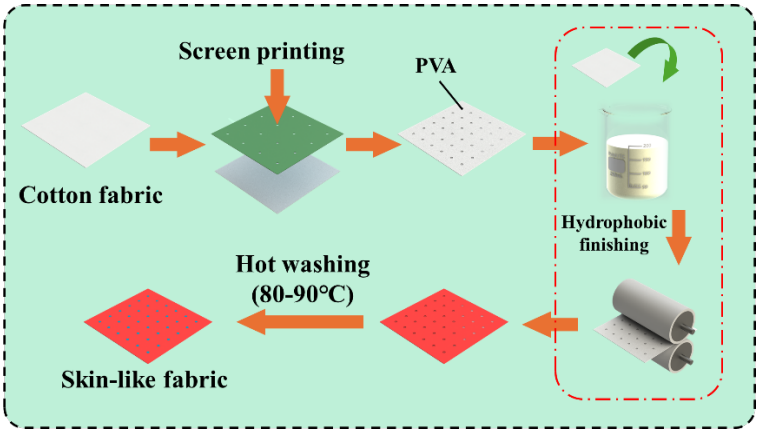

Figure 3.9 Illumination of preparation method for skin-like fabric via PVA-based (screen printing) treatment process.

After confirming the feasibility of this approach, the structure of the gradient wettability channels was optimized, leading to the redesign of an elongated hole screen (as shown in Figure 3.5b). The screen was also prepared by laser cutting using PET plates with thickness of 1 mm. The strip width was 1 mm, and strip length was 10 mm, with strip spacing being 10 mm and the thickness of the screen also being 1 mm. The

PVA solutions were printed on the plant-structured woven cotton fabric via the laser cut screens (Figure 3.10). The penetration capability of PVA solutions into the fabric substrate exhibited concentration-dependent behavior. Firstly, PVA solution with relatively lower concentration was printed on the fabric from the top surface via the round hole screen. Due to the high fluidity of the low concentration PVA solution, the printed fabric enabled quickly wetted by the solution. The solution easily penetrated to the back side of the fabric, establishing discrete dot patterned gradient wettability channels. Subsequently, the elongated hole screen was covered onto the printed fabric and precisely aligned to overlay these printed dots, enabling deposition of a high-concentration PVA solution on the top surface. The increased viscosity restricted the penetration of this solution, creating strip patterned channels exclusively on the top surface. This resulted in distinct wettability channel patterns on each side of the fabric surface: discrete dot shaped channels on the back side versus interconnected strip shaped channels on the top surface of the fabric. Finally, the printed fabric was dried at 60°C to solidify the printed PVA patterns.

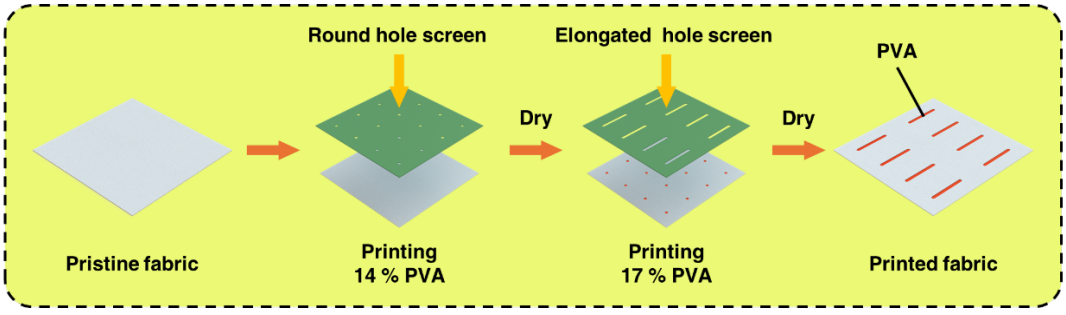

Figure 3.10 Schematic illustrating the printing of PVA solution onto the fabric.

The hydrophobic agent used in this section was the same as that in Section 3.2.2. The printed fabric was treated with the hydrophobic agent and then cured at 160° C for 1 minute. To complete the process, the cured fabric underwent continuous washing cycles for 30 min in hot water (>80°C) to thoroughly remove the printed PVA components. During the hydrophobic treatment, the PVA covered areas of the fabric were not exposed to the hydrophobic agent, and hence these areas remain hydrophilicity after the fabric was given a hot wash which removed the PVA, forming a wettability gradient through the cross section of the fabric for directional liquid transport. Elongated hydrophilic strips on the top side allow transported water accumulating on the top surface and then rolling down (see Figure 3.1).

3.3.3 Characterization

The wettability of the fabric was evaluated through water contact angle (WCA) measured by a contact angle tester (Model SDC-350, Dynetech Intelligent Technology Co., Ltd., Guangdong, China). Testing was performed with water droplet volume of 5 μL, with five measurements taken per sample and the results reported as mean values.

To demonstrate the directional liquid flow property, the skin-like fabric was suspended on a stand at an angle of 45°. Water was continuously supplied onto the back and top sides of the fabric via a syringe pump, respectively. The liquid transport behavior through the fabric was then observed.

The surface morphology of the fabric was observed using a scanning electron microscope (SEM, Model VEGA3, TESCAN, U.K.). A thin layer of gold was deposited

on the surface of the observed sample to increase the conductivity before testing for a better image quality.

Figure 3.11 The homemade apparatus for hydrostatic pressure test.

The water repellency of the fabric was characterized by the hydrostatic pressure test and the water shower test as well as the spray test. The hydrostatic pressure was measured by means of a homemade apparatus (see Figure 3.11). The sample was fixed in the middle of two acrylic tubes. Water was supplied continuously into the upper tube with water supply rate of 0.2 mmH_2O/s. When the first drip of water dropped through the sample to the lower tube, the height of water in the upper tube was recorded.

The water spray test was conducted to check the water repellency and directional liquid transport property of the fabric. A piece of fabric was fixed at the mouth of a glass vial, which contains hygroscopic color-changing silica gel. Then, the assembly was sprayed under a water pressure of 50 mmH_2O for 10 s. The color change of the silica gel inside the vial was then observed to evaluate the water repellency.

The shower test was conducted by a spray rating tester (Model M232, SDL International, U.K.) according to the standard AATCC 22. 250 mL of water was poured onto the top side of the fabric through a shower at the height of 150 mm and at temperature of 20°C, the water being dyed red to obtain a more visible result. The wetting area of the fabric was then observed and recorded.

The air permeability of the fabric was measured by means of an air permeability tester (KES-F8-AP1, KATO Tech Co., Ltd., Japan).

3.3.4 Results and Discussion

Effect of the concentration of PVA solutions on wettability of the fabric

Figure 3.12 Top side and back side of samples printed by the round hole screen using (a) 5 wt%, (b) 8 wt%, (c) 11 wt%, (d) 14 wt%, and (e) 17 wt%.

To achieve the best directional liquid transport properties of fabrics prepared by PVA-based process, the effect of PVA concentrations on wettability of the fabric was

explored. Five PVA solutions with different concentrations on weight (5%, 8%, 11%, 14%, 17%) were prepared. These five kinds of PVA solutions were printed onto the plant-structured cotton woven fabric from the top side via the round hole screen, respectively. Due to the hydrophilicity of the plant-structured cotton fabric, the solutions were easily absorbed by the fabric and forming polymer concentration gradients covering on the cross section (thickness direction) of the fabrics. As shown in Figure 3.12, the PVA solution demonstrated increased spreading behavior with the decrease of solution concentrations due to the lower viscosity. Therefore, the pattern printed with a higher concentration of PVA solution exhibited significantly improved clarity and accuracy. Additionally, solutions with higher viscosity showed reduced penetration through the fabric to the back side.

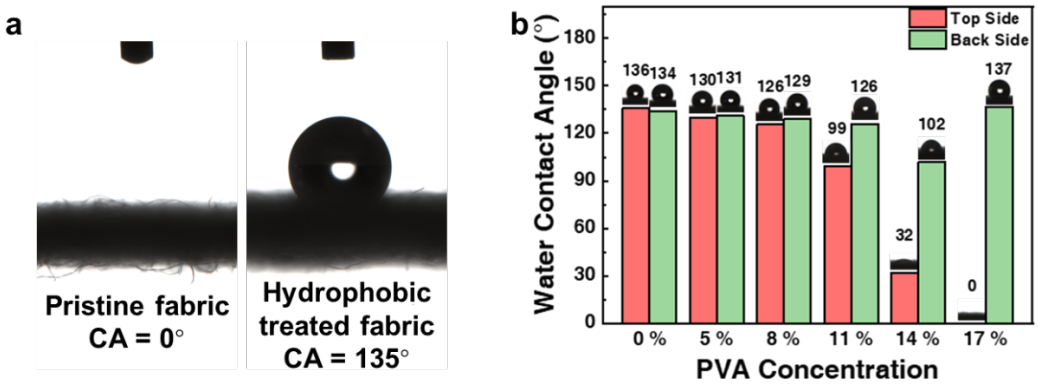

Figure 3.13 The wettability of the treated fabrics printed with different PVA concentrations in the solutions. (a) Contact angles of the pristine plant-structured cotton woven fabric and the hydrophobic treated area of the fabric. (b) Contact angles of the top side and back side of the wettability channels treated with solutions with various PVA concentrations.

After printing process, these fabrics were treated with commercial fluorine-free hydrophobic agent and were hot washed for PVA removal via the method mentioned in Section 3.3.2. The covering effect of PVA solution were checked with wettability of the printed areas. The water contact angles of these fabrics were measured. As shown in Figure 3.13a, the pristine plant-structured cotton fabric was superhydrophilic with the water contact angle of 0°. When the fabric was treated with hydrophobic agent, the fabric exhibited hydrophobicity with a water contact angle of 135°. The water contact angle of wettability channels on the fabric which was covered by PVA varied with the concentration of PVA solution due to the covering effect (see Figure 3.13). At lower PVA concentration, such as 5%, both the top side and the back side of the wettability channels areas were hydrophobic with water contact angles above 120°. Although the lower concentration PVA solutions were able to easily wet the fabric and penetrate to the back side of the fabric, its low viscosity leads to uncontrolled spreading, leading to an edge blurring and geometric deviation. Furthermore, the low concentration of PVA limited the covering efficiency, failing to prevent the pattered area from exposing to the hydrophobic agent. Consequently, unwanted hydrophobic properties occurred in protected areas. As the increase of PVA concentration in solutions, the water contact angle of the top side of the gradient wettability channels decreases, indicating the covering effect of the PVA solution improved. It is worth noting that, when the PVA concentration was 14%, the water contact angle of the top side of the wettability channels was 32°, while that of the back side of the wettability channels was 102°, which was slightly lower than that of the uncovered hydrophobic area. The water

contact angle difference was 70°, demonstrating that the 14% concentration of PVA solution was able to penetrate to the back side of the fabric with a suitable degree, forming a wettability gradient through the cross section of the fabric. As the PVA concentration increased to 17%, the PVA solution showed the best covering effect, with the contact angle of the top side of the wettability channels being 0°. However, since the solution was too thick to penetrate to the back side of the fabric, the back side of the wettability channels exhibited hydrophobicity with contact angle of 137°, which was almost the same as the uncovered hydrophobic area. Compared with selective plasma treatment, the PVA-based method exhibited durable hydrophilicity on the wettability gradient channels. As shown in Figure 3.14, the printed areas remain hydrophilic after being washed 10 times and then stored for 1 month. After being washed and stored, the hydrophilicity on the printed area remained. The results in this section showed that the PVA covering method is more suitable for preparing the skin-like fabric. In subsequent experiments, the PVA-based method was refined by adopting the dual-printing approach described in Section 3.3.2. The 14% PVA solution was selected to print dot pattern using the round hole screen, and the 17% PVA solution was used for printing the strip pattern via the elongated hole screen. Fabrics printed by this method exhibited a water contact angle difference of 102° between the two sides of the wettability gradient channels.

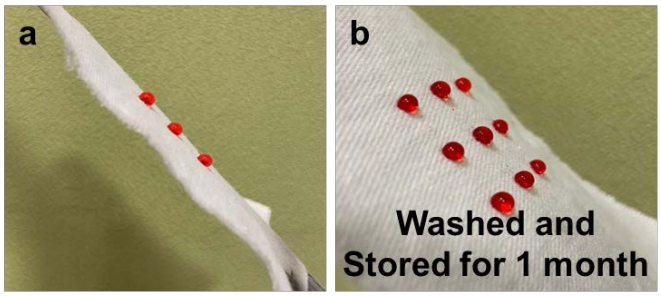

Figure 3.14 The fabric prepared by PVA-based method. (a) The hydrophilic printed areas and hydrophobic outer surface. (b) The wettability of the fabric after being washed and stored for 1 month. The water was dyed red to facilitate visual observation.

Effect of the PVA-based process on directional liquid transport property of the fabric

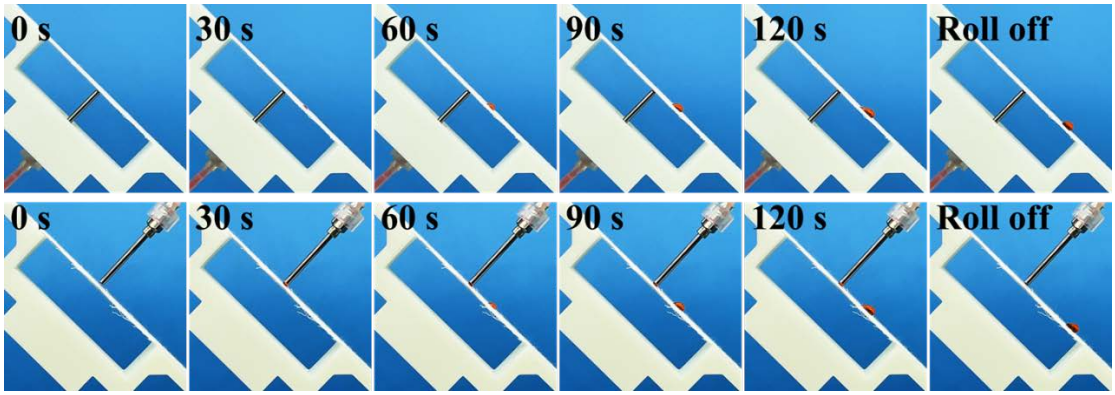

Figure 3.15 The directional liquid transport property of the fabric. The water was dyed red to facilitate visual observation.

Having explored the concentration of the PVA solution, the treated fabric via PVA-based method should have an excellent directional liquid transport property, which is a critical property for moisture management function of a fabric. In the prepared skin-like directional flow and water repellent fabric, there were gradient wettability channels with the top side being superhydrophilic (water contact angle was 0°) and back side being hydrophobic (water contact angle was 102°). The back side of the wettability

channels was slightly less hydrophobic than the uncovered hydrophobic area, allowing liquid easier to gather here and facilitation water transport. Due to the wettability difference between the two ends of the gradient wettability channels, water can be transported directionally from the more hydrophobic side to (back side) to the more hydrophilic side (top side) of the fabric. The key driving force of this directional liquid transport phenomenon is capillary pressure[20, 54]. As shown in Figure 3.15, water was transported to the top side of the fabric when it was supplied from the back side of the fabric. The transported water then accumulated along the hydrophilic strips on top side of the fabric and rolled off due to gravity. During the experiment, it takes 120 s for the first droplet to be transported and drip down. In contrast, when water was supplied onto the top side of the fabric, it just accumulated on the hydrophilic strips on the top side of the fabric and then rolled down rather than being transported to the back side of the fabric. Furthermore, the other area of the fabric was not wet by the water since most areas of the fabric were hydrophobic.

Effect of the PVA-based treatment on surface morphology of the fabric

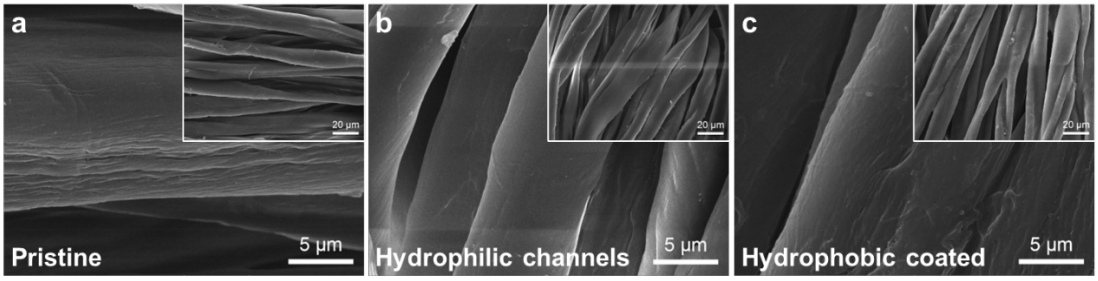

Figure 3.16 Surface morphology of the fabrics. SEM images of (a) pristine plant-structured cotton fabric, (b) Hydrophilic area (top surface) of the gradient wettability channels, and (c) hydrophobic treated area.

The properties of the fabric can be largely affected by the surface morphology of the fiber, not only wettability, but also mechanical properties, and air permeabilities. A scanning electron microscope (SEM) was used to observe the changes in the morphology of the fabric before and after the PVA-based treatment. As shown in the SEM images of the fabrics (Figure 3.16), there was a layer of coating on the surface of the hydrophobic treated area of the skin-like directional liquid flow fabric compared with the surface of the pristine fabric. It can also be observed in the inserted smaller magnification image that there are adhesions between fibers on the hydrophobic treated area due to the crosslink of the hydrophobic agent. The hydrophobic agent covered the fabric uniformly, resulting in a favorable hydrophobicity on the hydrophobic treated area of the fabric. Conversely, on the top side of the gradient wettability channels which covered by PVA, the surface morphology of the fibers was almost the same as the pristine plant-structured cotton fabric, indicating that these areas remain hydrophilicity

due to the excellent covering effect of PVA which prevented the fabric from being exposed to the hydrophobic agent. Furthermore, the treatment did not change the surface morphology and pore structure of the fabric, indicating that the mechanism properties and the air permeability were not affected.

Effect of PVA-based treatment on water repellency and air permeability of the fabric

Table 3.1 Hydrostatic pressure of the both sides of the skin-like directional flow fabric and air resistance of the pristine plant-structured cotton fabric and the skin-like directional flow fabric.

Sample	**Hydrostatic pressure (mmH_2O)**	**Air Resistance ($kPa·s·m^{-1}$)**	**Standard deviation of air resistance ($kPa·s·m^{-1}$)**
Pristine plant-structured cotton fabric	—	0.330	0.004
Skin-like directional flow fabric	Top side: 76 Back side: 22	0.329	0.007

Apart from the directional liquid flow property, the skin-like fabric also exhibited excellent water repellency due to the hydrophobicity of most areas of the fabric. The water repellency of the treated fabric was characterised by the hydrostatic pressure test. The hydrostatic pressure was tested via a homemade apparatus following the method detailed in Section3.3.3. As shown in Table 3.1, the hydrostatic pressure of the top side of the skin-like directional flow fabric was 76 mmH_2O, which was significantly higher than that of the back side of the fabric (22 mmH_2O). This indicated that it is easier for water to be transported from the back side to the top side of the fabric than the reverse

transport. This phenomenon clearly showed the directional water transport performance of the fabric and the water repellency from the top side of the fabric. To further evaluate the water repellency of the fabric, a water spray test and shower test was carried out. As shown in Figure 3.17, when water was sprayed onto the top side of the fabric, the silica gel in the vial remained unchanged in color, demonstrating that no water penetrated through to the back side of the skin-like fabric. Conversely, when water sprayed from the back side, water passed through the fabric to the top side, leading to the silica gel absorbing water and becoming red. As can be seen from Figure 3.18, the water selectively wetted only the hydrophilic area of the gradient wettability channels, leaving most of the top surface dry. No liquid penetrated to the back side of the skin-like fabric, resulting in a dry surface on the back side.

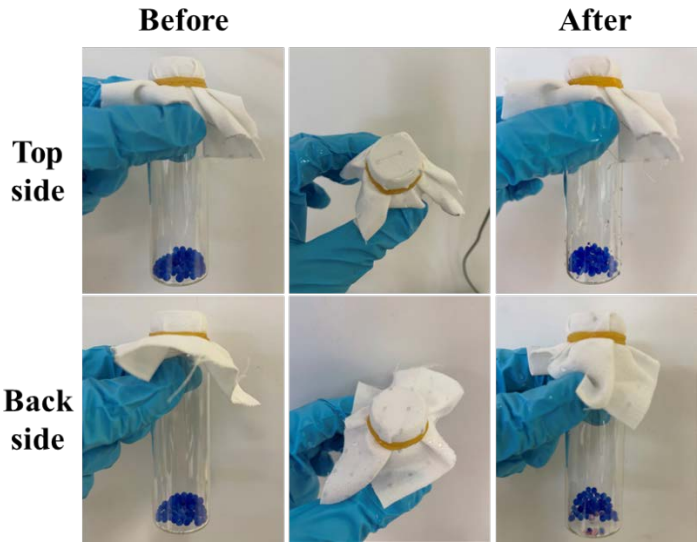

Figure 3.17 Water spray test of the skin-like directional flow fabric.

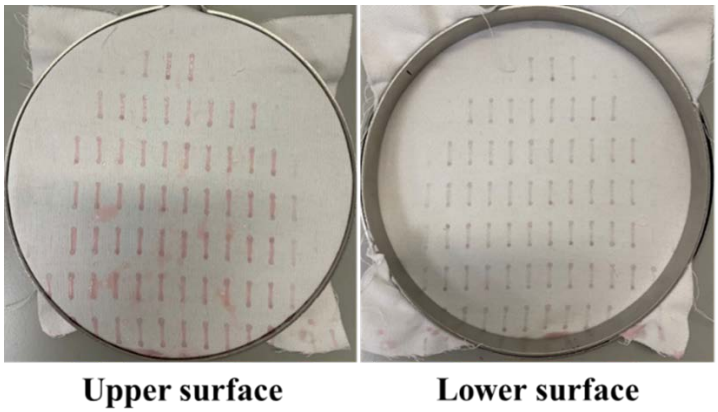

Figure 3.18 Image of shower test of skin-like directional flow fabric.

The air permeability of the fabric plays an important role in wearing comfort and thermal/moisture management. In this research, air permeability was evaluated through air resistance measurements, where lower air resistance represents higher air permeability. Air resistance is measured by the pressure generated when a certain amount of air passes through a unit area of fabric per unit time. The higher this value, the higher the air resistance. As shown in Table 3.1, the air resistance of the pristine plant-structured cotton fabric was 0.330 $kPa \cdot s \cdot m^{-1}$, while the treated skin-like fabric exhibited almost the same air resistance at 0.329 $kPa \cdot s \cdot m^{-1}$. The SEM image showed that the treatment did not affect the porous structure of the fabric, which can be attributed to the thin and uniform deposition of the hydrophobic agent without compromising the internal fiber architecture. As a result, the treated skin-like fabric remains an excellent air permeability.

Effect of substrates on directional liquid transport property during PVA-based treatment

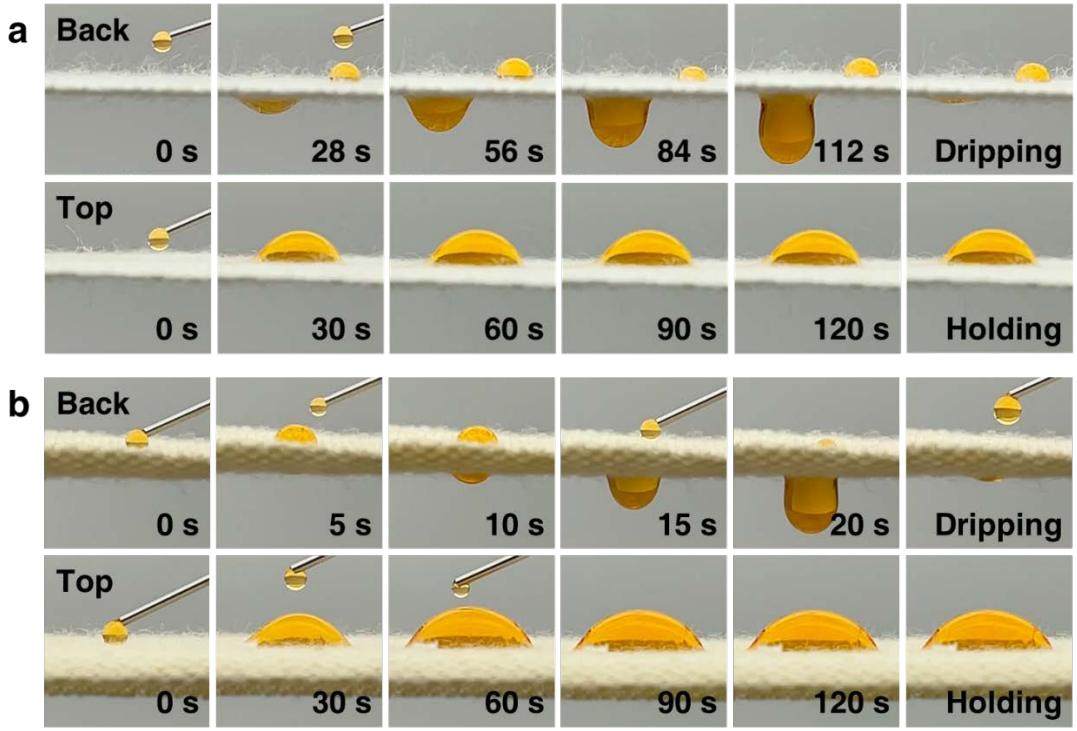

Figure 3.19 Directional liquid transport properties of skin-like fabrics prepared using different substrates. (a) Plain cotton woven fabric. (b) Cotton knitted fabric.

To demonstrate the general applicability of this method, in this section, we prepared three skin-like fabrics using different base materials including plain cotton woven fabric, plain cotton-polyester blended woven fabric, and cotton knitted fabric. Before the treatment, the cotton-polyester blended woven fabric was hydrolysed in 5% NaOH solution at 80°C for 2h to improve the hydrophilicity. The directional liquid transport properties of these fabrics were demonstrated in Figure 3.19. All treated fabrics exhibited effective directional liquid transport, allowing rapid water transport when water supplied from the back side of the fabrics while completely preventing

penetration from the top side of the fabrics. Among the tested substrates, the knitted cotton fabric showed the most rapid transport (Figure 3.19b), due to its inherently loose structural architecture which facilitated enhanced capillary flow. This experiment demonstrates the PVA-based method can be applied onto fabrics having different fabric constructions for creating skin-like directional liquid flow fabrics.

3.4 Summary

In this chapter, the preparation process of skin-like directional flow fabric was explored and improved. Gradient wettability channels were developed on the surface of hydrophobic fabrics via PVA-based method. This method primarily employs two mature industrial process: screen printing and dip coating, to achieve the desired functionalization. The developed gradient wettability channels allow water flows directionally from the skin side to the outer side of the fabric and accumulate on the outer surface and dripped down. Due to this property, the fabricated textile enables rapid sweat transport while preventing the heaviness and stickiness caused by saturation, maintaining dryness and lightweight comfort even after heavy sweating. Since most areas of the outer surface of the skin-like fabric is hydrophobic, the prepared fabric exhibits water repellency with the hydrostatic pressure of 76 mmH_2O. The shower test and water spray test also showed the water repellency of the fabric. Furthermore, the treatment did not affect the air permeability of the fabric, thus maintaining its air permeability. This treatment process has a broad applicability, could be used for

different substrates. Compared with existing plasma-based method, the PVA-based method exhibits significant potential for large-scale production.

Chapter 4 (PDMAPS)-based Temperature-responsive Skin-like Fabric

4.1 Introduction

Clothing plays an important role in assisting the human body's thermal and moisture regulation while providing necessary protection in the wide range of environments we live in[1-5]. An ideal clothing system should effectively promote heat dissipation during higher temperatures or extraneous activities while maintaining thermal insultation in cold conditions. Human skin has an exceptional temperature-responsive directional liquid flow property in that, it increases the secretion of sweat for evaporative cooling at high temperatures but minimizes water loss at low temperatures while providing protection from the external environment[5, 13, 14]. By mimicking the temperature-responsive directional liquid transport property of human skin in textiles can lead to a much-desired thermal and moisture regulation fabric that regulates sweat transport and the associated evaporative heat loss in response to thermal conditions.

In Chapter 3, the skin-like fabric with directional flow property and water repellency has been developed. However, these skin-like fabrics cannot regulate the moisture management properties with the change of temperature. The after-chill effect after vigorous exercise or the large temperature difference between outdoor and indoor may largely affect human comfort. To impart the temperature-responsive effect to a fabric, a simple strategy is to coat the temperature-responsive polymer on the surface

of the fabric. As discussed in Section 2.2, UCST-type polymers are more suitable for preparing thermal and moisture management textiles. These polymers exhibit hydrophobicity at a lower temperature and transform into hydrophilic when temperature rises[25]. This temperature-responsive property is similar with the intrinsic thermoregulatory properties of human skin. If this kind of polymer is coated on the gradient channels of the as-prepared skin-like directional flow fabric in Chapter 3, it is possible to impart the property that the water transport rate of the fabric changes with temperature, that is, the water transport rate is lower at a lower temperature, and the water transport rate rises at a higher temperature.

In this chapter, the UCST-type (PDMAPS)-based temperature-responsive skin-like directional flow and water repellent fabric is prepared by grafting the zwitterionic UCST-type polymer, poly([2-(Methacryloyloxy)ethyl]dimethyl-(3-sulfopropyl) ammonium hydroxide (PDMAPS), onto the surface of the plant-structured cotton woven fabric-based skin-like fabric prepared in Chapter 3 via a “grafting-from” method. The transition temperature (or UCST) of this polymer is about 26°C, which is close to the typical temperature of a fabric on the human body[134, 135]. Due to the switchable wettability of the PDMAPS, the prepared temperature-responsive skin-like fabric exhibits dynamic water transport rate driven by temperature. The coating existed only as a thin layer on the fabric surface, so the porosity of the fabric was not affected. The fabric exhibits high water transport rate (14202 $g \cdot m^{-2} \cdot h^{-1}$ at 40 ºC) when temperature higher than the transition temperature of PDMAPS (26-27°C). Conversely, when the temperature decreases below the transition temperature, the water transport capacity of

the fabric significantly reduces (8700 $g \cdot m^{-2} \cdot h^{-1}$ at 10 ºC) to prevent heat loss from the human body. Meanwhile, the water repellency of the fabric increases at lower temperature (hydrostatic pressure of 98 mmH_2O at 10 ºC), providing better protection for the human body. This kind of temperature-responsive skin-like moisture management fabric has wide potential applications in functional clothing due to its excellent temperature-dependent moisture management properties and water repellency.

4.2 Experimental Section

4.2.1 Materials

The skin-like directional liquid flow and water repellent fabric was prepared via the PVA-based method mentioned in Chapter 3, using the plant-structured cotton woven fabric as the substrate. The 3-(trimethoxysilyl) propyl methacrylate (TMSPMA, 98%) and the acetic acid (AR) were purchased from Dieckmann (Hong Kong) Chemical Industry Co., Ltd., Hong Kong. The ethyl alcohol (Absolute, ACS grade) as the solvent was supplied by Anaqua Global International Inc. Limited, Hong Kong. The [2-(methacryloyloxy) ethyl] dimethyl-(3-sulfopropyl) ammonium hydroxide (DMAPS, 98%) was obtained from Bide Pharmatech Co., Ltd., Shanghai, China. The 2-Hydroxy-4'-(2-hydroxyethoxy)-2-methylpropiophenone (HHMP, ≥98%) as the photo-initiator, ethylene glycol dimethacrylate (EGDMA, 98%) as the crosslinker, and 2,2,2-Trifluoroethanol (TFEA, 99.5%) as the solvent for HHMP and EGDMA were obtained from Shanghai Aladdin Biochemical Technology Co., Ltd., China.

4.2.2 Grafting the Coupling Agent onto the Skin-like Fabric

Due to the lack of grafting sites on the surface of skin-like cotton fabric, the temperature-responsive polymer PDMAPS cannot form covalent bonds with the substrate fabric and instead relies only on physical adhesion, which significantly compromises the strength of the coating and durability. Therefore, the fabric was treated with a coupling agent TMSPMA to introduce grafting sites for a stronger molecular binding before applying the temperature-responsive polymer onto the skin-like fabric. The coupling agent solution was prepared by dissolving 0.8 mL of TMSPMA in 39.2 mL ethyl alcohol and mixing with 130 μL acetic acid. The solution was stirred for 5 min at room temperature. Afterwards, a piece of skin-like fabric at the size of 10 × 10 cm was immersed into the solution at 30°C for 4 h while having magnetic stirring. The TMSPMA was hydrolyzed in the solution and combined with the cotton fabric through hydrogen bonds. Then, the fabric was cured at 105°C for 24 h in an oven. In this process, the hydrolyzed TMSPMA underwent condensation reaction with cotton fabrics, forming covalent bonding. Finally, the cotton fabric was rinsed three times with ethyl alcohol for 10 min to remove the unreacted chemicals and dried at 60°C in oven.

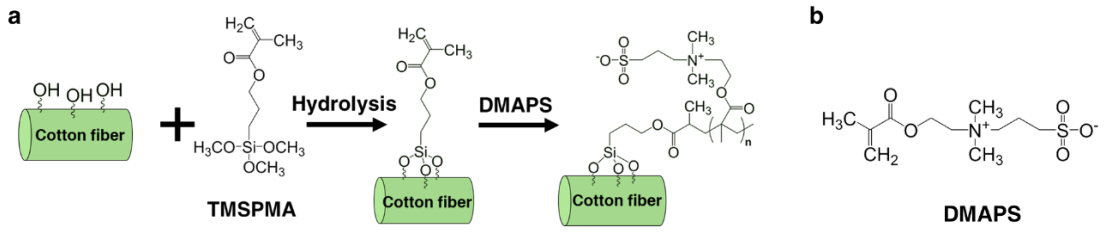

Figure 4.1 The chemical mechanism of grafting PDMAPS onto the cotton fabric. (a) Schematic of grafting PDMAPS on the cotton fabric. (b) Chemical structure of DMAPS monomer.

By introducing the coupling agent TMSPMA, the hydroxyl groups on the cotton surface were replaced by the double bonds on TMSPMA, providing a grafting site for graft polymerization of the temperature-responsive polymer PDMAPS. The TMSPMA provided covalent bonding between the fabric surface and the temperature-responsive polymer layers (see Figure 4.1a), enhancing the durability of the polymer coating. After treating the coupling agent, the hydrophilic area of the gradient wettability channels on the skin-like fabric became slightly hydrophobic due to the hydrophobic groups in TMSPMA. This hydrophobic modification regulates the wettability balance of the surface of the fabric, playing an important role in determining the temperature-responsive switchable wettability properties of the fabric.

4.2.3 Fabrication of the (PDMAPS)-based Temperature-responsive Skin-like Fabric

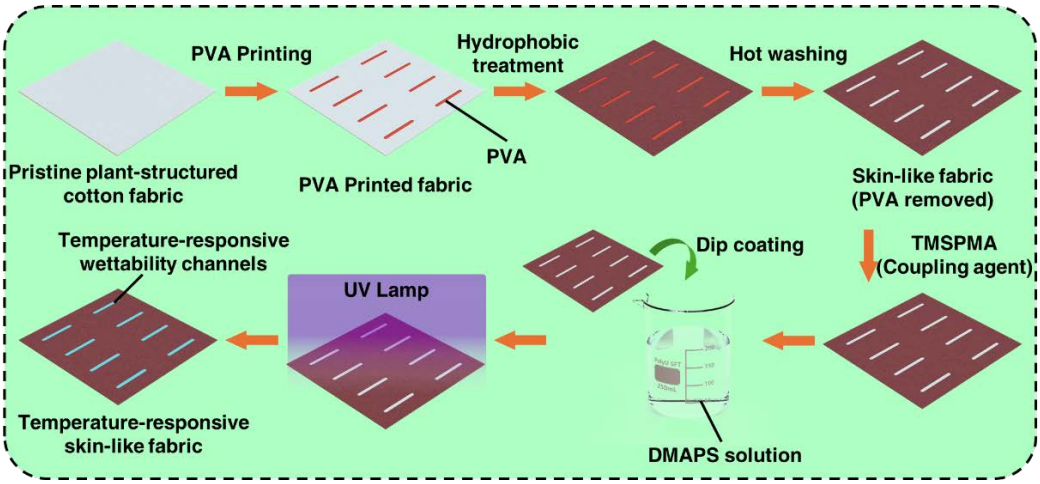

Figure 4.2 Illustration of preparation of (PDMAPS)-based temperature-responsive skin-like fabric.

The (PDMAPS)-based temperature-responsive skin-like fabric was prepared by grafting the temperature-responsive polymer PDMAPS onto the wettability channels

areas of the skin-like fabric via “grafting-from” method in a temperature-responsive monomer solution. To prepare the temperature-responsive monomer solution, different weight (2g, 3g, 4 g, 5g, 6g) of DMAPS monomer (Figure 4.1b), 20 μL of EGDMA as crosslinker, 40 mg of HHMP as photo-initiator, and 2 mL of TFEA as solvent for EGDMA and HHMP were dissolved in 20 mL of DI water. The solution was stirred for 1 h under a completely dark environment (for preventing initiation of polymerization) to get fully dissolved. Then, nitrogen (N_2) was pumped through the solution for 30 min to remove dissolved oxygen (O_2) in the solution. The skin-like fabric treated by coupling agent was dipped in the temperature-responsive monomer solution and then the fabric was processed through a padder for removing excess solution. The DMAPS solution only remained on the top side of the gradient wettability channels of the skin-like fabric (as shown in Figure 4.3, the DMAPS monomer solution was dyed red for obtaining a more visible result) since the other area of the skin-like fabric was hydrophobic. Then, the top side of the fabric was put under a UV lamp (365 nm, 120 W) at a distance of 5 cm. The grafting polymerization was initiated by the UV irradiation with a duration of 20 min. After the UV irradiation, the PDMAPS was grafted onto the fabric via covalent bonding with the assistance of the coupling agent. Finally, the fabric was alternately rinsed with cold (5°C) and hot water (80°C) for 1 h to remove unreacted monomers and solvents, after which it was dried at 60°C.

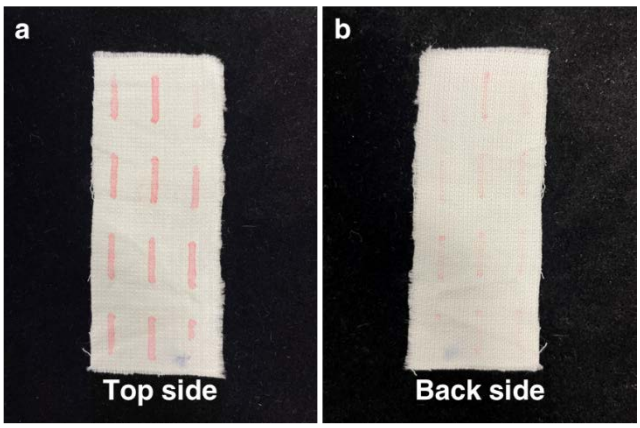

Figure 4.3 Photograph of the top side (a) and back side (b) of the TR-MM fabric. The red areas are the dyed DMAPS solution. It shows that the DMAPS solution is only picked up by the top side of the gradient channels.

4.2.4 Characterization

The wettability of the fabric was characterized by measuring the water contact angle with a contact angle tester (SDC-350, Dynetech Intelligent Technology Co., Ltd., Guangdong, China), a water droplet volume of 5 μL being used during the test. Each sample was tested for 5 times, and the mean of the data was taken.

A scanning electron microscope (SEM, VEGA3, TESCAN, U.K.) was used to observe the surface morphology of the fabric. A layer of gold was deposited on the surface of the fabric before testing to improve the conductivity of the surface for better image quality. Energy-dispersive X-ray spectroscopy (EDS) was used to analyze the element mapping of the surface of the fabric. A Fourier-transform infrared spectrometer (FTIR, Spectrum 100, PerkinElmer, USA) was used to characterize the chemical groups and composition of the fabric.

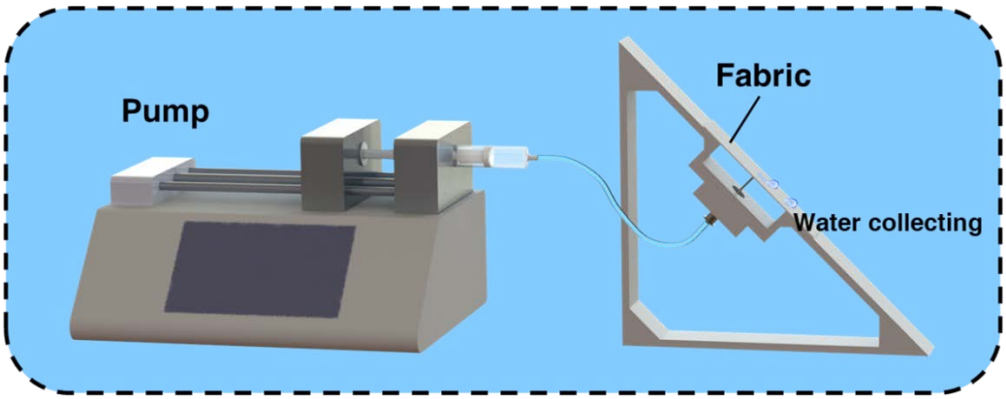

Figure 4.4 Schematic diagram of the homemade apparatus for water transport rate test.

The directional liquid transport rate of the fabric was tested by means of a homemade apparatus (see Figure 4.4). The fabric was fixed on a 3D printed triangular bracket at 45° inclination, and water was supplied continuously to the back side of the fabric at a rate of 10 ml/min by a syringe pump. The syringe needle for water supply is positioned at a distance from the fabric, approximately 2-3 mm. A portion of the water was conducted to the top side of the fabric and dripped down. The test was conducted for 1 hour. The dripped water was collected and weighed, then the water transport rate ($g \cdot min^{-1} \cdot m^{-2}$) can be calculated.

The water repellency property of the fabric was characterized by hydrostatic pressure test and shower test, following the same method detailed in Section 3.3.3. The air permeability of the fabric was measured by means of an air permeability tester (KES-F8-AP1, KATO Tech Co., Ltd., Japan).

The handle of the fabric was characterized by the low stress mechanical properties tests. The low stress mechanical properties of the fabric were tested using KEF-FB system, with the sample size being 20 cm × 20 cm. The tensile and shearing properties

were tested by KES-FB1 AUTO-A (KATO Tech Co., Ltd., Japan). The bending property was tested by KES-FB2 (KATO Tech Co., Ltd., Japan). The compression property was tested by KES-FB3 AUTO-A (KATO Tech Co., Ltd., Japan). The surface property was tested by KES-FB4 AUTO-A (KATO Tech Co., Ltd., Japan).

4.3 Results and discussion

4.3.1 Effect of the PDMAPS Coating on the Wettability of the Fabric

To achieve the temperature-responsive switchable wettability on the skin-like directional flow fabric, a UCST-type zwitterionic temperature-responsive polymer PDMAPS was grafted on the gradient wettability channels of the skin-like fabric. This polymer exhibits hydrophobicity at lower temperatures and becomes hydrophilic as temperature rises.

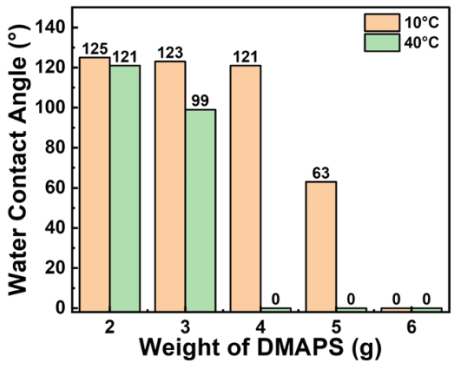

Figure 4.5 The effect of weight of DMAPS in the temperature-responsive solution (in 20 ml of solvent) on the water contact angle of the grafted fabric.

In order to explore the effect of monomer concentration of the solution on the wettability of the fabric, fabrics treated with five monomer solutions stated in Section

4.2.3 were prepared. The liquor pick-up was 120%. As shown in Figure 4.5, the hydrophilicity of the fabric increased with the increase of the monomer weight in the solution. At low DMAPS concentrations, the fabric maintained hydrophobic character (contact angle > 90°) at both high and low temperatures, indicating insufficient DMAPS to counterbalance the hydrophobicity of TMSPMA. When the weight of DMAPS reached 4 g, the grafted polymer density reached an optimal level that enabled temperature-responsive behavior, exhibiting a contact angle transition from 121° at low temperature to 0° at higher temperature. However, excessive DMAPS led to loss of temperature-responsiveness, as the high surface PDMAPS concentration turned the surface to hydrophilic even at lower temperatures.

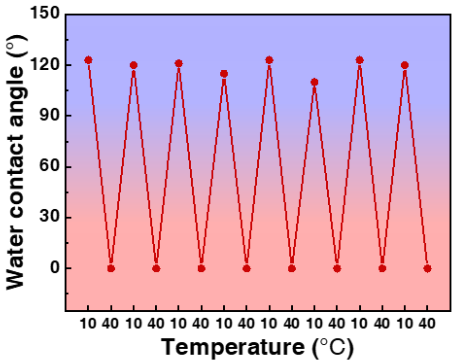

Figure 4.6 Repeated tests of water contact angle of the PDMAPS coated fabric at different ambient temperatures.

A fabric coated with the monomer solution with 4 g of DMAPS in 20 ml solvent was prepared to check the reversible wettability and durability of the temperature-responsive fabric. The water contact angles were tested alternatively for 8 cycles at 10°C and 40°C ambient temperature, respectively. According to the results of the

contact angle test (Figure 4.6), the surface of the fabric was hydrophobic with contact angles were all around 120° when the ambient temperature was 10°C, while the surface of the fabric became hydrophilic at 40°C with the contact angle of 0°. The contact angles did not change a lot after 8 cycles, which indicated that the temperature-responsive property of the fabric was reversible. The temperature-responsive wettability switching behavior is fundamentally governed by the distinctive molecular structure of the DMAPS monomer. Although electrically neutral overall, the DMAPS molecule incorporates both positively charged cationic and negatively charged anionic functional groups within its structure[136]. This zwitterionic characteristic drives the following temperature induced transitions: When the temperature is maintained below the UCST, zwitterionic groups undergo strong self-association through intensive dipole-dipole interactions between molecular chains, resulting in a hydrophobic state. Conversely, when the temperature is increased above the UCST, the thermal energy overcomes and disrupts these intermolecular dipole interactions, causing the molecular chains to extend and exposing the hydrophilic zwitterionic groups to the surface, thereby inducing a hydrophilic surface state[106]. The temperature-responsive property of the fabric is durable. The fabric also showed temperature-responsive property after being washed 30 times by an ultrasonic cleaner. As demonstrated in Figure 4.7, the fabric maintains its temperature-responsive characteristics, exhibiting various wetting behaviors at different temperatures. Water droplets rapidly roll off the surface at lower temperatures while completely spreading at increased temperatures.

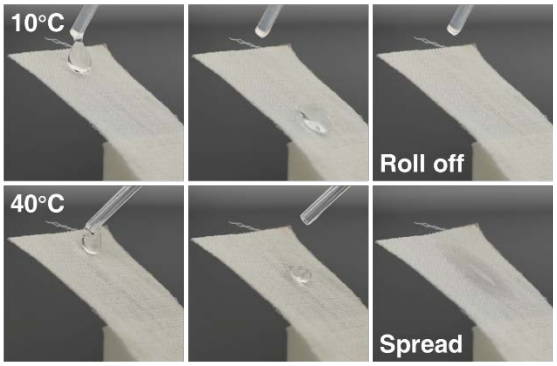

Figure 4.7 Wetting behaviors of PDMAPS coated fabric at different ambient temperatures after being washed for 30 times.

4.3.2 Effect of the PDMAPS Coating on the Surface Morphology and Chemical Composition of the Fabric

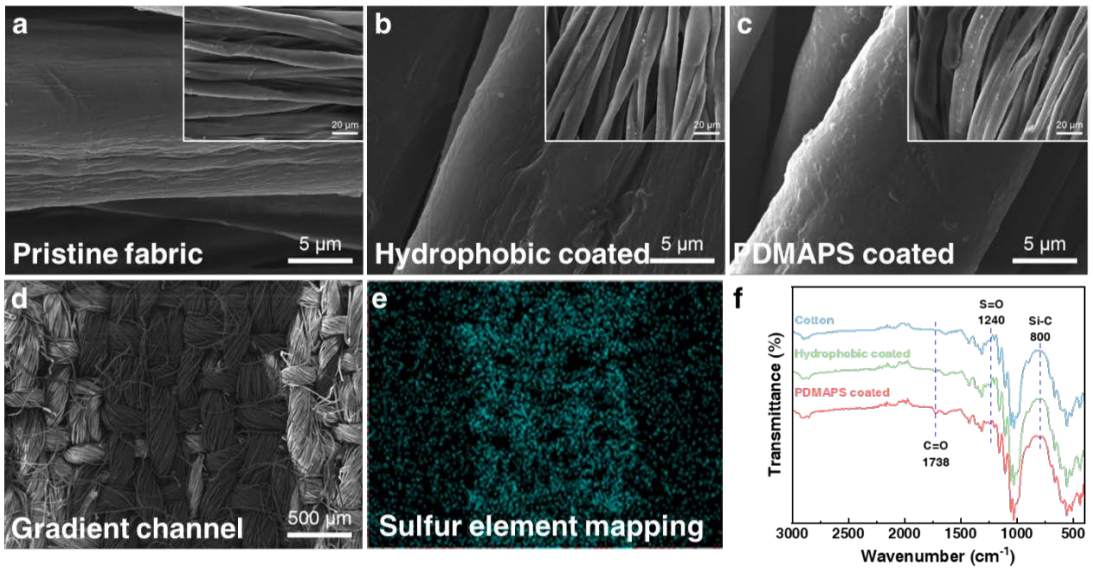

Figure 4.8 Surface morphology and chemical compounds of the (PDMAPS)-based temperature-responsive skin-like fabric. SEM images of (a) pristine fabric, (b) hydrophobic coated area of the fabric, and (c) PDMAPS coated area of the fabric. (d) SEM image and (e) sulfur element mapping of PDMAPS coated gradient wettability channels areas. (f) FTIR spectra of the pristine cotton fabric, the hydrophobic coated area, and the PDMAPS coated area of the temperature-responsive skin-like fabric.

After confirming the effects of PDMAPS on wettability of the fabric, the temperature-responsive skin-like fabric was prepared by grafting the monomer solution with 4 g of DMAPS in 20 ml solvent onto the gradient wettability channels of the skin-like fabric. As mentioned in Section 4.2.3, due to the hydrophobicity of the most area of the skin like fabric, the temperature-responsive polymer was only grafted on the top side of the gradient wettability channels during the “graft-from” process. A scanning electron microscope (SEM) was used to observe the changes of the surface morphology of the temperature-responsive skin-like fabric before and after the treatment. Compared with the pristine plant-structured cotton woven fabric (Figure 4.8a), a thin layer of coating on the surface of the PDMAPS grafted area can be clearly observed in the SEM image (see Figure 4.8c), which was very similar to the hydrophobic agent treated area (as shown in Figure 4.8b). However, when the two areas were observed within the same field of view, the PDMAPS grafted area and hydrophobic treated area exhibited distinct brightness contrast (Figure 4.8d). The gradient wettability channel area grafted with PDMAPS appeared darker than the hydrophobic agent treated area, which caused by the grafting of zwitterionic polymers enhanced electrical conductivity of the surface. This optical disparity confirms the compositional differences between the two surface treatments. Complementary EDS elemental mapping verified the sulfur distribution (characteristic element of PDMAPS), with significantly higher sulfur signal intensity (Figure 4.8e) in the darker PDMAPS region compared to the lighter hydrophobic-coated area, further validating the localized coating deposition.

The chemical composition of the fabric was characterized by FTIR spectroscopy (Figure 4.8f). Comparative analysis revealed distinct absorption peaks corresponding to carboxyl groups (C=O stretching at 1738 cm^{-1})[25, 137] and sulfonyl groups (S=O stretching at 1240 cm^{-1})[106, 135] in the PDMAPS coated region of the TR-MM fabric, which were absent in both the pristine plant-structured cotton fabric and the hydrophobic treated area of the (PDMAPS)-based temperature-responsive skin-like fabric. Additionally, the peak at 800 cm^{-1} was attributed to Si-C bonds from the TMSPMA coupling agent[16]. These spectroscopic results confirm the successful and uniform grafting of temperature-responsive PDMAPS polymer on the gradient wettability channels of the skin-like fabric, thereby imparting temperature-responsive properties to the functional textile.

4.3.3 Effect of the Grafting of PDMAPS on Directional Liquid Transport and Temperature-Responsive Properties of the Fabric

Table 4.1 Directional water transport rate and temperature-responsive property of the fabric.

Sample and Temperature		Weight of Transported water per hour	Water transport rate
(PDMAPS)-based temperature-responsive skin-like fabric	10°C	1.74 g	8700 $g \cdot m^{-2} \cdot h^{-1}$
	40°C	2.84 g	14202 $g \cdot m^{-2} \cdot h^{-1}$
Skin-like fabric prepared by the PVA-based method reported in Chapter 3	10°C	2.23 g	11150 $g \cdot m^{-2} \cdot h^{-1}$
	40°C	2.19 g	10950 $g \cdot m^{-2} \cdot h^{-1}$
Previous reported “skin-like” fabric[24]		—	6660 $g \cdot m^{-2} \cdot h^{-1}$

To evaluate the moisture management performance of the (PDMAPS)-based temperature-responsive skin-like fabric, the liquid water transport rate was measured by a homemade apparatus shown in Section 4.2.4. The results of the water transport rate are shown in Table 4.1. Here, the test was conducted for 1 hour, and the weight of transported water of every sample was weighed. There were 5000 channels per square meter in the samples, so the water transport rate ($g \cdot m^{-2} \cdot h^{-1}$) should be: *the weight of transported water per hour* × 5000 ($g \cdot m^{-2} \cdot h^{-1}$). According to the results obtained, the water transport rate of the skin-like fabric prepared by PVA method was similar at lower and higher temperatures, approximately 11000 $g \cdot m^{-2} \cdot h^{-1}$, which was almost 65% higher than that of the previous reported "skin-like" fabric by our group[24], which was 6660 $g \cdot m^{-2} \cdot h^{-1}$. This is caused by the structure of the gradient wettability channels on the fabric. The gradient wettability channels of previously reported skin-like fabric are small circles. Transported water accumulated on the outer side of the wettability channels in a hemispherical shape, which prevents the continuous transporting of water due to the surface tension. The liner wettability channels in this work enabled water to flow along the strip and drip faster. For the DMAPS-based temperature-responsive skin-like fabric, the water transport rate was 8700 $g \cdot m^{-2} \cdot h^{-1}$ at 10°C ambient temperature, since the coated temperature-responsive polymer was relative hydrophobic, resulting in a smaller wettability gradient between two sides of the wetting channels. When the ambient temperature was 40°C, the grafted PDMAPS became hydrophilic, and the water transport rate of the fabric increased to 14202 $g \cdot m^{-2} \cdot h^{-1}$. Compared to the commercial breathable and water repellent fabrics, the

(PDMAPS)-based temperature-responsive skin-like fabric allows liquid water to transport through. As a result, this temperature-responsive skin-like fabric is capable of transporting large amounts of sweat from the human body while also possessing water repellent properties[138].

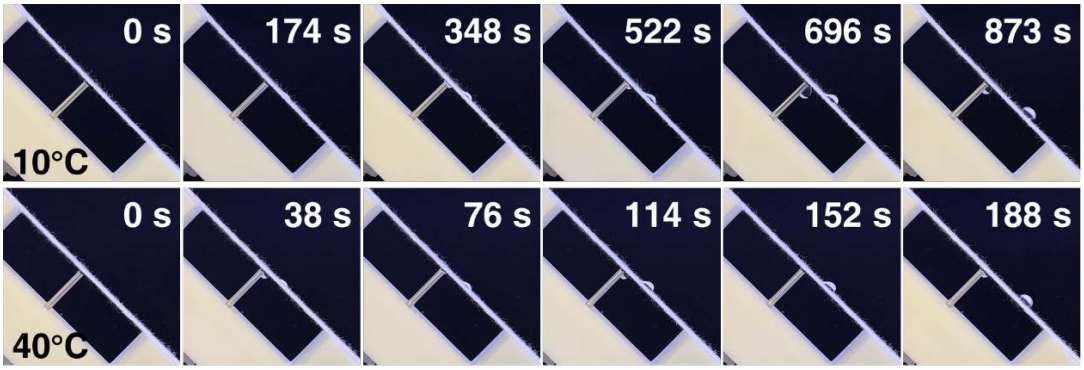

Figure 4.9 The directional liquid transport of artificial sweat through the (PDMAPS)-based temperature-responsive skin-like fabric.

In addition to water, the directional liquid transport properties of the (PDMAPS)-based temperature-responsive skin-like fabric were evaluated using artificial sweat prepared according to ISO 3160-2 (composition: 20 g/L NaCl, 17.5 g/L NH_4Cl, 5 g/L acetic acid, and 15 g/L lactic acid dissolved in deionized water, with pH adjusted to 4.7 using NaOH). As shown in Figure 4.9, the first droplet required 873 s to roll off the fabric at 10°C ambient temperature, significantly slower than the 188 s observed at 40°C. These results demonstrate the ability of (PDMAPS)-based temperature-responsive skin-like fabric to modulate its water (sweat) transport rate in response to environmental temperature changes, thereby enhancing its moisture management performance.

4.3.4 Effect of PDMAPS Coating on Water Repellency, Air Permeability, and Handle of the Fabric

The skin-like fabric prepared by PVA-based method exhibited excellent water repellency with hydrostatic pressure from the top side of the fabric being 76 mmH_2O. After applying PDMAPS on the surface, the water repellency of the fabric also changed as the variation of temperature. Figure 4.10a illustrates the hydrostatic pressure of the skin-like fabric prepared by PVA-based method and (PDMAPS)-based temperature-responsive skin-like fabric in different temperatures. Owing to the hydrophobic nature of the PDMAPS at 10°C, the hydrostatic pressure of the top and back sides of the fabric was 98 mmH_2O and 48 mmH_2O, respectively. Both of them are higher than that of the skin-like directional flow fabric, resulting in an enhanced water repellency of the fabric. When the ambient temperature increased to 40°C, the polymer PDMAPS transitioned to a hydrophilic state, leading to a lower hydrostatic pressure of both the top and back side of the fabric, which was 69 mmH_2O and 18 mmH_2O respectively. This dual-mode operation maintains water repellency while enabling facilitated water transport at elevated temperatures. To further evaluate the water repellency of the temperature-responsive skin-like fabric, the shower test was also conducted.

According to the result (Figure 4.10b), the water only remains on the top side of the gradient wettability channels after spraying with water with most of the top side being dry, which was similar with the skin-like directional flow fabric. On the back side of the fabric, there is no water penetrated, and it remains dry. The coating of the temperature-responsive polymer did not affect the water repellency of the fabric.

Figure 4.10 The water repellency and air permeability of the fabrics. (a) Hydrostatic pressure of the skin-like fabric and (PDMAPS)-based temperature-responsive skin-like fabrics. (b) Image of shower test of temperature-responsive skin-like fabrics and air resistance of the temperature-responsive skin-like fabric. (c) Demonstration of the air permeability and water repellency of the temperature-responsive skin-like fabric.

The air permeability of the temperature-responsive skin-like fabric was also checked. The air resistance of the temperature-responsive fabric (0.339 $kPa \cdot s \cdot m^{-1}$) was 2.7% higher than that of the pristine plant-structured cotton woven fabric and skin-like directional liquid flow fabric prepared in Chapter 3. The air resistance of the temperature-responsive skin-like fabric was slightly higher than that of the skin-like fabric due to the reduce of the pore size of the fabric caused by the grafting of PDMAPS. The demonstration of the air permeability and water repellency of the fabric was conducted using the apparatus shown in Figure 3.11. The fabric was fixed in the middle of two acrylic tubes, and the top side of the fabric is facing up. When a certain volume of water was introduced into the upper tube, no liquid penetration through the fabric was observed. Meanwhile, compressed air was pumped into the acrylic tube below the fabric through the valve on the acrylic tube. It was observed that the gas passed through

the fabric and created bubbles in the water. The observations conclusively demonstrate that the temperature-responsive skin-like fabric maintains exceptional air permeability and water repellency.

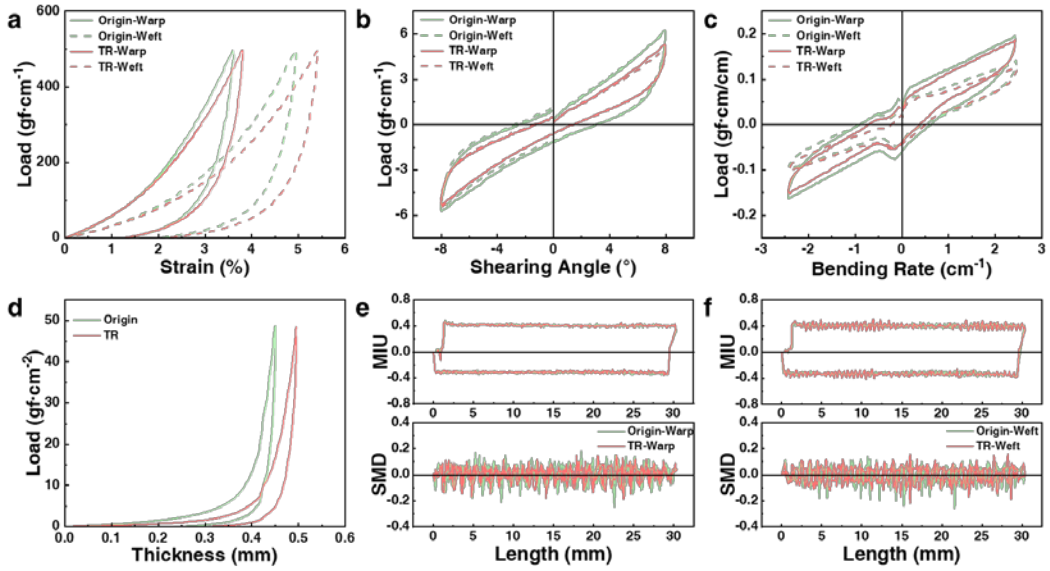

Figure 4.11 The low stress mechanical properties of the original fabric and the TR-MM fabric, including (a) tensile property, (b) shearing property, (c) bending property, (d) compression property, and surface properties in (e) warp direction and (f) weft direction. The MIU represents the frictional coefficients and the SMD means the surface roughness.

In addition, the low stress mechanical properties tested using KES-FB system (Figure 4.11) show that the handle of the treated TR-MM fabric is almost the same as the original fabric. The coating of PDMAPS on the fabric did not affect the mechanical properties of the fabric, and this kind of temperature-responsive self-adjusting fabric has the potential to greatly improve the comfort of clothing.

4.3.5 Discussion on the Mechanism of Temperature-responsive Skin-like Directional Liquid Flow Fabric

The mechanisms involved in the directional water transport and moisture management of the temperature-responsive skin-like fabric have been analyzed, with the directional flow of the liquid in the gradient channels of the fabric being explained in terms of the Gibbs pinning criterion[72, 77, 139]. The cross-section of the yarn can be approximated by a circle, with the water flowing through the channels between the yarns, the channels varying in size along the flow direction (see Figure 4.12a-c). Here, the wall angle α of the channel is used to represent the slope (expanding and narrowing) of the channels, it being the angle between the tangent to the cross-section of the yarn and the liquid flow direction and ranging from -90° to 90°. When $\alpha > 0$, the channel is expanding, and when $\alpha < 0$, it is narrowing.

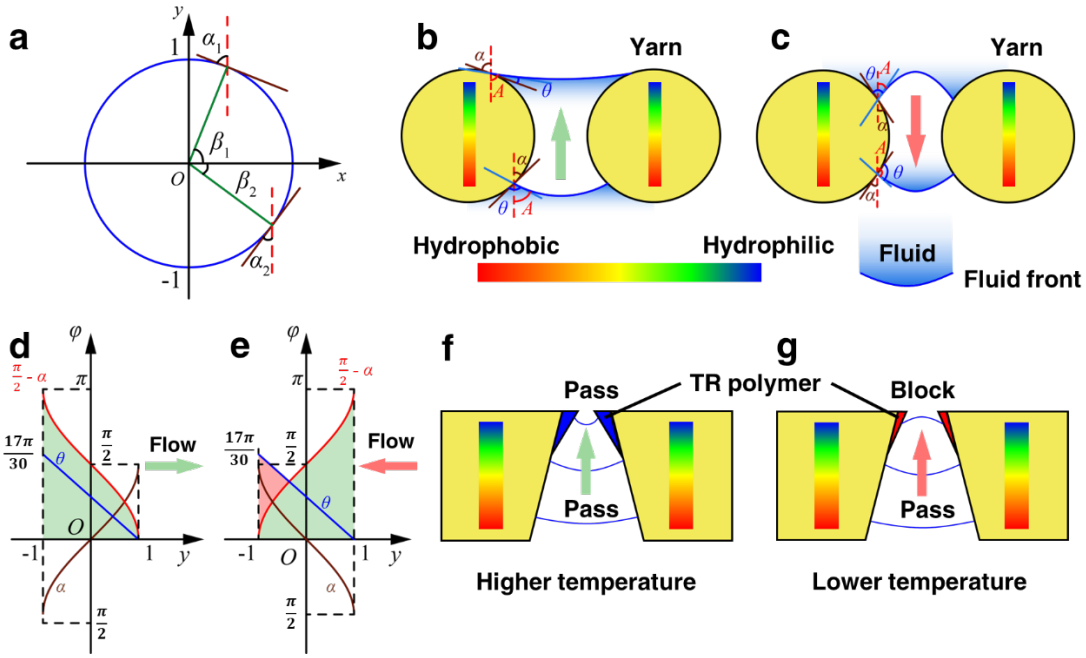

Figure 4.12 Mechanism of temperature-responsive skin-like directional flow fabric. (a) Illustration of the circular yarn cross-section and wall angle α. (b) and (c) Illustration of the directional water

transport through the gradient channel between yarns. (d) and (e) The range of contact angles θ which satisfies the condition of directional water transport. (f) and (g) Illustration of water transport through the temperature-responsive skin-like fabric at lower and higher temperatures.

As illustrated in Figure 4.12a, the unit circle in the figure represents the cross-section of the yarn, with the liquid flow direction along the positive direction of the *y*-axis, α_1 being a positive value and α_2 a negative value. Here, β represents the acute angle between the x-axis and the line connecting the point on the fiber to the center of the circle. It is clear from the figure that α and β are numerically equal, so that the relationship between α and the fluid front *y* is $\alpha = \arcsin y$. The possible mechanism of the directional liquid transport for the temperature-responsive skin-like fabric is illustrated in Figure 4.12b-c. The contact angle between the water and the yarn surface is represented by θ. The advance angle, $A = \alpha + \theta$, represents the angle between the liquid surface and the direction of liquid advancement. The value of *A* determines the shape of the liquid surface. When $A < 90°$, the liquid surface is concave, and the surface tension of the liquid pulls the liquid forward; when $A > 90°$, the liquid surface is convex, and the surface tension hinders the liquid flow[72, 77]. If water flows from the hydrophobic side (Figure 4.12b), even if the contact angle $\theta > 90°$, the liquid can still flow to the hydrophilic side, with $A < 90°$ since $\alpha < 0$. When the water reaches the hydrophilic side, although $\alpha > 0$, the contact angle θ is small and close to 0, so *A* is still less than 90°. In fact, as shown in Fig. Figure 4.12d, as long as $A < \frac{\pi}{2}$, that is, $\theta < \frac{\pi}{2} - \alpha$ (green area in Figure 4.12d-e), the water will move forward continuously. According to the experimental data shown in Figure 3.13b, the water contact angle on the hydrophobic

side is 102° ($\frac{17\pi}{30}$rad). There is a wettability gradient (contact angle gradient) between two sides of the gradient wettability channels on the skin-like fabric. The blue curve in the figure can represent the contact angle gradient in the wettability channel ($0 < \theta < \frac{17\pi}{30}$). When water flows from the hydrophobic side to the hydrophilic side, the contact angle always satisfies $\theta < \frac{\pi}{2} - \alpha$. As a result, water can flow (i.e., be transported) easily. Similarly, when water flows from the hydrophilic side to the hydrophobic side (Figure 4.12c), the contact angle θ on the hydrophilic side is less than 90°, and $\alpha < 0$, so $A < 90°$, the liquid front surface is a concave and the liquid moves forward spontaneously. Nevertheless, when the water reaches the hydrophobic side, the water flow is blocked, since the contact angle $\theta > 90°$ and $\alpha > 0$, $A > 90°$. In Figure 4.12e, the water flows in the negative direction of the *y*-axis. The red region in the figure does not satisfy $\theta < \frac{\pi}{2} - \alpha$, and the water flow is hindered. Hence, it is more difficult for the water to flow from the hydrophilic side to the hydrophobic side.

The plant-structured fabric is used as the substrate for the temperature-responsive skin-like fabric, hence the gradient wetting channel can be simplified to a trapezoidal one as illustrated in Figure 4.12f-g. If the water flows from the larger pores side to the smaller pores side, the channel is narrowing ($\alpha < 0$). At a higher temperature (Figure 4.12f), the temperature-responsive polymer becomes hydrophilic, $\theta < 90°$, and water passes through it more easily, with the polymer swelling after absorbing water, resulting in a smaller α, which is more conducive to the water flow. At a lower temperature (Figure 4.12g), the temperature-responsive polymer becomes hydrophobic, $\theta > 90°$, even though $\alpha < 0$ at this time, with the water transport being hindered somewhat.

Hence, the temperature-responsive skin-like fabric has a higher water transport rate at higher temperatures than at lower temperatures.

4.4 Summary

In this chapter, a temperature-responsive skin-like fabric with directional liquid flow and water repellent properties was developed. The temperature-responsive polymer PDMAPS was applied to the surface of the gradient wettability channels on the skin-like fabric prepared in Chapter 3. The temperature-responsive water transport behavior of the fabric originates from the inherent properties of the grafted temperature-responsive polymer. As temperature rises, sweat transport from the skin was significantly accelerated. Conversely, under decreased temperatures, both water and sweat transport rates reduced while the outer surface of the fabric transitioned to a more hydrophobic state, consequently enhancing its hydrostatic pressure resistance (i.e., improved water repellency). The underlying liquid transport mechanism follows the Gibbs pinning criterion. Meanwhile, the treatment process preserved fiber structure of the fabric, and hence neither are the fabric mechanical nor wear properties. The optimized fabric exhibited a high directional water transport rate of 14202 $g \cdot m^{-2} \cdot h^{-1}$ at higher temperatures and performed well in terms of water repellency (hydrostatic pressure resistance) and air permeability. These characteristics render the fabric particularly suitable for advanced smart moisture management apparel applications.

Chapter 5 [Poly(AAm-co-AN)]-based Non-ionic UCST-type Temperature-responsive Skin-like Textiles

5.1 Introduction

Temperature-responsive textiles exhibit dynamic, reversible modulation of wettability, morphological structure, and thermal insulation properties in response to temperature variations[95, 97, 140], rendering them highly promising functional materials for extreme temperature variations[88, 98, 141-143]. By adaptively regulating heat dissipation and moisture transfer, these smart fabrics significantly improve personal thermal and moisture comfort under extreme or rapidly change of the temperature[84, 144], providing dual benefits of health preservation and energy efficiency. These properties have drawn considerable research interest, leading to diverse applications in temperature-variable scenarios, such as moisture harvesting[85, 86], oil-water separation[87], soft robotics[145], and thermal/moisture management[146]. In Chapter 4, the (PDMAPS)-based temperature-responsive skin-like fabric was prepared by grafting the zwitterionic UCST-type polymer onto the skin-like fabric. Although this fabric offers advantages such as facile fabrication and rapid response to temperature, it still faces the following issues: (i) limited transition temperature tunability, restricting their operational temperature range[107]; (ii) electrolyte-dependent transition temperature instability in ionic-type temperature-responsive polymers[109]; (iii) inadequate control over surface hydrophobic-hydrophilic balance, leading to loss of temperature-responsive functionality at

interfaces[114]. These intrinsic limitations hinder the application of (PDMAPS)-based temperature-responsive skin-like fabric in next-generation functional garments.

Current UCST research primarily focuses on zwitterionic poly(sulfobetaine)[25, 27]. Their temperature-responsiveness originates from temperature-driven ionic group association/dissociation[105, 109]. However, several fundamental constraints hinder their practical application. The phase transition temperature of zwitterionic polymers is highly sensitive to both polymer and electrolyte concentrations[93, 109]. In wearable or wound dressing applications, individual differences in body fluids composition and pathological conditions[110-112], which would unpredictably modulate the transition temperature, leading to inconsistent performance across users. Seawater or industrial wastewater with complex ionic compositions also lead to unreliable performance when these materials are used in oil-water separation. In addition, most zwitterionic polymers suffer from limited tunability of transition temperatures and inability to adapt to application-specific requirements, restricting their operational scope.

A breakthrough came in 2012 when Seuring and Agarwal[109] pioneered a universal approach for synthesizing non-ionic UCST type polymers. Unlike conventional zwitterionic systems, these polymers achieve temperature-responsiveness through hydrogen bonding networks rather than ionic interactions[113-115]. Among these non-ionic UCST type polymers, poly(acrylamide-co-acrylonitrile) [poly(AAm-co-AN)] has emerged as particularly promising due to precise UCST tunability via comonomer ratio adjustment and minimal thermal hysteresis during heating/cooling cycles. Despite these advantages, some limitations hinder textile applications. The polymer exhibits

hydrophilicity at high concentration. It is difficult to precisely balance the hydrophilicity and hydrophobicity of the surface applied with poly(AAm-co-AN). While previous studies have demonstrated successful creation of temperature-responsive surfaces by incorporating hydrophobic components onto poly(AAm-co-AN)-coated AAO substrates[28], these approaches prove inadequate for textile applications due to the difficulty in precisely controlling the surface hydrophilic-hydrophobic balance on fibrous substrates. The complex three-dimensional structure and chemical heterogeneity of textile surfaces further exacerbate these limitations, making conventional coating techniques ineffective for achieving reliable temperature-responsive performance.

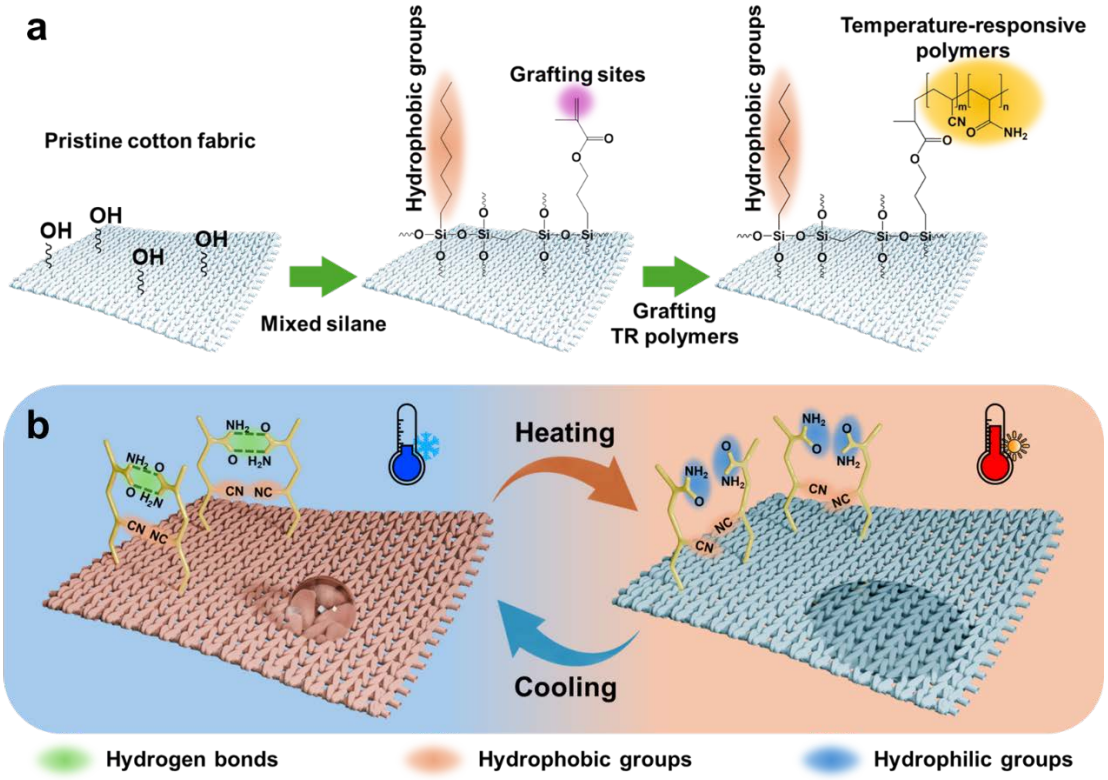

Figure 5.1 Scheme of the non-ionic UCST type temperature-responsive smart fabric. (a) Surface modification of fabric. (b) Reversible wettability of the temperature-responsive fabric.

To address the limitations, in this chapter, a novel [poly(AAm-co-AN)]-based non-ionic UCST-type temperature-responsive (NiTR) skin-like fabric was developed. Fristly, the NiTR cotton knitted fabric was prepared as the substrate of skin-like fabric using a “grafting-from” method. We developed a novel mixed silane treatment strategy that enables precise control over both polymer concentration and surface wettability in textile substrates. Our approach involves sequential treatment of cotton fabric with an optimized mixture of hydrophobic silane, silane crosslinker, and grafting-functionalized silanes, followed by in-situ grafting of poly(AAm-co-AN) via a “graft-from” polymerization technique (Figure 5.1). By systematically varying the silane composition and monomer ratios (AAm:AN), we successfully fabricated a NiTR fabric with tunable transition temperatures that exhibits excellent reversibility and electrolyte-independent behavior. This smart textile demonstrates a sharp hydrophobic-to-hydrophilic transition (contact angle change from >120° to 0°) at the UCST threshold, maintaining stability under physiological and high-salinity conditions. Finally, the NiTR fabric was treated by PVA-based method to develop the NiTR skin-like fabric (As shown in Figure 5.14). This breakthrough overcomes the major limitations of conventional zwitterionic UCST materials, offering promising applications in intelligent sportswear, where reliable temperature-responsive performance is critical.

5.2 Fabrication and Evaluation of the NiTR Fabric as the Substrate

5.2.1 Materials

Cotton, polyester, and Coolmax knitted fabrics were purchased from local stores. 1,2-Bis(triethoxysilyl)ethane (BTEOSE, 96%), n-Octyltrimethoxysilane (OTMS, 97%), 3-(Trimethoxysilyl)propyl methacrylate (TMSPMA,97%), Sodium hydroxide (NaOH, AR, 96%), and Acrylamide (AAm, AR, 99.0%) were purchased from Shanghai Aladdin Biochemical Technology Co., Ltd. in China. Acrylonitrile (AN, 99%) was obtained from Shanghai Macklin Biochemical Technology Co., Ltd., China. Acetic acid (AR) and 2-Hydroxy-2-methylpropiophenone (photo-initiator 1173, 98%) were purchased from Dieckmann (Hong Kong) Chemical Industry Co., Ltd. Ethyl alcohol (ethanol, absolute, ACS grade) and Dimethyl sulfoxide (DMSO, ACS grade) was supplied by Anaqua Global International Inc. Limited, Hong Kong.

5.2.2 Fabrication Processes

Pretreatment of the Fabric using Mixed Silane Solution

To precisely balance the hydrophilicity and hydrophobicity of the surface applied with poly(AAm-co-AN), we present a novel mixed silane surface engineering approach that can control both surface wettability and temperature-responsive polymer concentration in textile substrates. This strategy involves a mixed silane pretreatment system comprising OTMS as a hydrophobic modifier, BTEOSE as a crosslinker to enhance durability, and TMSPMA as a polymer grafting anchor. This unique

combination creates a tunable interface where the OTMS:TMSPMA ratio regulates the hydrophilic-hydrophobic balance and the density of available grafting sites. During the silanization process, the mixed silane components underwent hydrolysis, converting the alkoxy groups (Si-O-CH_3 or Si-O-CH_2CH_3) to reactive silanol groups (Si-OH). These newly formed silanol groups then established hydrogen bonds with the hydroxyl groups (-OH) present on the fabric surface. Subsequent thermal curing induced a dehydration condensation reaction, resulting in the covalent immobilization of the silane network onto the textile substrate through stable Si-O-Si and Si-O-cellulose linkages (as shown in Figure 5.2).

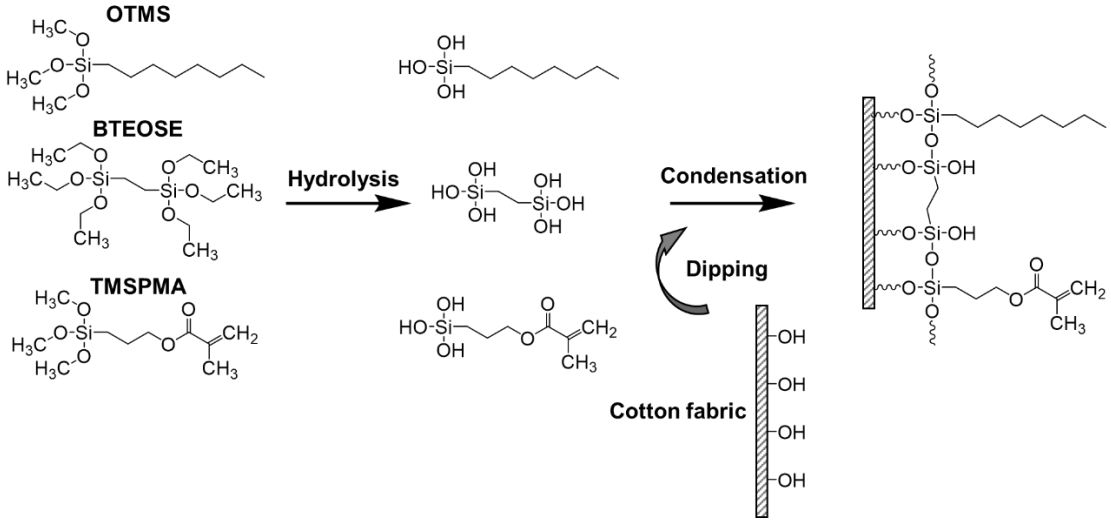

Figure 5.2 Chemical reaction mechanism of mixed silane treatment.

The mixed silane solutions were prepared by dissolving OTMS, BTEOSE, and TMSPMA in a 90 vol% aqueous ethanol solution at specific concentrations. To explore the optimal ratio of mixed silane solutions, five silane solutions were prepared. The total silane concentration in the solution was 0.9 mol/L, and the molar ratio of these

three silanes is listed in Table 5.1. Acetic acid was then added to adjust the pH to 4-5. The mixture was stirred overnight at room temperature on a magnetic stirrer to facilitate hydrolysis. The pristine cotton knitted fabric was thoroughly cleaned with a 0.5 wt% NaOH solution at 80°C for 2 h. The fabric was then rinsed three times with deionized (DI) water and dried in an oven at 60°C. Next, the mixed silane solution was applied to the fabric via dip coating, with a liquor pick-up of 120%. Finally, the coated fabric was cured at 105°C for 2 h.

Table 5.1 Mixed silane solution with different molecular ratio of silanes.

Sample	OTMS : BTEOSE : TMSPMA (mol)
1	0.3 : 0.3 : 0.3
2	0.35 : 0.3 : 0.25
3	0.4 : 0.3 : 0.2
4	0.45 : 0.3 : 0.15
5	0.5 : 0.3 : 0.1

Preparation of the NiTR Fabric

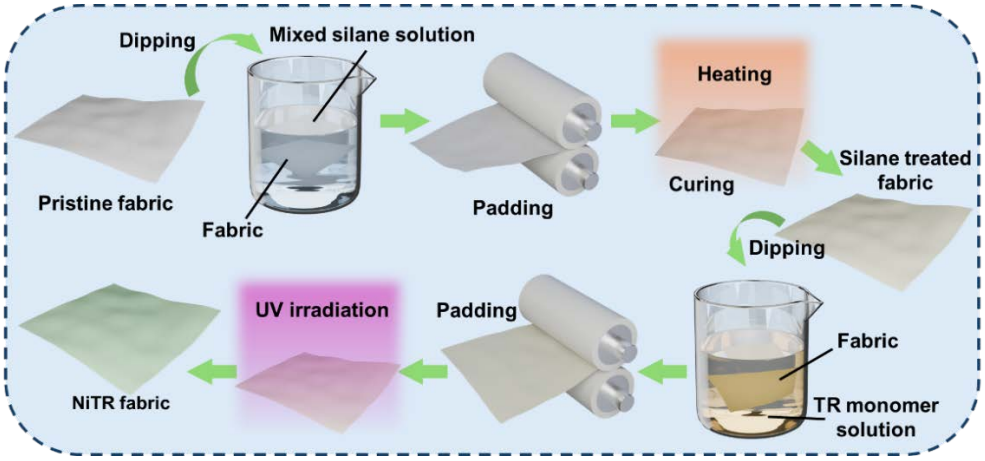

Figure 5.3 Preparation of the NiTR fabric.

Being pretreated with the mixed silane solution, the subsequent poly(AAm-co-AN) grafting process occurs exclusively at the double bond of TMSPMA through a dip coating and free radical polymerization process (Figure 5.3). This site-specific grafting approach ensures covalent attachment of poly(AAm-co-AN) chains, preservation of the silane-modified surface properties, and controlled polymer loading on the surface (see Figure 5.1a).

The monomer solutions of the temperature-responsive polymer, poly(AAm-co-AN) were prepared. Firstly, AAm and photo-initiator 1173 were dissolved in DMSO. Nitrogen gas was pumped into the solution for 15 min to remove the dissolved oxygen in the solution. Finally, AN was added to the solution before grafting. The concentration of the monomers was 3 mol/L, and the molar ratios of AN were 11 mol%, 12 mol%, 13 mol%, 14 mol%, and 15 mol%, respectively. The pretreated fabric was immersed in the monomer solution. A padder was used to remove the excess liquid, achieving a liquor pick-up of 120%. Afterwards, the fabric was exposed to a UV lamp with a wavelength of 365 nm to initiate the grafting process. After 20 minutes, the fabric was rinsed three times with DI water and dried at 60°C.

5.2.3 Characterization

The wettability of the fabrics was characterized by measuring the contact angle of the surface using a contact angle tester (SDC-350, Dynetech, Guangdong, China), with a droplet volume of 5 μL during the test.

The surface morphology of the fabric was observed using a scanning electron microscope (SEM, VEGA3, TESCAN, U.K.), with a thin layer of gold deposited on the fabrics to enhance conductivity.

The chemical composition of the fabrics was analyzed using energy-dispersive X-ray spectroscopy (EDS, VEGA3, TESCAN, U.K.) and Fourier-transform infrared spectroscopy (FTIR, Spectrum 100, PerkinElmer, USA).

The temperature-responsive wettability was also measured with the contact angle tester, equipped with a temperature-controlled platform to regulate the surface temperature of the fabrics.

The air permeability of the fabric was tested by an air permeability tester (KES-F8-AP1, KATO Tech Co., Ltd., Japan). The water vapor permeability of the fabric was measured following BS 7209:1990 standard.

The handle of the fabric was characterized by measuring the low stress mechanical properties of the fabric using KES-FB system (KATO Tech Co., Ltd., Japan), with the sample size being 20 cm × 20 cm.

5.2.4 Results and Discussion

Effect of the Ratio of the Mixed Silane Solution on the Wettability of the Fabric

The poly(AAm-co-AN) copolymer exhibits well-defined UCST behavior with a tunable phase transition temperature controlled by the acrylamide-to-acrylonitrile ratio. This temperature-responsive behavior stems from the association and dissociation of

inter- and intra-molecular hydrogen bonds as well as the interactions between hydrophilic amide and hydrophobic nitrile groups in its molecular chains[147, 148] (Figure 5.4a). Below the UCST threshold, the aqueous solution became turbid due to polymer aggregation driven by dominant hydrogen bonding networks and hydrophobic microdomain formation, while heating above the UCST resulted in complete dissolution characterized by solution clarification through hydrogen bond disruption and polymer chain hydration (As shown in Figure 5.4b). However, the surface functionalization of textiles with poly(AAm-co-AN) to develop temperature-responsive fabrics faces substantial technical challenges. The hydrophilicity of the polymer at high concentrations, arising from the abundant amide groups in its structure, results in completely hydrophilic textile surfaces regardless of temperature when directly applied to naturally hydrophilic cotton substrates. This behavior fundamentally eliminates the desired temperature-responsive wettability switching capability.

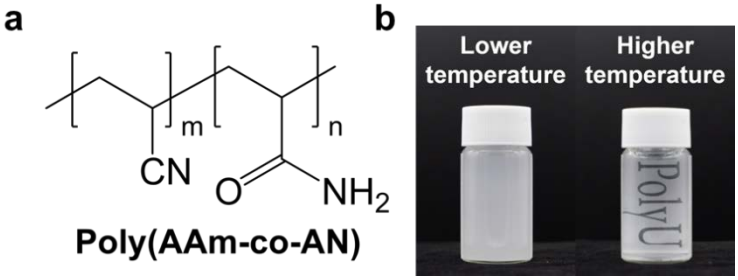

Figure 5.4 (a) Molecular structure of poly(AAm-co-AN). (b) Different forms of poly(AAm-co-AN) aqueous solution at high and low temperatures.

To establish the optimal hydrophobic-hydrophilic balance, cotton knitted fabrics were treated with different silane solutions (As shown in Table 5.1). The molar ratio of

OTMS to TMSPMA ranged from 0.3:0.3 to 0.5:0.1. The treated cotton fabrics became hydrophobic due to the introduction of silane. Subsequently, poly(AAm-co-AN) with 13 mol% AN content was grafted onto the five fabrics mentioned above. Previous studies have reported that the phase transition temperature of poly(AAm-co-AN) with 13.5% of AN in aqueous solution is approximately 30°C[109]. Therefore, the water contact angles of these five fabrics were measured at both 15°C and 40°C to evaluate their temperature-responsive wettability.

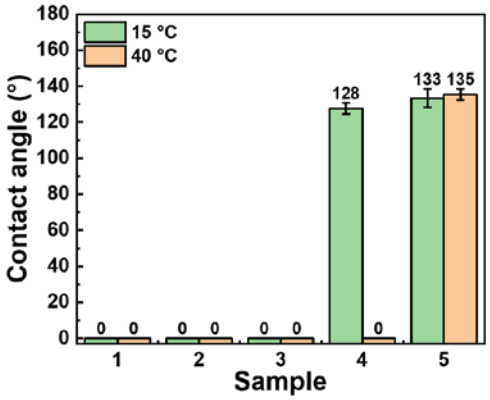

Figure 5.5 Water contact angle of the NiTR fabrics treated with different mixed silane solutions at different temperatures.

As shown in Figure 5.5 and referring to Table 5.1, as the molar ratio of OTMS to TMSPMA was lower than 0.4:0.2, the fabrics grafted with poly(AAm-co-AN) were completely hydrophilic, exhibiting a water contact angle of 0° at both lower and higher temperatures. This behavior can be explained by the high proportion of TMSPMA, which leads to an excessive grafting of poly(AAm-co-AN) and results in a predominantly hydrophilic fabric surface. In contrast, as the molar ratio of TMOS to

TMSPMA increased to 0.5:0.1, the surface properties changed, and the fabric became hydrophobic, with water contact angles exceeding 130° at both higher and lower temperatures. The increase in TMOS content promotes the presence of hydrophobic groups on the fabric surface, rendering hydrophobicity the dominant property. It should be noted that when the ratio of OTMS to TMSPMA was 0.45:0.15 according to Table 5.1, the poly(AAm-co-AN) grafted fabric exhibited temperature-responsive wettability, with a water contact angle of 128° at 15°C and 0° at 40°C. The optimized OTMS:TMSPMA molar ratio achieves the ideal hydrophilic-hydrophobic balance for poly(AAm-co-AN) to exhibit its temperature-responsive properties. Therefore, in subsequent experiments, this optimized mixed silane solution formulation will be employed for fabric pretreatment.

Effect of the Ratio of the Temperature-responsive Monomer Solution on the Transition Temperature of the NiTR Fabric

The transition temperature of the NiTR fabric can be tuned by controlling the AN content during poly(AAm-co-AN) synthesis[118], demonstrating a positive correlation between AN concentration and transition temperature. Five fabric samples were prepared by grafting poly(AAm-co-AN) with varying AN content (11-15 mol%) onto optimally silane (OTMS:TMSPMA=0.45:0.15) pretreated cotton knitted fabric. Contact angle measurements revealed sharp hydrophobic-to-hydrophilic transitions (>120° to 0°) for all samples Figure 5.6a), with transition temperatures systematically increasing with AN content (Figure 5.6b). The tunablility of the transition temperature

expands the NiTR fabric's potential for a wide range of applications. Of particular significance, the 13 mol% AN formulation achieved a transition between 32.5-35°C, which is close to human skin temperature. This enables the fabric to be a promising candidate for applications in the apparel industry. Unless otherwise noted, the subsequent tests in this study employed this 13 mol% AN formulation.

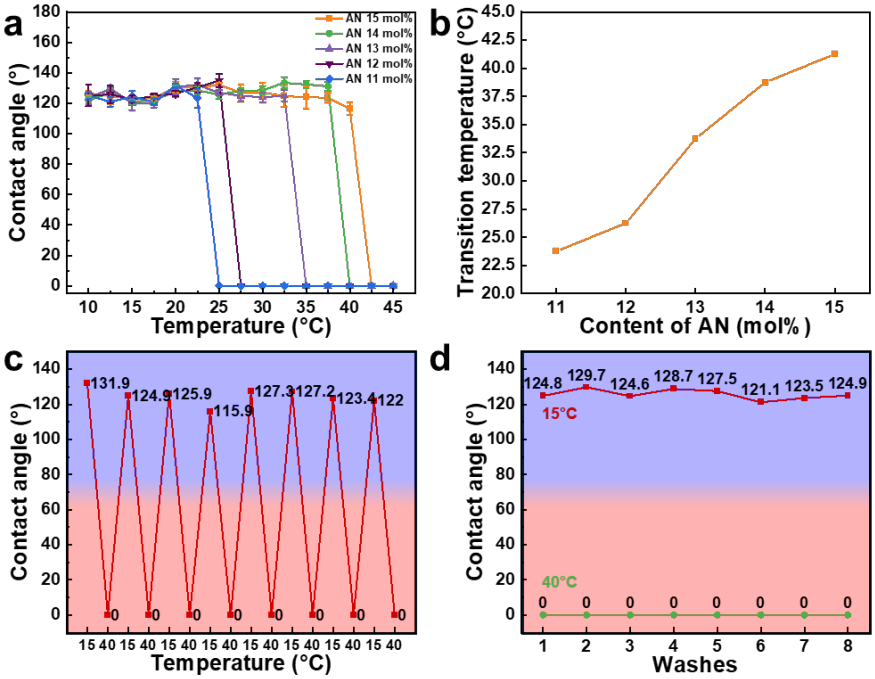

Figure 5.6 Temperature-responsive properties of the NiTR fabrics. (a) Water contact angles of NiTR fabrics grafted with monomer solutions with different AN content at different temperatures. (b) Transition temperatures of the fabrics treated with monomer solution with different AN content. (c) Repeated tests of water contact angles of the NiTR fabric at both higher and lower temperatures. (d) Water contact angles of NiTR fabrics at both higher and lower temperatures after multiple washes.

The wetting behavior of the fabric was recorded at both lower and higher temperatures using a contact angle tester, with 5 μL of water. At 15°C, the fabric

maintained a high water contact angle for 90 seconds. In contrast, at 40°C, the fabric quickly became wetted, with the contact angle decreasing within 10 seconds (see Figure 5.7). The temperature-responsive wettability of the fabric is also reversible. The water contact angle of the NiTR fabric was alternately measured at 15°C and 40°C for 8 cycles (Figure 5.6c). All contact angles at 40°C were 0°, while those at 15°C remained consistently above 115°, showing minimal change after 8 cycles. This excellent wettability reversibility is attributed to the breaking and reorganization of hydrogen bonds within the poly(AAm-co-AN) molecules[109].

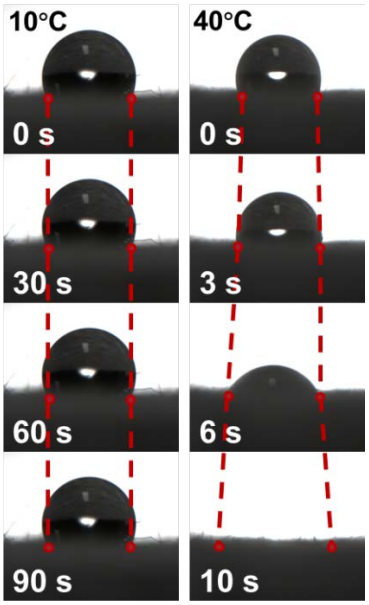

Figure 5.7 Wetting time of the NiTR fabric at lower and higher temperatures.

Moreover, the NiTR polymer also demonstrated remarkable durability. The NiTR fabric was subjected to 8 washing cycles in ethanol using an ultrasonic cleaner, with each cycle lasting 10 min. Subsequently, the contact angles of the fabric were measured after each wash at both 15°C and 40°C. Even after 8 washes, the fabric retained its

temperature-responsive wettability (Figure 5.6d), which can be attributed to the covalent bonding between the polymer and the fabric.

Effect of the Poly(AAm-co-AN) coating on the Morphology and Chemical Compound of the Fabric

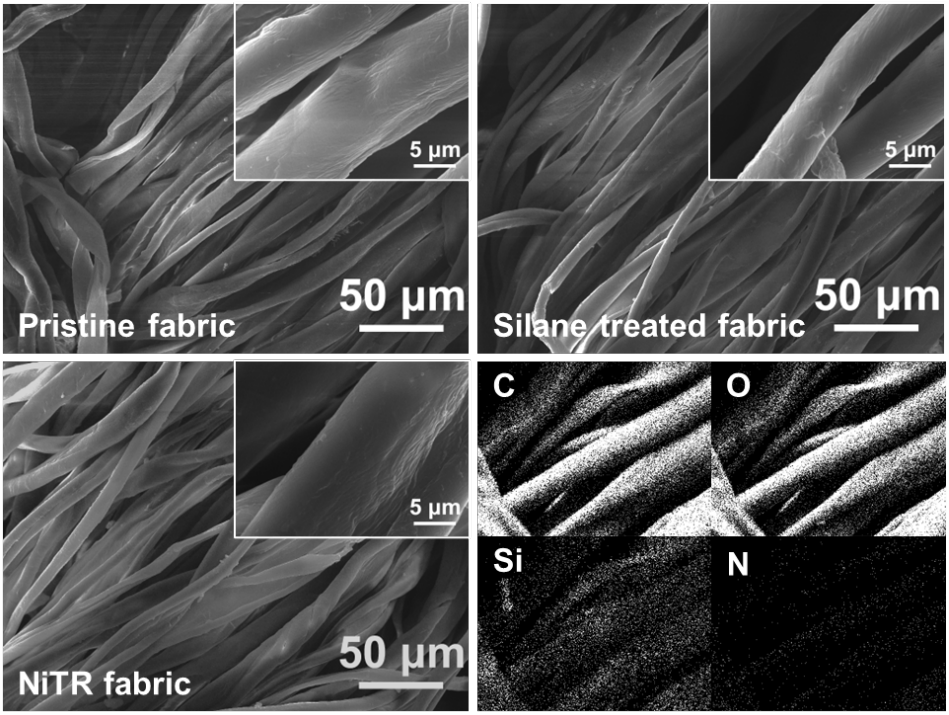

Figure 5.8 SEM image of pristine fabric, silane treated fabric and NiTR fabric as well as the element mapping of NiTR fabric.

The surface morphology and chemical compounds of the pristine cotton fabric, silane treated cotton fabric, and NiTR cotton fabric were also evaluated by scanning electron microscope (SEM), energy-dispersive X-ray spectroscopy (EDS) and Fourier-transform infrared spectroscopy (FTIR). As observed in the SEM images (Figure 5.8), there was no significant difference between these three fabrics, indicating that the silane

and poly(AAm-co-AN) primarily interact with the outermost surface of the fabric without causing any disruption to the fiber structure. Thus, this treatment will not affect other fundamental properties of the fabric, such as mechanical properties, air permeability, water vapor transmission, and pore size distribution. The elemental mapping of the fabric revealed that the surface elements of the fabric have changed after treatment. The silicon element was attributed to mixed silane, while the nitrogen element originated from poly(AAm-co-AN). The FTIR spectrum (Figure 5.9) also showed changes in the chemical composition of the fabrics. Compared to the pristine fabric, the silane treated fabric exhibited a peak at 800 cm^{-1} and 1724 cm^{-1}, which was attributed to Si-C in silane[16] and C=O in TMSPMA[131], respectively. The peak 1670 and 1450 observed in the NiTR fabric were caused by C=O (in amide) and -CH_2 groups in the poly(AAm-co-AN)[149].

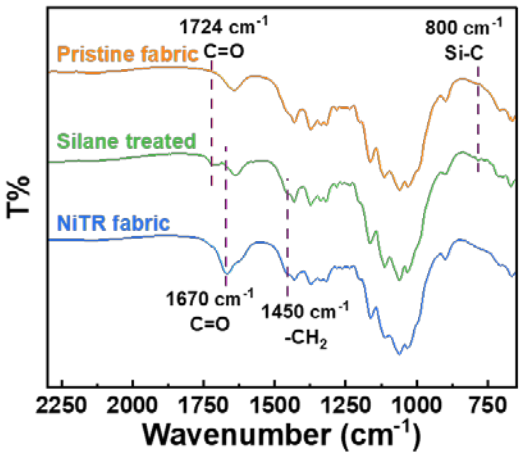

Figure 5.9 FTIR spectrum of pristine fabric, silane treated fabric and NiTR fabric.

Effect of the Electrolyte Concentration on the Transition Temperature of the Temperature-responsive Fabrics

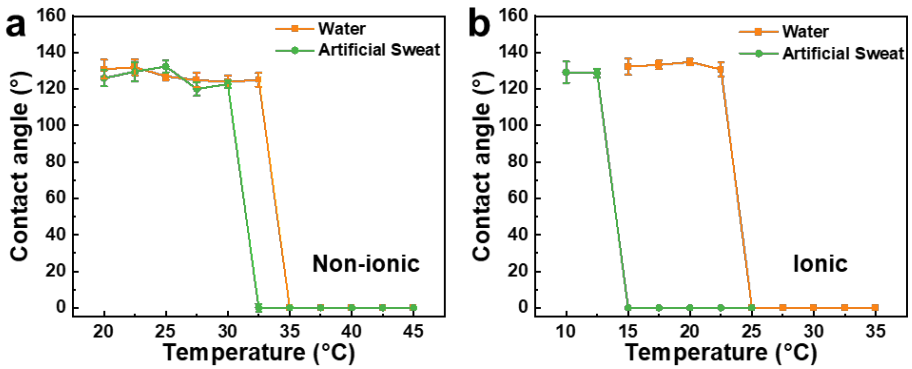

Figure 5.10 Water and artificial sweat contact angles of (a) poly(AAm-co-AN) grafted fabric (non-ionic) and (b) PDMAPS grafted fabric (ionic).

Compared to zwitterionic UCST type polymers, non-ionic UCST type polymers exhibit enhanced stability against electrolyte variation. To demonstrate the merits of the non-ionic polymer, ionic temperature-responsive cotton fabrics grafted with the zwitterionic polymer PDMAPS were prepared using the same method as described in Chapter 4. The contact angles of the zwitterionic temperature-responsive fabric and NiTR fabric were measured using both deionized (DI) water and artificial sweat (prepared according to ISO 3160-2, as described in Section 4.3.3) at different surface temperatures. As shown in Figure 5.10a-b, the transition temperature of the NiTR fabric was observed 32.5-35°C when tested with DI water, and 30-32.5°C when tested with artificial sweat. In contrast, the transition temperature of the zwitterionic temperature-responsive fabric exhibited electrolyte-dependent transition behavior, with the transition temperature shifting significantly from 22.5-25°C in DI water to 12.5-15°C

in artificial sweat. The temperature-responsive wettability of ionic temperature-responsive polymers arises from the association and dissociation of ionic bonds within the molecular chains[150], which is strongly influenced by the concentration of electrolytes. The electrolyte composition of bodily fluids exhibits significant individual variation[110-112] depending on health status and physical activity levels. This variability causes ionic temperature-responsive fabrics to demonstrate user-dependent transition temperatures, while non-ionic systems maintain consistent temperature-responsive properties across all physiological conditions.

Effect of the Substrates on the Temperature-responsive Property of the NiTR Fabric

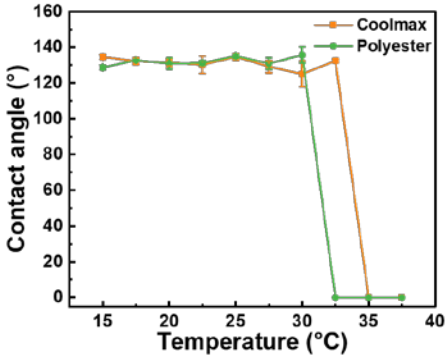

Figure 5.11 Water contact angles of the NiTR fabrics prepared using Coolmax and polyester as substrates at different temperatures.

The developed method in this chapter exhibits broad substrate compatibility. To demonstrate the broad applicability of this fabrication process, the non-ionic UCST-type temperature-responsive polymer, poly(AAm-co-AN) was successfully grafted onto various fabrics including polyester and Coolmax based on the method described

in this chapter. Before the grafting of poly(AAm-co-AN), the polyester and Coolmax were hydrolyzed in a 5% NaOH solution to increase active groups such as hydroxyl groups. The grafted NiTR fabrics demonstrated temperature-responsive wettability on both substrates as shown in Figure 5.11. These fabrics exhibited hydrophobicity at lower temperatures and became hydrophilic with the temperature increased, with the transition temperatures between 30-35°C, confirming the method's compatibility with synthetic textiles.

Effect of the Poly(AAm-co-AN) coating on the Wearing Performance of the NiTR Fabric

Table 5.2 Air resistance, water vapor permeability of pristine fabric and NiTR fabric.

Sample	**Air Resistance ($kPa \cdot s \cdot m^{-1}$)**	**Water Vapor Permeability ($g \cdot m^{-2}/day$)**
Pristine fabric	0.5126	850.073
NiTR fabric	0.6312	834.981

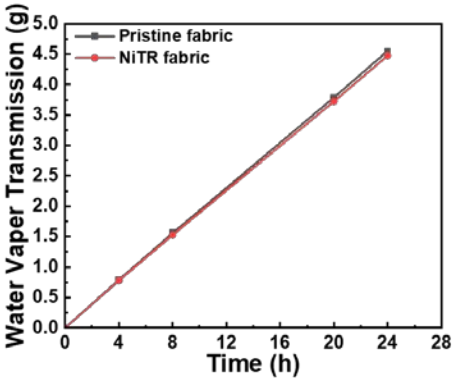

Figure 5.12 Water vapor transmission curve of the pristine fabric and NiTR fabric over 24 hours.

Despite the remarkable temperature-responsive behavior of NiTR fabrics, factors such as air permeability, water vapor transmission, and handle are essential for ensuring their comfort and practicality in garment use. Here, the air permeability of the fabric was characterized by air resistance, and the water vapor permeability was measured according to the standard BS 7209:1990. As shown in Table 5.2, the air resistance of the pristine fabric was 0.5126 $kPa \cdot s \cdot m^{-1}$, and although the NiTR fabric showed a slight increase to 0.6312 $kPa \cdot s \cdot m^{-1}$, the values remained comparable. Similarly, the water vapor permeability of the pristine fabric was 850.073 $g \cdot m^2/day$, while the NiTR fabric demonstrated a nearly identical value of 834.981 $g \cdot m^2/day$. In Figure 5.12, the water vapor transmission curve over 24 hours reveals that the lines for both the pristine fabric and the TR fabric overlap closely, indicating no significant difference in the amount of liquid evaporated within the 24-hour period. It appears that the grafting of the polymer slightly reduced the pore size of the fabric. Based on the SEM images shown in Figure 5.8, the polymer was grafted only onto the outermost surface, without altering the fiber structure. As a result, the air permeability and water vapor permeability of the fabric were not significantly affected.

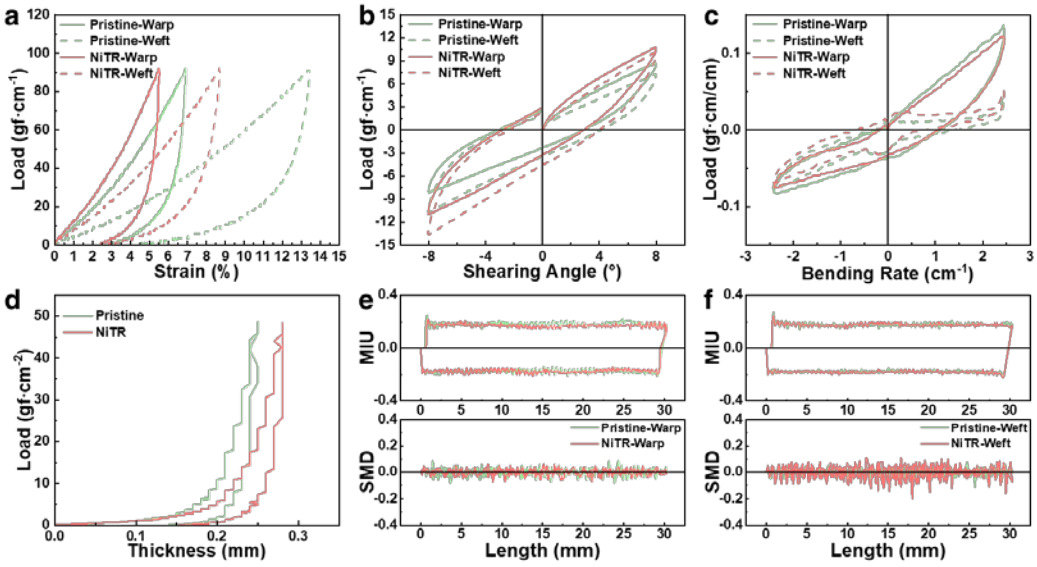

Figure 5.13 The tactile properties of the pristine fabric and the NiTR fabric, including (a) tensile property, (b) shearing property, (c) bending property, (d) compression property, and surface properties in (e) warp direction and (f) weft direction. The MIU represents the frictional coefficients and the SMD means the surface roughness.

The tactile properties of the fabrics were assessed using the Kawabata Evaluation System of Fabric (KES-FB). The evaluated properties included tensile, shearing, bending, and compressional characteristics, as well as surface fraction and roughness (as shown in Figure 5.13). The data suggested that the NiTR fabrics exhibited slightly higher stiffness compared to the pristine fabric. The modulus of the NiTR fabric was increased, requiring greater loads to stretch, shear, bend, and compress the fabric in both the weft and warp directions. This change is likely due to the crosslinking of the silane on the surface of the NiTR fabric, which contributed to enhanced stiffness. Nevertheless, the surface fraction and roughness of the NiTR fabric remained similar

to those of the pristine fabric. In general, despite the increase in stiffness, the NiTR fabric maintained comparable wearing comfort to the pristine fabric.

5.3 Fabrication and Evaluation of NiTR Skin-like Fabric for Personal Thermal Management

5.3.1 Preparation of the NiTR Skin-like Fabric by PVA-based Method

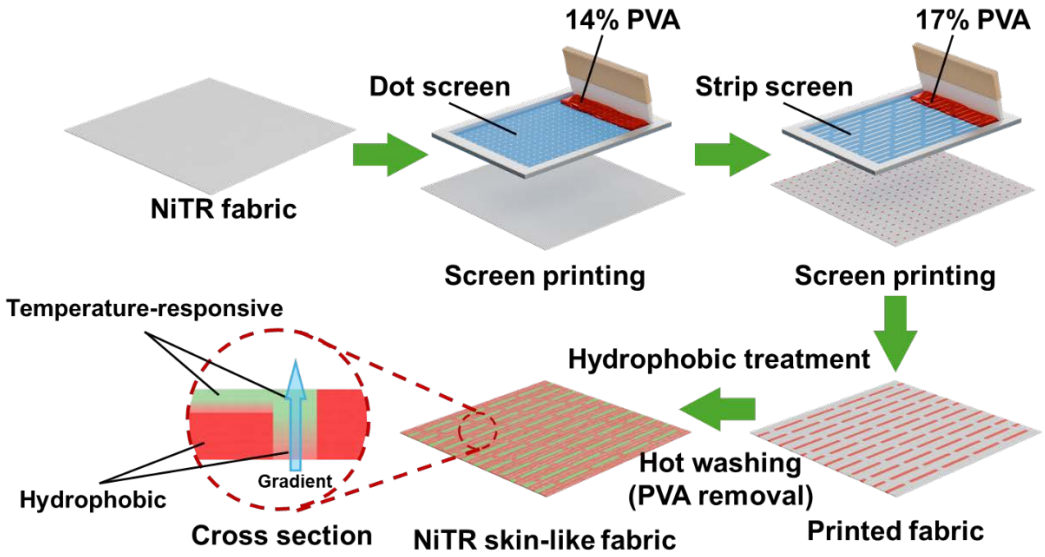

Figure 5.14 Fabrication process of NiTR skin-like fabric via PVA-based method.

In Chapter 3, PVA-based method for preparing the skin-like directional liquid flow and water repellent fabric was proposed. Wettability gradient channels were developed on the surface of a hydrophobic treated fabric. These channels allow water to be transported directionally from the back side to the top side of the fabric, while most areas of the fabric remain hydrophobic, thereby repelling external water like human skin. In this section, the developed NiTR fabric can also serve as the substrate for such

a skin-like fabric. Specifically, NiTR skin-like fabric was prepared using the PVA-based printing method outlined in Section 3.3 (see Figure 5.14). The NiTR fabric with 13 mol% AN content was selected as the substrate for this process. The water transport properties of the NiTR skin-like fabric were then demonstrated.

5.3.2 The Temperature-responsive liquid property of the NiTR Skin-like Fabric

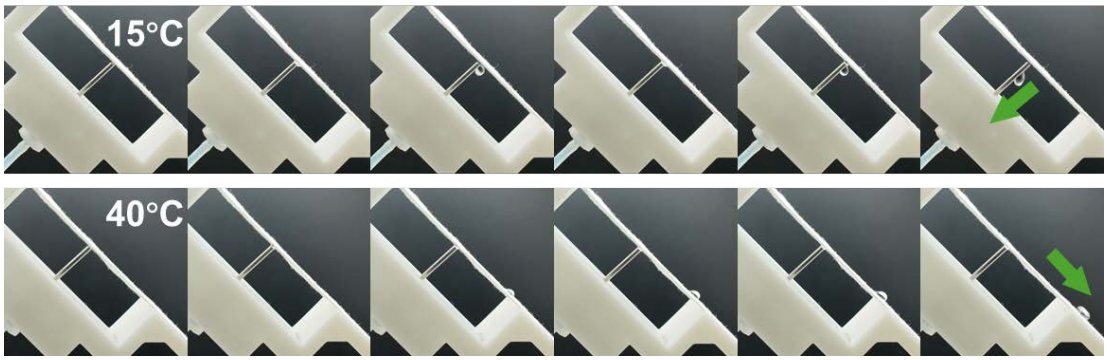

Figure 5.15 Temperature-responsive liquid water transport of the NiTR skin-like fabric.

As shown in Figure 5.15, at a temperature of 15°C, the fabric exhibited hydrophobicity, preventing water from being transported to the top side through the wettability channels. However, when the temperature was increased to 40°C, the wettability channels of the fabric turned hydrophilic, resulting in the formation of a wettability gradient within the channels. This allows water to be directionally transported to the top side of the fabric. Importantly, since most of the fabric remains hydrophobic, the transported water does not spread but rather accumulates on the top side and rolls off. Such NiTR skin-like fabric is highly suitable for sportswear applications. During physical activity, as the body's temperature increases and excessive sweating occurs, the fabric facilitates the transport of sweat away from the

skin to the outer side, allowing it to drip off. The hydrophobic outer surface prevents the fabric from becoming heavier or sticky due to sweat absorption. After exercise, when the body temperature decreases, the fabric reverts to its hydrophobic state, halting further water transport and preventing evaporative cooling. This helps reduce the after-chill effect typically experienced following physical exertion. The electrolyte stability nature of this non-ionic system ensures reliable performance under heavy sweating conditions compared to the (PDMAPS)-based temperature-responsive skin-like fabric developed in Chapter 4.

5.4 Summary

In this chapter, a non-ionic UCST-type temperature-responsive skin-like fabric with reversible wettability was successfully developed. By being pretreated with mixed silane solution, the grafted polymer concentration and surface hydrophilic-hydrophobic balance can be precisely controlled. The transition temperature of the fabric can be easily tuned by varying the monomer ratios (AAm:AN) when grafting the poly(AAm-co-AN) onto the fabric. Then, the prepared NiTR fabric was served as substrate for PVA-based treatment. With this treatment, skin-like structure was built on the NiTR fabric, forming the NiTR skin-like fabric. The NiTR fabric exhibited hydrophobic behavior at temperatures below the transition temperature and transitioned to hydrophilic at temperatures above it. Furthermore, the transition in wettability occurs rapidly and stable against electrolyte variation. A detailed exploration of the relationship between transition temperature and AN concentration highlighted the

fabric’s ability to adapt to various temperature conditions. Importantly, the temperature-responsive treatment did not compromise the fabric’s other properties, such as wearing comfort. The NiTR skin-like fabric also exhibited excellent temperature-responsive directional liquid transport properties. These fabric also demonstrated considerable potential for a wide array of applications, which will be introduced in the next chapter, with oil-water separation, wound dressing. This research bridges the gap in the application of non-ionic UCST-type polymers for temperature-responsive smart fabrics. With their stable temperature-responsive properties, these polymers open up broader possibilities for future applications.

Chapter 6 Other Potential Applications of [Poly(AAm-co-AN)]-based Non-ionic UCST-type Temperature-responsive Textiles

The tunable and electrolyte stability of the [poly(AAm-co-AN)]-based non-ionic UCST-type temperature-responsive textiles developed in Chapter 5 enables a wide range of applications in scenarios involving temperature and electrolyte fluctuations. These include adaptive clothing, wearable devices, medical textiles, and environmental monitoring, where the fabric's ability to dynamically adjust to temperature changes offers significant advantages. In addition to serving as the substrate material for skin-like fabric in personal thermal management systems, in this chapter, several other potential applications of the NiTR fabric were proposed, including oil-water separation and wound dressing.

6.1 Oil-Water Separation

The temperature-induced change in wettability enables the NiTR fabric to be applied in smart oil-water separation systems. Below the transition temperature, the fabric exhibited hydrophobic and oleophilic properties, while above the transition temperature, it became hydrophilic and oleophobic in water (see

Figure 6.1a). This distinct difference in wettability towards oil and water allows for effective oil-water separation. Two scenarios were illustrated here: one in which a small amount of water is present in the oil, and another where a small amount of oil is present in the water (

Figure 6.1b). In the case of separating water from oil, the temperature should be maintained below the fabric's transition temperature. In this condition, the fabric's hydrophobic and oleophilic properties allow oil to pass through while blocking water. Conversely, for the separation of oil from water, the temperature must be raised above the transition temperature, at which point the fabric becomes hydrophilic and oleophobic, allowing water to pass while blocking the oil (

Figure 6.1c). The stability against electrolytes variation of the NiTR fabric enables the fabric to be used in seawater or industrial wastewater. Furthermore, by adjusting the AN content, the transition temperature of the fabric can be fine-tuned. Thus, depending on the required application temperature, this fabric can be used in a variety of oil-water separation scenarios, which will not be exhaustively listed here.

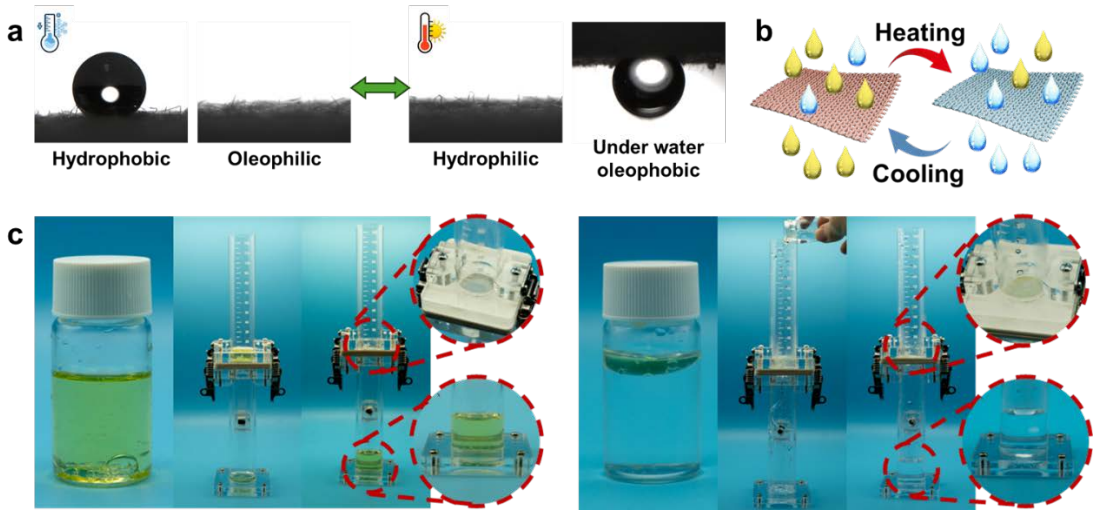

Figure 6.1 Potential application for oil-water separation of the NiTR fabric. (a) Wettability of TR fabric by water and oil at lower and higher temperatures. (b) Illustration of switchable oil-water separation of NiTR fabric. (c) Switchable oil-water separation application of NiTR fabric.

6.2 Wound Dressing

Table 6.1 Directional Liquid Transport Fabric Test of pristine fabric based directional liquid flow fabric and NiTR fabric based directional liquid flow fabric at different temperatures.

Substrate	Upper paper water content	Fabric water content	Lower paper water content	Transmission ratio
Pristine fabric-10 ºC	2.15%	75.90%	21.95%	10.21
Pristine fabric-40 ºC	2.23%	77.03%	20.74%	9.30
NiTR-10 ºC	10.87%	71.82%	17.31%	1.59
NiTR-40 ºC	1.20%	84.05%	14.75%	12.29

The NiTR fabrics can also serve as versatile substrates, onto which additional functional treatments can be applied to create fabrics with enhanced or supplementary properties. A temperature-responsive directional water transport fabric (NiTR directional flow fabric) was prepared by applying a commercial hydrophobic agent onto one side of the fabric via screen printing. The printed side became hydrophobic while the other side remains its temperature-responsive wettability. This asymmetric design enabled the fabric to exhibit complete hydrophobicity below the UCST while demonstrating directional water transport capability above the transition temperature. Here, directional water transport fabrics were prepared using NiTR fabric and pristine fabric as substrate. The directional liquid transport properties were evaluated using the Directional Liquid Transport Fabric Tester (DLTFT), developed by our group[151]. The DLTFT is a device for evaluating the directional liquid transport properties of textiles developed by our research group. 1 mL of DI water was supplied onto the upper surface of the fabric in 180 s, followed by a 60 s waiting time to ensure complete fabric wetting.

Then, two highly absorbent filter paper were placed on the upper and lower surface of the fabric. 100 g of load was applied onto the fabric for 60 s. Finally, weight of water absorbed by upper filter paper (m_u), lower filter paper (m_l), and water remains on the fabric (m_f) can be measured using a balance. The liquid transmission ratio (*LTR*) can be calculated as:

$$LTR = \frac{m_l}{m_u} \tag{6.1}$$

As shown in Table 6.1, the pristine fabric based directional flow fabric exhibited a liquid transmission ratio of 10.21 at lower temperatures and 9.30 when temperature rose. The liquid transmission ratios were similar at different temperatures. For the NiTR directional flow fabric, at lower temperatures, the liquid transmission ratio was relatively low at 1.59, while at higher temperatures, it increased to 12.29. This change in wettability enabled the fabric to smartly transition between a hydrophobic fabric and a directional water transport fabric, demonstrating its versatility.

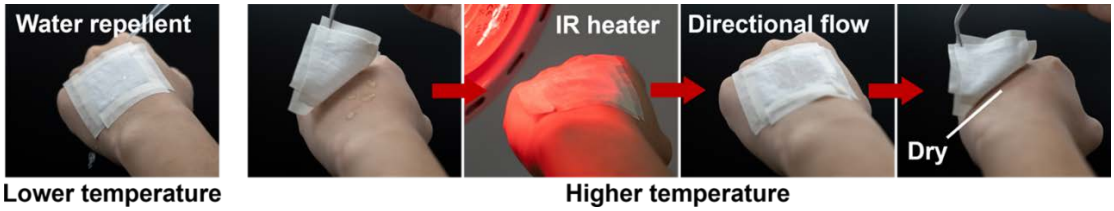

Figure 6.2 Potential application for wound dressing of the NiTR fabric.

The NiTR directional flow fabric demonstrates significant potential for advanced wound care applications (Figure 5b), where its transition temperature can be precisely tuned to ~40° C by adjusting the AN content. Under ambient conditions, the fabric maintains a hydrophobic state that effectively repels external contaminants and liquids,

while gentle heating via infrared radiation triggers its transformation into a directional liquid transport system that actively drains tissue fluid to maintain optimal wound dryness. The non-ionic nature of the system ensures remarkable stability, with the transition temperature remaining unaffected by physiological electrolyte variations caused by individual health differences. Moreover, this versatile technology can be adapted for personal moisture management applications by simply modifying the transition temperature range, demonstrating its broad potential in both medical and everyday textile applications.

Chapter 7 Conclusion and Suggestions for Future Research

7.1 Conclusion

In this study, temperature-responsive skin-like fabrics with directional liquid flow and water repellent properties were developed. The fabrics enable sweat to be transported directionally from the skin side to the outer side through the gradient wettability channels, while exhibiting water repellency. Moreover, the grafted temperature-responsive polymers endow the fabrics with variable liquid transport properties, allowing the liquid transport rate dynamically regulating as the temperature changes. Additionally, this study developed a non-ionic temperature-responsive textile, which exhibits tunable liquid transport behavior and enhanced stability against electrolyte concentrations variation, making it suitable for diverse applications. The novelty of this study is primarily demonstrated in three aspects. First, the structure of the skin-like fabric was improved, and a novel method for its large-scale preparation, the PVA-based method, was proposed. Second, PDMAPS was successfully grafted onto the aforementioned skin-like fabric to prepare a skin-like fabric with temperature-responsive wettability. Third, poly(AAm-co-AN) was grafted onto cotton fabric for the first time to prepare NiTR fabric, which features a tunable transition temperature and stability against electrolyte concentration, expanding the application scenarios of temperature-responsive fabrics.

In the first part of the study, the existing plasma-based fabrication method of skin-like fabric was evaluated. In this method, the pristine fabric was treated with a

commercial hydrophobic agent. Then, the fabric was covered with a laser cut PET plate screen with round hole pattern before plasma treatment. Due to the coverage of the screen, the gradient wettability channels only formed at the uncovered areas. Finally, a selective hydrophilic treatment was conducted on the gradient wettability channels to maintain the hydrophilicity of these areas. The prepared skin-like fabric using this method exhibited directional liquid transport through the gradient wettability channels and water repellency. However, this approach suffers from limitations including high energy consumption, low processing efficiency, and poor durability, which may limit the industrialization of this method.

Subsequently, the PVA-based fabrication method of skin-like fabric was proposed. The proposed method involves applying PVA solutions onto the surface of the pristine fabric using patterned screens via printing method to establish a controlled gradient of PVA concentration along the thickness direction of the fabric. Following the printing, hydrophobic treatment was applied to the fabric by dip coating. Notably, the fibers in PVA covered areas were not exposed to the hydrophobic agent due to the protection of the polymer, thereby preserving the inherent hydrophilicity on these areas. Subsequent hot washing removed the printed PVA on the surface of the fabric, resulting in the formation of gradient wettability channels in the previously coated areas. In this part, the effect of PVA concentration on wettability of the printed areas was explored, and optimized PVA concentration for printing was investigated. The directional liquid transport property through the gradient wettability channels exhibited excellent durability. The skin-like fabric prepared by PVA-based fabrication method exhibited

excellent directional liquid transport property and water repellency, with the transport rate being 10998 $g \cdot m^{-2} \cdot h^{-1}$ and hydrostatic pressure being 76 mmH_2O from the top side of the fabric. Meanwhile, the skin-like fabric demonstrated unaffected air permeability compared to the pristine fabric since the surface structure and pore structure were not affected by the treatment. This approach used mature technologies including printing and dip coating, offering significant scalability potential for industrial implementation.

In the second part of the study, the (PDMAPS)-based temperature-responsive skin-like fabric was developed by grafting zwitterionic UCST-type temperature-responsive polymer PDMAPS onto the surface of the gradient wettability channel areas of the skin-like fabric. The skin-like fabric was first treated with coupling agent TMSPMA to create double bonds on the surface. In this step, the hydroxyl groups on the cotton fabric were replaced by double bonds from TMSPMA, introducing both hydrophobicity and grafting sites onto the fabric. The temperature-responsive polymer PDMAPS was applied onto the fabric by photoinitiated “grafting-from” polymerization method.

The effect of the PDMAPS coating on the wettability of the fabric was explored. An optimal monomer solution concentration imparted temperature-responsive reversible wettability to the fabric surface, enabling temperature-dependent contact angle variation. In addition to the characteristics of skin-like fabric, the prepared (PDMAPS)-based temperature-responsive skin-like fabric exhibited temperature-responsive liquid transport capacity. Compared with the skin-like fabric prepared by PVA-based method, the water transport rate increased up to 14202 $g \cdot m^{-2} \cdot h^{-1}$ with a higher temperature, while at a lower temperature, the water transport rate decreased to

8700 $g \cdot m^{-2} \cdot h^{-1}$. The dynamic moisture management capacity improved the wearing comfort of the fabric. Furthermore, the water repellency of the temperature-responsive fabric could also be improved at lower temperatures, with 28.9% improvement (up to 98 mmH_2O) in hydrostatic pressure resistance at lower temperatures compared to skin-like fabric. The fabric also maintains comparable handle and breathability to both skin-like fabrics and pristine fabrics. Since the grafting process is exclusively surface modification, the fibrous architecture remains unchanged, thereby preserving the wear comfort performance. Furthermore, the mechanism of temperature-responsive directional water transport was systematically analyzed and explained, providing critical insights for performance optimization and advanced functional design.

In the third part of the study, a more widely used [poly(AAm-co-AN)]-based UCST-type temperature-responsive (NiTR) fabric was reported, which addressed some limitations of the (PDMAPS)-based temperature-responsive skin-like fabric. Compared to the zwitterionic UCST-type polymers, the non-ionic UCST-type polymers offer superior stability, yet present significant challenges in both fabrication and grafting onto the textile surface. In this study, the non-ionic UCST-type temperature-responsive polymer, poly(AAm-co-AN) was grafted onto the cotton knitted fabric for the first time via a novel site-specific grafting method. The pristine cotton knitted fabric was pretreated with a mixed silane solution, including a hydrophobic silane, a silane crosslinker, and a grafting-functionalized silane. The fabric treated with mixed silane solution was dipped into a monomer solution and then graft polymerization was initiated under UV radiation. The polymerization was selectively confined to silane-

functionalized regions, enabling precise control over grafted polymer quantity through systematic adjustment of the mixed silane composition ratio.

The effect of the mixed silane solution ratio on the wettability of the grafted fabric was explored firstly. In the mixed silane solution, the grafting-functionalized silane provided grafting site while the hydrophobic silane adjusted the wettability of the fabric. By adjusting the ratio of these two components, both the surface-grafted polymer density and the hydrophilic-hydrophobic balance of the grafted textile can be precisely modulated. The results showed when OTMS : BTEOSE : TMSPMA was 0.45 : 0.3 : 0.15, the optimal grafting density was achieved, and the fabric exhibited best temperature-responsive performance. Then, the effect of the temperature-responsive monomer solution ratio on the transition temperature was also investigated. The ratio of AAm to AN in poly(AAm-co-AN) largely influenced the transition temperature of this temperature-responsive polymer. The results showed the transition temperature was positively correlated with the content of AN. Specifically, at 13 mol% of AN, the transition temperature was tuned to 32.5-35°C, which is similar with the human skin temperature. The NiTR fabric exhibited tunable transition temperature and stability against electrolyte concentration variations compared to (PDMAPS)-based temperature-responsive fabrics, demonstrating broad application potential across multiple domains. The fabric can serve as a substrate for skin-like fabric to prepare the novel moisture management fabrics and can also be applied in wound dressing and smart switchable oil-water separation.

7.2 Suggestions for Future Research

7.2.1 Limitations of this Research

Although the proposed work in this research has been completed, there are several limitations remaining to be addressed in the future work. The key limitations of this research include:

1. The industrial scale fabrication of the skin-like fabric has not been achieved. Although the proposed PVA-based fabrication method used mature technologies with demonstrated scalability potential, the large-scale production of the skin-like fabric still faces challenges. The current printing screens in this research are laser cut PET plates, while industrial production employs mesh screens. The mesh structure hinders the penetration of PVA solution to the back side of the fabric, preventing it from forming the wettability gradient channels. Additionally, PVA becomes viscous during prolonged production, generating bubbles during printing, which adversely affects industrialized printing processes. Future work could explore incorporating various additives into the PVA solution to optimize its properties.

2. Although the PVA-based method can be applied to cotton fabrics with different structures, the application on polyester fabrics for developing polyester-based skin-like fabrics still faces limitations, as the PVA solution penetrates too rapidly through the polyester fibers, leading it difficult to control the infiltration.

3. The current directional liquid transport rate testing device is a homemade apparatus, that only enables single-point water supply, potentially rendering inaccurate test results. The testing device still needs to be improved.

4. The existing printing screens utilize only two patterns, dot pattern and stripe pattern. The effect of pattern shape on water transport efficiency and water repellency of the fabric have not been investigated. The shape of the printed pattern may be optimized.

5. Temperature-responsive fabrics have not yet achieved large-scale production. Currently, the grafting of the temperature-responsive polymers remains at the laboratory stage. The solvents used for temperature-responsive monomers in this research may affect human health and environment, making them unsuitable for industrial production. During large-scale UV-induced polymerization, uneven grafting may occur, compromising the quality of the fabricated textiles.

7.2.2 Industrialization of Skin-like Fabric

To achieve industrial production of skin-like fabric using PVA-based fabrication method, the primary challenge is improving the penetration of PVA solution through the fabric through the mesh printing screen. Further research could focus on optimizing the PVA solution formulation. Using PVA solution with lower molecular weight for printing may improve the penetration of the solution. Additionally, since PVA solution becomes viscous due to self-crosslinking during printing, additives could be introduced

to reduce hydrogen bonding, such as urea. Foaming during PVA printing may affect quality, so defoamers could be added to mitigate this issue.

Future studies could also optimize the shape and density of patterns on the printing screen. The shape of the patterns could be triangles or spindles, as well as varying pattern arrangements. By refining the design of patterns on printing screen, the fabric may achieve optimal water transport efficiency and water repellency.

7.2.3 Industrial Grafting of the Non-Ionic UCST-type Polymers onto Fabrics

To achieve the industrial grafting of the non-ionic UCST-type polymer, poly(AAm-co-AN), onto the fabrics for preparing the NiTR fabrics, the primary issue to address is the solvent system. The currently used DMSO solvent presents safety and environment concerns for large-scale production. A potential solution for this problem is to develop a water-based grafting solution. Due to the low solubility of initiators and crosslinkers in water, a “grafting-to” approach could be employed. This involves first synthesizing long-chain poly(AAm-co-AN) with reactive end groups in organic solvent, then isolating and dispersing it in aqueous solution. For the grafting process, thermal initiation and crosslinking could be utilized, allowing conventional dip coating and curing processes to graft the polymer onto the fabric surface, enabling large-scale production of NiTR fabrics.

References

(1) Nakamura, K.; Morrison, S. F. A thermosensory pathway that controls body temperature. *Nat. Neurosci.* **2008**, *11* (1), 62-71. DOI: 10.1038/nn2027.

(2) Lou, L.; Shou, D.; Park, H.; Zhao, D.; Wu, Y. S.; Hui, X.; Yang, R.; Kan, E. C.; Fan, J. Thermoelectric air conditioning undergarment for personal thermal management and HVAC energy saving. *Energy Build.* **2020**, *226*. DOI: 10.1016/j.enbuild.2020.110374.

(3) Song, Y.-N.; Li, Y.; Yan, D.-X.; Lei, J.; Li, Z.-M. Novel passive cooling composite textile for both outdoor and indoor personal thermal management. *Composites, Part A* **2020**, *130*. DOI: 10.1016/j.compositesa.2019.105738.

(4) Tabor, J.; Chatterjee, K.; Ghosh, T. K. Smart Textile‐Based Personal Thermal Comfort Systems: Current Status and Potential Solutions. *Adv. Mater. Technol.* **2020**, *5* (5). DOI: 10.1002/admt.201901155.

(5) Ullah, H. M. K.; Lejeune, J.; Cayla, A.; Monceaux, M.; Campagne, C.; Devaux, É. A review of noteworthy/major innovations in wearable clothing for thermal and moisture management from material to fabric structure. *Text. Res. J.* **2021**. DOI: 10.1177/00405175211027799.

(6) Zeng, C.; Wang, H.; Zhou, H.; Lin, T. Directional Water Transport Fabrics with Durable Ultra‐High One‐Way Transport Capacity. *Adv. Mater. Interfaces* **2016**, *3* (14). DOI: 10.1002/admi.201600036.

(7) Wang, H.; Zhou, H.; Wei, X.; Niu, H.; Lin, T. Highly Permeable, Directional Water Transport Cotton Fabrics. *Adv. Mater. Interfaces* **2018**, *5* (19). DOI: 10.1002/admi.201800815.

(8) Zhao, Y.; Wang, H.; Zhou, H.; Lin, T. Directional Fluid Transport in Thin Porous Materials and its Functional Applications. *Small* **2017**, *13* (4), 1601070. DOI: 10.1002/smll.201601070.

(9) Li, J.; Li, J.; Sun, J.; Feng, S.; Wang, Z. Biological and Engineered Topological Droplet Rectifiers. *Adv Mater* **2019**, *31* (14), e1806501. DOI: 10.1002/adma.201806501.

(10) de Groot, B. L.; Grubmuller, H. Water permeation across biological membranes: mechanism and dynamics of aquaporin-1 and GlpF. *Science* **2001**, *294* (5550), 2353-2357.

(11) Wheeler, T. D.; Stroock, A. D. The transpiration of water at negative pressures in a synthetic tree. *Nature* **2008**, *455* (7210), 208-212.

(12) Zheng, Y.; Bai, H.; Huang, Z.; Tian, X.; Nie, F.-Q.; Zhao, Y.; Zhai, J.; Jiang, L. Directional water collection on wetted spider silk. *Nature* **2010**, *463* (7281), 640-643.

(13) Pedersen, L.; Jemec, G. B. Mechanical properties and barrier function of healthy human skin. *Acta dermato-venereologica* **2006**, *86* (4), 308-311.

(14) Montagna, W. *The structure and function of skin*; Elsevier, 2012.

(15) Xin, B.; Hao, J. Reversibly switchable wettability. *Chem Soc Rev* **2010**, *39* (2), 769-782. DOI: 10.1039/b913622c.

(16) Pu, Y.; Yang, J.; Russell, S. J.; Ning, X. Cotton nonwovens with unidirectional water-transport properties produced by atmospheric plasma deposition. *Cellulose* **2021**, *28* (7), 4427-4438. DOI: 10.1007/s10570-021-03794-x.

(17) Huang, G.; Jin, Y.; Huo, L.; Yuan, S.; Zhao, R.; Zhao, J.; Li, Z.; Li, Y. An All-Hydrophobic Fluid Diode for Continuous and Reduced-Wastage Water Transport. *ACS Appl. Mater. Interfaces* **2021**, *13* (43), 51708-51717. DOI: 10.1021/acsami.1c14724.

(18) Wu, J.; Zhou, H.; Wang, H.; Shao, H.; Yan, G.; Lin, T. Novel Water Harvesting Fibrous Membranes with Directional Water Transport Capability. *Adv. Mater. Interfaces* **2019**, *6* (5). DOI: 10.1002/admi.201801529.

(19) Wu, J.; Wang, N.; Wang, L.; Dong, H.; Zhao, Y.; Jiang, L. Unidirectional water-penetration composite fibrous film via electrospinning. *Soft Matter* **2012**, *8* (22). DOI: 10.1039/c2sm25514f.

(20) Miao, D.; Huang, Z.; Wang, X.; Yu, J.; Ding, B. Continuous, Spontaneous, and Directional Water Transport in the Trilayered Fibrous Membranes for Functional Moisture Wicking Textiles. *Small* **2018**, *14* (32), 1801527. DOI: 10.1002/smll.201801527.

(21) Wang, H.; Niu, H.; Zhou, H.; Wei, X.; Yang, W.; Lin, T. Multifunctional Directional Water Transport Fabrics with Moisture Sensing Capability. *ACS Appl. Mater. Interfaces* **2019**, *11* (25), 22878-22884. DOI: 10.1021/acsami.9b06787.

(22) Chi, H.; Xu, Z.; Wei, Z.; Zhang, T.; Wang, H.; Lin, T.; Zhao, Y. Fabrics with Novel Air-Oil Amphibious, Spontaneous One-Way Water-Transport Capability for Oil/Water Separation. *ACS Appl. Mater. Interfaces* **2021**, *13* (24), 29150-29157. DOI: 10.1021/acsami.1c06489.

(23) Huang, G.; Xu, H.; Jin, Y.; Huo, L.; Zhao, J.; Li, Z. Electrospun Janus fabrics with directional water transport property for efficient water collection. *Mater. Lett.* **2021**, *289*, 129424. DOI: https://doi.org/10.1016/j.matlet.2021.129424.

(24) Lao, L.; Shou, D.; Wu, Y.; Fan, J. "Skin-like" fabric for personal moisture management. *Sci. Adv.* **2020**, *6* (14), eaaz0013. DOI: doi:10.1126/sciadv.aaz0013.

(25) Lei, Z.; Wu, P. Zwitterionic Skins with a Wide Scope of Customizable Functionalities. *ACS Nano* **2018**, *12* (12), 12860-12868. DOI: 10.1021/acsnano.8b08062.

(26) Bansal, K. K.; Upadhyay, P. K.; Saraogi, G. K.; Rosling, A.; Rosenholm, J. M. Advances in thermo-responsive polymers exhibiting upper critical solution temperature (UCST). *eXPRESS Polym. Lett.* **2019**, *13* (11), 974-992. DOI: 10.3144/expresspolymlett.2019.85.

(27) Woodfield, P. A.; Zhu, Y.; Pei, Y.; Roth, P. J. Hydrophobically Modified Sulfobetaine Copolymers with Tunable Aqueous UCST through Postpolymerization Modification of Poly(pentafluorophenyl acrylate). *Macromolecules* **2014**, *47* (2), 750-762. DOI: 10.1021/ma402391a.

(28) Chen, L.; Yang, T.; Niu, Y.; Mu, X.; Gong, Y.; Feng, Y.; de Rooij, N. F.; Wang, Y.; Li, H.; Zhou, G. Building a smart surface with converse temperature-dependent wettability based on poly(acrylamide-co-acrylonitrile). *Chem. Commun.* **2020**, *56* (19), 2837-2840. DOI: 10.1039/c9cc09479b.

(29) Liang, L.; Feng, X.; Liu, J.; Rieke, P. C.; Fryxell, G. E. Reversible surface properties of glass plate and capillary tube grafted by photopolymerization of N-isopropylacrylamide. *Macromolecules* **1998**, *31* (22), 7845-7850.

(30) Yim, H.; Kent, M.; Mendez, S.; Balamurugan, S.; Balamurugan, S.; Lopez, G.; Satija, S. Temperature-dependent conformational change of PNIPAM grafted chains at high surface density in water. *Macromolecules* **2004**, *37* (5), 1994-1997.

(31) Yim, H.; Kent, M.; Huber, D.; Satija, S.; Majewski, J.; Smith, G. Conformation of end-tethered PNIPAM chains in water and in acetone by neutron reflectivity. *Macromolecules* **2003**, *36* (14), 5244-5251.

(32) Kidoaki, S.; Ohya, S.; Nakayama, Y.; Matsuda, T. Thermoresponsive structural change of a poly (N-isopropylacrylamide) graft layer measured with an atomic force microscope. *Langmuir* **2001**, *17* (8), 2402-2407.

(33) Huang, G.; Wei, X.; Gu, Y.; Kang, Z.; Lao, L.; Li, L.; Fan, J.; Shou, D. Heterogeneously engineered porous media for directional and asymmetric liquid transport. *Cell Rep. Phys. Sci.* **2022**, *3* (1). DOI: 10.1016/j.xcrp.2021.100710.

(34) Huang, K.; Si, Y.; Hu, J. Fluid Unidirectional Transport Induced by Structure and Ambient Elements across Porous Materials: From Principles to Applications. *Adv Mater* **2024**, *36* (32), e2402527. DOI: 10.1002/adma.202402527.

(35) Prakash, M.; Quéré, D.; Bush, J. W. Surface tension transport of prey by feeding shorebirds: the capillary ratchet. *science* **2008**, *320* (5878), 931-934.

(36) Parker, A. R.; Lawrence, C. R. Water capture by a desert beetle. *Nature* **2001**, *414* (6859), 33-34. DOI: 10.1038/35102108.

(37) Wang, X.; Huang, Z.; Miao, D.; Zhao, J.; Yu, J.; Ding, B. Biomimetic Fibrous Murray Membranes with Ultrafast Water Transport and Evaporation for Smart Moisture-Wicking Fabrics. *ACS Nano* **2018**, *13* (2), 1060-1070. DOI: 10.1021/acsnano.8b08242.

(38) Bonn, D.; Eggers, J.; Indekeu, J.; Meunier, J.; Rolley, E. Wetting and spreading. *Rev. Mod. Phys.* **2009**, *81* (2), 739-805. DOI: 10.1103/RevModPhys.81.739.

(39) Quéré, D. Wetting and Roughness. *Annu. Rev. Mater. Res.* **2008**, *38* (1), 71-99. DOI: 10.1146/annurev.matsci.38.060407.132434.

(40) Bonn, D. Wetting transitions. *Current opinion in colloid & interface science* **2001**, *6* (1), 22-27.

(41) Wenzel, R. N. Surface roughness and contact angle. *The Journal of Physical Chemistry* **1949**, *53* (9), 1466-1467.

(42) Liu, T. L.; Chen, Z.; Kim, C. J. A dynamic Cassie-Baxter model. *Soft Matter* **2015**, *11* (8), 1589-1596. DOI: 10.1039/c4sm02651a From NLM Medline.

(43) Hao, J.-H.; Wang, Z.-J. Modeling Cassie–Baxter State on Superhydrophobic Surfaces. *J. Dispersion Sci. Technol.* **2015**, *37* (8), 1208-1213. DOI: 10.1080/01932691.2015.1089407.

(44) Kuang, X.; Zhang, Z.; Ma, X.; Zhu, L.; Li, Y.; Li, P.; Fu, Y.; Ma, T.; He, H.; Ramakrishna, S.; et al. Advances in Directional Liquid Transport Textiles: Mechanism, Construction, and Applications. *Adv. Funct. Mater.* **2024**, *34* (42). DOI: 10.1002/adfm.202406906.

(45) Rayleigh, L. On the theory of the capillary tube. *Proceedings of the Royal Society of London. Series A, Containing Papers of a Mathematical and Physical Character* **1916**, *92* (637), 184-195.

(46) Zhang, G.; Liu, J.; Miao, Y.; Ge, S.; Rezakazemi, M.; Chang, R.; Zhang, X.; Li, Y.; Fan, W. Advances in Controllable Water Transport of Textile Porous Materials: Mechanism, Structure Design, Fabrication and Application. *Adv. Fiber Mater.* **2025**. DOI: 10.1007/s42765-025-00533-w.

(47) Liu, S.; Li, S.; Liu, J. Jurin’s law revisited: Exact meniscus shape and column height. *The European Physical Journal E* **2018**, *41*, 1-7.

(48) Rodríguez-Valverde, M. Á.; Miranda, M. T. Derivation of Jurin's law revisited. *Eur. J. Phys.* **2010**, *32* (1), 49.

(49) Fengzhi, L.; Yi, L.; Yingxi, L.; Zhongxuan, L. Numerical simulation of coupled heat and mass transfer in hygroscopic porous materials considering the influence of atmospheric pressure. *Numerical Heat Transfer, Part B: Fundamentals* **2004**, *45* (3), 249-262.

(50) Wang, Z.; Li, Y.; Li, S.; Guo, J.; Zhang, S. Janus porous membrane with conical nanoneedle channel for rapid unidirectional water transport. *Chem. Commun.* **2018**, *54* (78), 10954-10957.

(51) Dong, J.; Peng, Y.; Wang, D.; Li, L.; Zhang, C.; Lai, F.; He, G.; Zhao, X.; Yan, X. P.; Ma, P. Quasi‐Homogeneous and Hierarchical Electronic Textiles with Porosity‐Hydrophilicity Dual‐Gradient for Unidirectional Sweat Transport, Electrophysiological Monitoring, and Body‐Temperature Visualization. *Small* **2023**, *19* (14), 2206572.

(52) Si, Y.; Shi, S.; Dong, Z.; Wu, H.; Sun, F.; Yang, J.; Hu, J. Bioinspired Stable Single-Layer Janus Fabric with Directional Water/Moisture Transport Property for Integrated Personal Cooling Management. *Adv. Fiber Mater.* **2022**, *5* (1), 138-153. DOI: 10.1007/s42765-022-00200-4.

(53) Li, Y.; Fan, J.; Zhang, S.; Xia, Z.; Wang, L.; Liu, Y. Directional Water Transport in Fabrics by Varying Yarn Coordination and Texture Design. *Fibers Polym.* **2023**, *24* (2), 759-769. DOI: 10.1007/s12221-023-00092-0.

(54) Ren, B.; Pi, H.; Zhao, X.; Hu, M.; Zhang, X.; Wang, R.; Wu, J. Janus membrane with novel directional water transport capacity for efficient atmospheric water capture. *Nanoscale* **2021**, *13* (20), 9354-9363. DOI: 10.1039/d1nr01120k.

(55) Liu, J.; Xu, Z.; Wang, H.; Zhao, Y.; Lin, T. Directional Liquid Transport in Thin Fibrous Matrices: Enhancement of Advanced Applications. *ACS Nano* **2025**, *19* (6), 5913-5937. DOI: 10.1021/acsnano.4c17351.

(56) Wang, Z.; Yang, X.; Cheng, Z.; Liu, Y.; Shao, L.; Jiang, L. Simply realizing “water diode” Janus membranes for multifunctional smart applications. *Mater. Horiz.* **2017**, *4* (4), 701-708.

(57) Tian, X.; Li, J.; Wang, X. Anisotropic liquid penetration arising from a cross-sectional wettability gradient. *Soft Matter* **2012**, *8* (9), 2633-2637.

(58) Mates, J. E.; Schutzius, T. M.; Qin, J.; Waldroup, D. E.; Megaridis, C. M. The fluid diode: tunable unidirectional flow through porous substrates. *ACS Appl. Mater. Interfaces* **2014**, *6* (15), 12837-12843.

(59) Huang, G.; Liang, Y.; Wang, J.; Zeng, X.; Li, Z.; Zhang, X. Effect of asymmetric wettability on directional transport of water through Janus fabrics prepared by an electrospinning technique. *Mater. Lett.* **2019**, *246*, 76-79. DOI: 10.1016/j.matlet.2019.03.011.

(60) Chen, X.; Wu, C.; Lv, Y.; Zhang, C.; Zhang, X.; Nie, L.; Zhang, Y.; Zhao, L.; Huang, C.; Liu, W. Self-driven lithium extraction by directional liquid transport nonwoven. *Matter* **2022**, *5* (9), 3053-3065. DOI: 10.1016/j.matt.2022.06.050.

(61) Peng, Z.; Liu, R.; Xu, Z.; Chi, H.; Wang, Z.; Zhao, Y. Directional sweat transport window based on hydrophobic/hydrophilic Janus fabric enables continuous transfer and monitoring of sweat. *Appl. Mater. Today* **2022**, *29*. DOI: 10.1016/j.apmt.2022.101623.

(62) Zhou, H.; Wang, H.; Lin, T.; Niu, H. A novel Janus fabric with stable amphibious directional oil transport function. *Chem. Eng. J.* **2022**, *427*. DOI: 10.1016/j.cej.2021.131936.

(63) Liu, L.; Sun, H.; Zhang, J.; Xu, B.; Gao, Y.; Qi, D.; Mao, Z.; Wu, J. Trilayered Fibrous Dressing with Wettability Gradient for Spontaneous and Directional Transport of Massive Exudate and Wound Healing Promotion. *Adv. Fiber Mater.* **2022**, *5* (2), 574-587. DOI: 10.1007/s42765-022-00239-3.

(64) Fan, W.; Zhang, G.; Zhang, X.; Dong, K.; Liang, X.; Chen, W.; Yu, L.; Zhang, Y. Superior Unidirectional Water Transport and Mechanically Stable 3D Orthogonal Woven Fabric for Human Body Moisture and Thermal Management. *Small* **2022**, *18* (10), e2107150. DOI: 10.1002/smll.202107150.

(65) Zhou, H.; Wang, H.; Niu, H.; Lin, T. Superphobicity/philicity Janus fabrics with switchable, spontaneous, directional transport ability to water and oil fluids. *Sci Rep* **2013**, *3*, 2964. DOI: 10.1038/srep02964.

(66) Lin, Y.; Wang, C.; Miao, D.; Cheng, N.; Meng, N.; Babar, A. A.; Wang, X.; Ding, B.; Yu, J. A Trilayered Composite Fabric with Directional Water Transport and Resistance to Blood Penetration for Medical Protective Clothing. *ACS Appl Mater Interfaces* **2022**, *14* (16), 18944-18953. DOI: 10.1021/acsami.2c03136.

(67) Lin, Y.; Liu, X.; Babar, A. A.; Wang, X.; Yu, J.; Ding, B. Sweat Gland-Inspired Skin-like Fabric with Directional Water Transport and Durability for Efficient Personal Moisture Management. *ACS Appl. Mater. Interfaces* **2023**, *15* (45), 53105-53112. DOI: 10.1021/acsami.3c11006.

(68) Soltani, M.; Lahiri, S. K.; Shabanian, S.; Golovin, K. Surface-engineered double-layered fabrics for continuous, passive fluid transport. *Mater Horiz* **2023**, *10* (10), 4293-4302. DOI: 10.1039/d3mh00634d.

(69) Fan, Z.; Wang, Y.; Zhao, W.; Hou, K.; Li, X.; Jin, K.; Ji, Y.; Tam, K. C.; Cai, Z. Unidirectional water transport fabric with nanoscale Hydrophilic/hydrophobic pattern for personal moisture and thermal management. *Chem. Eng. J.* **2024**, *480*. DOI: 10.1016/j.cej.2023.148204.

(70) Yang, Y.; Chen, L.; Naveed, T.; Zhang, P.; Farooq, A. Influence of fabric structure and finishing pattern on the thermal and moisture management properties of unidirectional water transport knitted polyester fabrics. *Text. Res. J.* **2018**, *89* (10), 1983-1996. DOI: 10.1177/0040517518783349.

(71) Zhao, H.; Fan, Z.; Jia, C.; Cai, Z. One-way water transport and enhanced heating and cooling for cotton fabrics. *Cellulose* **2023**, *30* (5), 3351-3361. DOI: 10.1007/s10570-023-05073-3.

(72) Shou, D.; Fan, J. An All Hydrophilic Fluid Diode for Unidirectional Flow in Porous Systems. *Adv. Funct. Mater.* **2018**, *28* (36). DOI: 10.1002/adfm.201800269.

(73) Du, L.; Xu, Y.; Xu, H.; Ye, X.; Li, Y. Highly directional water transport membrane made from a hybrid manufacturing approach: Unleashing the power of melt electrowriting. *Colloids Surf., A* **2022**, *641*. DOI: 10.1016/j.colsurfa.2022.128486.

(74) Dai, B.; Li, K.; Shi, L.; Wan, X.; Liu, X.; Zhang, F.; Jiang, L.; Wang, S. Bioinspired Janus Textile with Conical Micropores for Human Body Moisture and Thermal Management. *Adv Mater* **2019**, *31* (41), e1904113. DOI: 10.1002/adma.201904113.

(75) Qing, C.; Jintu, F.; Sarkar, M.; Gaoming, J. Biomimetics of Plant Structure in Knitted Fabrics to Improve the Liquid Water Transport Properties. *Text. Res. J.* **2009**, *80* (6), 568-576. DOI: 10.1177/0040517509340600.

(76) Wang, L.; Shou, D.; Owad, T. T. A.; Zhang, J.; Zheng, R.; Chen, Q.; Fan, J. Bioinspired Multilayered Knitted Fabric with Directional Water Transport and Collection for Personal Sweat Management. *ACS Appl Mater Interfaces* **2024**, *16* (31), 41504-41517. DOI: 10.1021/acsami.4c07080.

(77) Zou, C.; Lao, L.; Chen, Q.; Fan, J.; Shou, D. Nature-inspired moisture management fabric for unidirectional liquid transport and surface repellence and resistance. *Energy Build.* **2021**, *248*. DOI: 10.1016/j.enbuild.2021.111203.

(78) Ma, J.; Lin, J.-H.; Feng, Y.; Huang, X.; Chi, S.; Liu, Y.; Lou, C.-W.; Dong, T. Durable antibacterial cotton fabric imitating skin wet management with synchronous liquid gating and directional liquid transfer. *Ind. Crops Prod.* **2022**, *184*. DOI: 10.1016/j.indcrop.2022.114994.

(79) Peng, Y.; Zhou, J.; Yang, Y.; Lai, J. C.; Ye, Y.; Cui, Y. An Integrated 3D Hydrophilicity/Hydrophobicity Design for Artificial Sweating Skin (i-TRANS) Mimicking Human Body Perspiration. *Adv Mater* **2022**, *34* (44), e2204168. DOI: 10.1002/adma.202204168.

(80) Chen, Q.; Xiao, X.; Shou, D.; Chen, H.; Zheng, W.; Fu, B.; Zheng, R.; Fan, J. Directional Water Transport Property of Cotton–Polyester Knitted Plating Fabric with Multiple Gradient Concentration Coatings. *Fibers Polym.* **2023**, *24* (8), 2933-2939. DOI: 10.1007/s12221-023-00208-6.

(81) Liu, L.-Y.; Liu, G.-H.; Shou, B.-B.; Li, T.-T.; Ren, H.-T.; Lin, J.-H.; Lou, C.-W.; Xu, Y.-M. Design of nature-inspired patterns on knitted fabrics for directional transportation of sweat and study of their performances. *Text. Res. J.* **2024**, *95* (7-8), 767-782. DOI: 10.1177/00405175241276521.

(82) Zhou, H.; Wang, H.; Niu, H.; Zeng, C.; Zhao, Y.; Xu, Z.; Fu, S.; Lin, T. One‐Way Water‐Transport Cotton Fabrics with Enhanced Cooling Effect. *Adv. Mater. Interfaces* **2016**, *3* (17). DOI: 10.1002/admi.201600283.

(83) Pi, H.; Xi, Y.; Wu, J.; Hu, M.; Tian, B.; Yang, Y.; Wang, R.; Zhang, X. Janus fibrous membrane with directional liquid transport capacity for wound healing promotion. *Chem. Eng. J.* **2023**, *455*. DOI: 10.1016/j.cej.2022.140853.

(84) Yang, T.; Wang, S.; Yang, H.; Gui, H.; Du, Y.; Liang, F. Temperature‐Triggered Dynamic Janus Fabrics for Smart Directional Water Transport. *Adv. Funct. Mater.* **2023**, *33* (18). DOI: 10.1002/adfm.202214183.

(85) Chang, X.; Li, S.; Li, N.; Wang, S.; Li, J.; Guo, C.; Yu, L.; Murto, P.; Xu, X. Marine biomass-derived, hygroscopic and temperature-responsive hydrogel beads for atmospheric water harvesting and solar-powered irrigation. *J. Mater. Chem. A* **2022**, *10* (35), 18170-18184. DOI: 10.1039/d2ta04919h.

(86) Yang, H.; Zhu, H.; Hendrix, M. M.; Lousberg, N. J.; de With, G.; Esteves, A. C.; Xin, J. H. Temperature-triggered collection and release of water from fogs by a sponge-like cotton fabric. *Adv Mater* **2013**, *25* (8), 1150-1154, 1149. DOI: 10.1002/adma.201204278.

(87) Wang, Y.; Lai, C.; Hu, H.; Liu, Y.; Fei, B.; Xin, J. H. Temperature-responsive nanofibers for controllable oil/water separation. *RSC Adv.* **2015**, *5* (63), 51078-51085. DOI: 10.1039/c5ra08851h.

(88) Sun, C.; Luo, J.; Yan, S.; Li, K.; Li, Y.; Wang, H.; Hou, C.; Zhang, Q. Thermally Responsive Fibers for Versatile Thermoactivated Protective Fabrics. *Adv. Funct. Mater.* **2022**, *33* (9). DOI: 10.1002/adfm.202211035.

(89) Zhu, H.; Geng, Q.; Chen, W.; Zhu, Y.; Chen, J.; Du, J. Antibacterial high-genus polymer vesicle as an "armed" drug carrier. *J Mater Chem B* **2013**, *1* (40), 5496-5504. DOI: 10.1039/c3tb20713g.

(90) Chen, J.-P.; Kuo, C.-Y.; Lee, W.-L. Thermo-responsive wound dressings by grafting chitosan and poly(N-isopropylacrylamide) to plasma-induced graft polymerization modified non-woven fabrics. *Appl. Surf. Sci.* **2012**, *262*, 95-101. DOI: 10.1016/j.apsusc.2012.02.106.

(91) Yang, H.; Esteves, A. C. C.; Zhu, H.; Wang, D.; Xin, J. H. In-situ study of the structure and dynamics of thermo-responsive PNIPAAm grafted on a cotton fabric. *Polymer* **2012**, *53* (16), 3577-3586. DOI: 10.1016/j.polymer.2012.05.053.

(92) Gu, S.-Y.; Wang, Z.-M.; Li, J.-B.; Ren, J. Switchable Wettability of Thermo-Responsive Biocompatible Nanofibrous Films Created by Electrospinning. *Macromol. Mater. Eng.* **2010**, *295* (1), 32-36. DOI: 10.1002/mame.200900215.

(93) Roy, D.; Brooks, W. L.; Sumerlin, B. S. New directions in thermoresponsive polymers. *Chem Soc Rev* **2013**, *42* (17), 7214-7243. DOI: 10.1039/c3cs35499g.

(94) Higashi, N.; Sonoda, R.; Koga, T. Thermo-responsive amino acid-based vinyl polymers showing widely tunable LCST/UCST behavior in water. *RSC Adv.* **2015**, *5* (83), 67652-67657. DOI: 10.1039/c5ra13009c.

(95) Kotsuchibashi, Y. Recent advances in multi-temperature-responsive polymeric materials. *Polym. J.* **2020**, *52* (7), 681-689. DOI: 10.1038/s41428-020-0330-0.

(96) Zhang, X. Z.; Xu, X. D.; Cheng, S. X.; Zhuo, R. X. Strategies to improve the response rate of thermosensitive hydrogels. *Soft Matter* **2008**, *4* (3), 385-391. DOI: 10.1039/b713803m.

(97) Bai, S.; Xu, R.; Wang, W.; Yu, D. Dual-response of temperature and humidity asymmetrical cotton fabric prepared based on thiol-ene click chemistry. *Colloids Surf., A* **2019**, *567*, 104-111. DOI: 10.1016/j.colsurfa.2019.01.050.

(98) ter Schiphorst, J.; van den Broek, M.; de Koning, T.; Murphy, J. N.; Schenning, A. P. H. J.; Esteves, A. C. C. Dual light and temperature responsive cotton fabric functionalized with a surface-grafted spiropyran–NIPAAm-hydrogel. *J. Mater. Chem. A* **2016**, *4* (22), 8676-8681. DOI: 10.1039/c6ta00161k.

(99) Reed, J. A.; Lucero, A. E.; Cooperstein, M. A.; Canavan, H. E. The effects of cell culture parameters on cell release kinetics from thermoresponsive surfaces. *J Appl Biomater Biomech* **2008**, *6* (2), 81-88. From NLM.

(100) Li, Y.; Tanaka, T. Study of the universality class of the gel network system. *The Journal of Chemical Physics* **1989**, *90* (9), 5161-5166. DOI: 10.1063/1.456559.

(101) Wu, J.; Jiang, Y.; He, J.; Zhao, S.; Cai, G.; Wang, J. Thermo-responsive poly(N-isopropylacrylamide) grafted polyester textiles with switchable surface wettability. *Text. Res. J.* **2016**, *86* (7), 677-684. DOI: 10.1177/0040517515599748.

(102) Zhang, C.; Zhu, Y.; Zhou, C.; Yuan, W.; Du, J. Antibacterial vesicles by direct dissolution of a block copolymer in water. *Polym. Chem.* **2013**, *4* (2), 255-259. DOI: 10.1039/c2py20719b.

(103) Jiang, B.; Zhang, L.; Liao, B.; Pang, H. Self-assembly of well-defined thermo-responsive fluoropolymer and its application in tunable wettability surface. *Polymer* **2014**, *55* (21), 5350-5357. DOI: 10.1016/j.polymer.2014.08.050.

(104) Seuring, J.; Agarwal, S. Polymers with upper critical solution temperature in aqueous solution. *Macromol Rapid Commun* **2012**, *33* (22), 1898-1920. DOI: 10.1002/marc.201200433.

(105) Qi, B.; Fan, B.; Xu, B.; Zhou, M.; Yu, Y.; Cui, L.; Wang, Q.; Wang, P. Enzymatic construction of temperature-responsive PDMAPS-decorated textiles for oil-water separation. *Colloids Surf., A* **2023**, *656*. DOI: 10.1016/j.colsurfa.2022.130340.

(106) Wang, Y.; Liang, X.; Zhu, H.; Xin, J. H.; Zhang, Q.; Zhu, S. Reversible Water Transportation Diode: Temperature - Adaptive Smart Janus Textile for Moisture/Thermal Management. *Adv. Funct. Mater.* **2019**, *30* (6). DOI: 10.1002/adfm.201907851.

(107) Liang, J.; Ding, L.; Yu, Z.; Zhang, X.; Chen, S.; Wang, Y. Smart and programmed thermo-wetting yarns for scalable and customizable moisture/heat conditioning textiles. *J Colloid Interface Sci* **2023**, *651*, 612-621. DOI: 10.1016/j.jcis.2023.08.013.

(108) Pu, Y.; Fan, J. Thermoresponsive Skin-like Fabric for Personal Comfort and Protection. *ACS Appl Mater Interfaces* **2024**, *16* (8), 10960-10968. DOI: 10.1021/acsami.3c17270.

(109) Seuring, J.; Agarwal, S. First Example of a Universal and Cost-Effective Approach: Polymers with Tunable Upper Critical Solution Temperature in Water and Electrolyte Solution. *Macromolecules* **2012**, *45* (9), 3910-3918. DOI: 10.1021/ma300355k.

(110) Shirreffs, S.; Maughan, R. Whole body sweat collection in humans: an improved method with preliminary data on electrolyte content. *Journal of Applied Physiology* **1997**, *82* (1), 336-341.

(111) Coltman Jr, C. A.; Atwell, R. J. The electrolyte composition of normal adult sweat. *American Review of Respiratory Disease* **1966**, *93* (1), 62-69.

(112) Baker, L. B.; De Chavez, P. J. D.; Ungaro, C. T.; Sopeña, B. C.; Nuccio, R. P.; Reimel, A. J.; Barnes, K. A. Exercise intensity effects on total sweat electrolyte losses and regional vs. whole-body sweat [Na+],[Cl−], and [K+]. *Eur. J. Appl. Physiol.* **2019**, *119*, 361-375.

(113) Otsuka, C.; Wakahara, Y.; Okabe, K.; Sakata, J.; Okuyama, M.; Hayashi, A.; Tokuyama, H.; Uchiyama, S. Fluorescent Labeling Method Re-Evaluates the Intriguing Thermoresponsive Behavior of Poly(acrylamide-co-acrylonitrile)s with Upper Critical Solution Temperatures. *Macromolecules* **2019**, *52* (20), 7646-7660. DOI: 10.1021/acs.macromol.9b00880.

(114) Lertturongchai, P.; Ibrahim, M. I. A.; Durand, A.; Sunintaboon, P.; Ferji, K. Synthesis of Thermoresponsive Copolymers with Tunable UCST-Type Phase Transition Using Aqueous Photo-RAFT Polymerization. *Macromol Rapid Commun* **2020**, *41* (9), e2000058. DOI: 10.1002/marc.202000058.

(115) Hua, L.; Xie, M.; Jian, Y.; Wu, B.; Chen, C.; Zhao, C. Multiple-Responsive and Amphibious Hydrogel Actuator Based on Asymmetric UCST-Type Volume Phase Transition. *ACS Appl. Mater. Interfaces* **2019**, *11* (46), 43641-43648. DOI: 10.1021/acsami.9b17159.

(116) Seuring, J.; Bayer, F. M.; Huber, K.; Agarwal, S. Upper Critical Solution Temperature of Poly(N-acryloyl glycinamide) in Water: A Concealed Property. *Macromolecules* **2011**, *45* (1), 374-384. DOI: 10.1021/ma202059t.

(117) Seuring, J.; Agarwal, S. Non-Ionic Homo- and Copolymers with H-Donor and H-Acceptor Units with an UCST in Water. *Macromol. Chem. Phys.* **2010**, *211* (19), 2109-2117. DOI: 10.1002/macp.201000147.

(118) Asadujjaman, A.; Bertin, A.; Schonhals, A. Dielectric analysis of the upper critical solution temperature behaviour of a poly(acrylamide-co-acrylonitrile) copolymer system in water. *Soft Matter* **2017**, *13* (12), 2384-2393. DOI: 10.1039/c6sm02684b.

(119) Zubair, N. A.; Moawia, R. M.; Nasef, M. M.; Hubbe, M.; Zakeri, M. A Critical Review on Natural Fibers Modifications by Graft Copolymerization for Wastewater Treatment. *J. Polym. Environ.* **2021**, *30* (4), 1199-1227. DOI: 10.1007/s10924-021-02269-1.

(120) Bhattacharya, A. Grafting: a versatile means to modify polymersTechniques, factors and applications. *Prog. Polym. Sci.* **2004**, *29* (8), 767-814. DOI: 10.1016/j.progpolymsci.2004.05.002.

(121) Roy, D.; Semsarilar, M.; Guthrie, J. T.; Perrier, S. Cellulose modification by polymer grafting: a review. *Chem Soc Rev* **2009**, *38* (7), 2046-2064. DOI: 10.1039/b808639g.

(122) Ma, H.; Davis, R. H.; Bowman, C. N. A novel sequential photoinduced living graft polymerization. *Macromolecules* **2000**, *33* (2), 331-335.

(123) Chauhan, G. S.; Lal, H. Novel grafted cellulose-based hydrogels for water technologies. *Desalination* **2003**, *159* (2), 131-138.

(124) Ghosh, J.; Rupanty, N. S.; Khan, F.; Noor, T.; Jahangir, R.; Mirmohammadsadeghi, S.; Islam, T. Grafting modification for textile functionalization: innovations and applications. *Discover Applied Sciences* **2025**, *7* (1). DOI: 10.1007/s42452-024-06364-5.

(125) Wang, P.; Zhang, M.; Qu, J.; Wang, L.; Geng, J.; Fu, F.; Liu, X. Antibacterial cotton fabric prepared by a “grafting to” strategy using a QAC copolymer. *Cellulose* **2022**, *29* (6), 3569-3581. DOI: 10.1007/s10570-022-04469-x.

(126) Xu, Q.; Shen, L.; Duan, P.; Zhang, L.; Fu, F.; Liu, X. Superhydrophobic cotton fabric with excellent healability fabricated by the “grafting to” method using a diblock copolymer mist. *Chem. Eng. J.* **2020**, *379*. DOI: 10.1016/j.cej.2019.122401.

(127) Sangermano, M.; Razza, N. Light induced grafting-from strategies as powerfull tool for surface modification. *eXPRESS Polym. Lett.* **2019**, *13* (2), 135-145. DOI: 10.3144/expresspolymlett.2019.13.

(128) Gangopadhyay, R.; Ghosh, P. Uncatalyzed photografting of polyacrylamide from functionalized cellulosic and lignocellulosic materials. *J. Appl. Polym. Sci.* **1999**, *74* (7), 1623-1634. DOI: 10.1002/(sici)1097-4628(19991114)74:7<1623::Aid-app3>3.0.Co;2-z.

(129) Sekine, A.; Seko, N.; Tamada, M.; Suzuki, Y. Biodegradable metal adsorbent synthesized by graft polymerization onto nonwoven cotton fabric. *Radiat. Phys. Chem.* **2010**, *79* (1), 16-21. DOI: 10.1016/j.radphyschem.2009.08.007.

(130) Yeqiu, L.; Jinlian, H.; Yong, Z.; Zhuohong, Y. Surface modification of cotton fabric by grafting of polyurethane. *Carbohydr. Polym.* **2005**, *61* (3), 276-280.

(131) Yang, Y.; Bao, X.; Wang, Q.; Wang, P.; Zhou, M.; Yu, Y. Thermo-responsive cotton fabric prepared by enzyme-initiated “graft from” polymerization for moisture/thermal management. *Cellulose* **2021**, *28* (3), 1795-1808. DOI: 10.1007/s10570-020-03626-4.

(132) Mohammadi Sejoubsari, R.; Martinez, A. P.; Kutes, Y.; Wang, Z.; Dobrynin, A. V.; Adamson, D. H. “Grafting-Through”: Growing Polymer Brushes by Supplying Monomers through the Surface. *Macromolecules* **2016**, *49* (7), 2477-2483. DOI: 10.1021/acs.macromol.6b00183.

(133) Sarkar, M.; Fan, J.; Szeto, Y.-c.; Tao, X. Biomimetics of Plant Structure in Textile Fabrics for the Improvement of Water Transport Properties. *Text. Res. J.* **2009**, *79* (7), 657-668. DOI: 10.1177/0040517508095604.

(134) Sun, J. T.; Yu, Z. Q.; Hong, C. Y.; Pan, C. Y. Biocompatible zwitterionic sulfobetaine copolymer-coated mesoporous silica nanoparticles for temperature-responsive drug release. *Macromol Rapid Commun* **2012**, *33* (9), 811-818. DOI: 10.1002/marc.201100876.

(135) Zou, W.; Chen, Y.; Zhang, X.; Li, J.; Sun, L.; Gui, Z.; Du, B.; Chen, S. Cytocompatible chitosan based multi-network hydrogels with antimicrobial, cell anti-adhesive and mechanical properties. *Carbohydr. Polym.* **2018**, *202*, 246-257. DOI: 10.1016/j.carbpol.2018.08.124.

(136) Willcock, H.; Lu, A.; Hansell, C. F.; Chapman, E.; Collins, I. R.; O'Reilly, R. K. One-pot synthesis of responsive sulfobetaine nanoparticles by RAFT polymerisation: the effect of branching on the UCST cloud point. *Polym. Chem.* **2014**, *5* (3), 1023-1030. DOI: 10.1039/c3py00998j.

(137) Elzein, T.; Nasser-Eddine, M.; Delaite, C.; Bistac, S.; Dumas, P. FTIR study of polycaprolactone chain organization at interfaces. *J. Colloid Interface Sci.* **2004**, *273* (2), 381-387. DOI: 10.1016/j.jcis.2004.02.001.

(138) Gohlke, D. J.; Tanner, J. C. Gore-Tex® waterproof breathable laminates. *Journal of Coated Fabrics* **1976**, *6* (1), 28-38.

(139) Herminghaus, S.; Brinkmann, M.; Seemann, R. Wetting and Dewetting of Complex Surface Geometries. *Annu. Rev. Mater. Res.* **2008**, *38* (1), 101-121. DOI: 10.1146/annurev.matsci.38.060407.130335.

(140) Jiang, S.; Zhou, S.; Du, B.; Luo, R. Preparation of the temperature-responsive superhydrophobic paper with high stability. *ACS Omega* **2021**, *6* (24), 16016-16028.

(141) Gao, X.; Meng, J.; Wang, Y.; Liu, Y.; Zhi, C.; Yang, L.; Chen, Y.; Wang, C. Humidity /temperature/ pH multi-responsive fabric-based colorimetric sensor for

detection and information encryption. *Dyes Pigm.* **2024**, *225*. DOI: 10.1016/j.dyepig.2024.112090.

(142) Wang, J.; He, J.; Ma, L.; Zhang, Y.; Shen, L.; Xiong, S.; Li, K.; Qu, M. Multifunctional conductive cellulose fabric with flexibility, superamphiphobicity and flame-retardancy for all-weather wearable smart electronic textiles and high-temperature warning device. *Chem. Eng. J.* **2020**, *390*. DOI: 10.1016/j.cej.2020.124508.

(143) Shi, Y.; Ma, C.; Peng, L.; Yu, G. Conductive "Smart" Hybrid Hydrogels with PNIPAM and Nanostructured Conductive Polymers. *Adv. Funct. Mater.* **2015**, *25* (8), 1219-1225. DOI: 10.1002/adfm.201404247.

(144) Liu, J.; He, H.; Yu, Z.; Suryawanshi, A.; Li, Y.; Lin, X.; Sun, Z. Investigation of temperature-responsive and thermo-physiological comfort of modified polyester fabric with Sericin/PNIPAAm/Ag NPs interpenetrating polymer network hydrogel. *Text. Res. J.* **2020**, *90* (23-24), 2622-2638. DOI: 10.1177/0040517520931475.

(145) Tian, X.; Guo, Y.; Zhang, J.; Ivasishin, O. M.; Jia, J.; Yan, J. Fiber Actuators Based on Reversible Thermal Responsive Liquid Crystal Elastomer. *Small* **2024**, *20* (24). DOI: 10.1002/smll.202306952.

(146) Zhang, X.; Wang, Z.; Huang, G.; Chao, X.; Ye, L.; Fan, J.; Shou, D. Soft Robotic Textiles for Adaptive Personal Thermal Management. *Adv Sci (Weinh)* **2024**, *11* (21), e2309605. DOI: 10.1002/advs.202309605.

(147) Asadujjaman, A.; Kent, B.; Bertin, A. Phase transition and aggregation behaviour of an UCST-type copolymer poly(acrylamide-co-acrylonitrile) in water: effect of

acrylonitrile content, concentration in solution, copolymer chain length and presence of electrolyte. *Soft Matter* **2017**, *13* (3), 658-669. DOI: 10.1039/c6sm02262f.

(148) Hou, L.; Wu, P. Understanding the UCST-type transition of P(AAm-co-AN) in H2O and D2O: dramatic effects of solvent isotopes. *Soft Matter* **2015**, *11* (35), 7059-7065. DOI: 10.1039/c5sm01745a.

(149) Sivanantham, M.; Kesavamoorthy, R.; Sairam, T. N.; Sabharwal, K. N.; Raj, B. Stimulus response and molecular structural modification of polyacrylamide gel in nitric acid: A study by Raman, FTIR, and photoluminescence techniques. *J. Polym. Sci., Part B: Polym. Phys.* **2008**, *46* (7), 710-720. DOI: 10.1002/polb.21402.

(150) Gui, Z.; Qian, J.; Zhao, Q.; Ji, Y.; Liu, Y.; Liu, T.; An, Q. Controllable disintegration of temperature-responsive self-assembled multilayer film based on polybetaine. *Colloids Surf., A* **2011**, *380* (1-3), 270-279. DOI: 10.1016/j.colsurfa.2011.02.049.

(151) Yuan, L.; Hong, Y.; Shahzad, A.; Wu, Y.; Huang, G.; Fan, J. Simple, direct and accurate measurement of one-way liquid transport across fabric thickness: A directional liquid transport fabric tester. *J. Ind. Text.* **2024**, *54*. DOI: 10.1177/15280837241302017.